Informing salmon conservation with population models that account for individual heterogeneity

Mark Sorel

A dissertation

submitted in partial fulfillment of the

requirements for the degree of

Doctor of Philosophy

University of Washington

2022

Reading Committee:

Sarah Converse, Chair

Mark Scheuerell

Richard Zabel

Program Authorized to Offer Degree:

School of Aquatic and Fishery Sciences

University of Washington

Abstract

Informing salmon conservation with population models that account for individual heterogeneity

Mark Sorel

Chair of the Supervisory Committee:
Sarah Converse
School of Aquatic and Fishery Sciences

Managing threatened species requires information on their status and predictions of their response to management and environmental change. To develop this information, we often collect data and use them to parameterize population models capable of projecting populations into the future under different conditions. Within many populations, individuals vary in traits such as survival, age at maturity, and migration behavior that affect the variability in population abundance through time and how they respond to environmental conditions. In these cases, it may be necessary to develop more complex population models that account for this heterogeneity among individuals to inform conservation. Anadromous salmonids (*Salmonidae spp.*) face several threats that put populations at risk globally, and information is needed to make decisions about the allocation of resources for their conservation. They also commonly exhibit individual heterogeneity in life history traits like migratory behavior and habitat use within

freshwater, which are known to affect population dynamics and can affect population responses to management.

To inform salmon conservation, I developed and applied an integrated population model for Chinook salmon (*Oncorhynchus tshawytscha*) listed as Endangered under the Endangered Species Act, which spawn in the Wenatchee River Basin in Washington State. I first developed a model of the production of juveniles expressing different life history pathways (LHPs) of migration age from natal streams (Chapter 2) and used it to test hypotheses about drivers of the production of different LHPs. I developed a model of the survival and marine-return rates of fish between emigrating from their natal stream and returning to the Wenatchee River basin to spawn (Chapter 3) and examined how lifetime demographic rates varied among fish that had expressed different juvenile LHPs. Next, I combined the models of juvenile production and of subsequent survival and return rate, along with additional data, within a full integrated population model (Chapter 4) and projected the population into the future to assess its trajectory and examine how individual heterogeneity affects population stability. Finally, I worked with decision makers and scientific experts to develop management strategies for habitat restoration and hatcheries (Chapter 5), which I simulated the consequences of for the population.

TABLE OF CONTENTS

LIST OF FIGURES

No table of figures entries found.

LIST OF TABLES

Chapter 1. INTRODUCTION

1.1 BACKGROUND

To effectively manage threatened species, information is needed on population statuses and the effects of management actions on populations. This kind of information is often generated by fitting population models to data to project future trajectories in population abundance and risk of extinction (Beissinger and Westphal 1998) under future climate scenarios and management strategies. The accuracy and precision of such projections depend upon the information available in data or other forms of knowledge, model structures, and the way that information is harnessed to inform model parameter values (Zipkin and Saunders 2018).

Individual heterogeneity refers to variability in traits such as migration timing, survival, and age at maturity among individuals within a population, and can affect population trajectories in interesting and important ways (Forsythe et al. 2021). When population components with different traits respond differently to environmental variability such that their abundances vary asynchronously through time, the variability in the total population abundance is dampened, contributing to the viability of small populations and the sustainable provisioning of ecosystem services (Kendall and Fox 2002, Schindler et al. 2010). This is often referred to as the portfolio effect (Schindler et al. 2010). Another way that individual heterogeneity affects populations is when individuals use resources in diverse ways, reducing competition and allowing for larger population sizes (Werner and Gilliam 1984, Raffard et al. 2019). Individual heterogeneity provides the variability that natural selection acts on, so is critical to the ability of populations to adapt to changing environments over time (Hamel et al. 2018). Phenotypic plasticity also

contributes to individual heterogeneity and enables adaptation to variable environments (West-Eberhard 1989).

It may be advantageous to consider individual heterogeneity in population models used for conservation management (Plard et al. 2019). When fitting population models to data, accounting for individual heterogeneity may be necessary to meet model assumptions such as binomial variance in survival (Gimenez et al. 2018). Furthermore, considering heterogeneity in population models enables explicit accounting for different responses by diverse population components to environmental variability and management interventions, which may improve the accuracy of model predictions (Armstrong et al. 2021).

For population models to be most useful in informing decisions about the management of threatened species, alternative management strategies and metrics to evaluate them must be developed with decision makers and scientific experts (Nel et al. 2016, Cooke et al. 2021). Decision analysis provides a framework for collaboratively structuring conservation decision problems by defining the problem, identifying desired outcomes, and generating management alternatives to consider (Gregory et al. 2012, Runge et al. 2020). While the process of structuring a decision problem is sometimes sufficient to identify an optimal choice (Keeney 2004), in some cases population models may be needed to predict the effects of strategies in order to assess tradeoffs and select among alternatives (e.g., Servanty et al. 2014).

Anadromous salmonids, which use freshwater habitats for reproduction and saltwater habitats for rearing, face several threats that have led to the decline and extirpation of multiple populations globally (Nehlsen et al. 1991, Slaney et al. 1996, Gibson 2017). Some of the greatest threats include habitat degradation in rivers, including the damming of migration corridors, overharvest,

and the deleterious effects of introgression and competition with fish born in hatcheries (Hoekstra et al. 2007, Forseth et al. 2017). Given the tremendous importance of anadromous salmonids to people and ecosystems (National Research Council 1996, Hilderbrand et al. 1999, Ford et al. 2010), considerable resources are being devoted to conserve them and there are multiple actions available to do so. Consequently, information is needed to help allocate resources among alternative management strategies to best conserve these critically important fish (Newbold and Siikamäki 2009, Walsh et al. 2020, Fonner et al. 2021). Furthermore, salmon populations are known to exhibit individual heterogeneity in juvenile habitat use, age at return, and spawning location, which may be important considerations for assessing population statuses and predicting the effects of management interventions.

1.2 Research Objectives

I developed and applied a population model for an endangered populations of Chinook salmon (*Oncorhynchus tshawytscha*) that spawn in the Wenatchee River Basin of Washington State to evaluate its status and alternative management strategies to conserve it. I accounted for individual heterogeneity in the timing of juvenile emigration from natal streams, the return age of adults, and spawning location. Given the diversity of data sets considered, the complexity of the salmon life cycle, and need to work with decision makers on the analysis, I took a stepwise approach.

First, I tested the hypotheses that annual streamflow conditions and the density of spawners affects the production of juvenile salmon expressing different life history pathways (LHPs) in timing of emigration from natal streams (Chapter 2). I then assessed differences in lifetime demographic rates, including return-age probabilities, among fish that were born in different natal streams and that had expressed different LHPs as juveniles (Chapter 3). I next combined

models of the production of juveniles and their lifetime demographic rates developed in the second and third chapters respectively, along with additional data, within a full population model (Chapter 4). Finally, in Chapter 5, I worked with decision makers and scientific experts working on salmon management in the Wenatchee River Basin to develop management strategies, which I assessed the population outcomes of using a version of the model developed in Chapter 4.

1.3 Broader Impacts

My work provides insights into drivers of individual heterogeneity, the carryover effects of juvenile life history diversity on lifetime demographic rates, and the effects of heterogeneity on population dynamics. The models that I developed provide examples of ways to account for individual heterogeneity within population models, including density dependence in the production of alternative life LHPs and synchronous and asynchronous variability in demographic rates through time among fish that express different LHPs. The results of my final chapter can be used by decision makers in the Wenatchee River Basin to assess tradeoffs among alternative management strategies and to guide the development of new strategies. The modeling framework that I developed can be used to assess the outcomes of additional management strategies in the future.

1.4 REFERENCES

Armstrong, D. P., E. H. Parlato, and P. G. H. Frost. 2021. Incorporating individual variation in survival, reproduction and detection rates when projecting dynamics of small populations. Ecological Modelling 455:109647.

Beissinger, S. R., and M. I. Westphal. 1998. On the use of demographic models of population viability in endangered species management. The Journal of wildlife management:821–841.

Cooke, S. J., V. M. Nguyen, J. M. Chapman, A. J. Reid, S. J. Landsman, N. Young, S. G. Hinch, S. Schott, N. E. Mandrak, and C. A. D. Semeniuk. 2021. Knowledge co-production: A pathway to effective fisheries management, conservation, and governance. Fisheries 46:89–97.

Fonner, R., J. Honea, J. C. Jorgensen, M. Plummer, and M. McClure. 2021. Considering intervention intensity in habitat restoration planning: An application to Pacific salmon. Journal of Environmental Management 299:113536.

Ford, J. K. B., G. M. Ellis, P. F. Olesiuk, and K. C. Balcomb. 2010. Linking killer whale survival and prey abundance: food limitation in the oceans' apex predator? Biology Letters 6:139–142.

Forseth, T., B. T. Barlaup, B. Finstad, P. Fiske, H. Gjøsæter, M. Falkegård, A. Hindar, T. A. Mo, A. H. Rikardsen, E. B. Thorstad, and others. 2017. The major threats to Atlantic salmon in Norway. ICES Journal of Marine Science 74:1496–1513.

Forsythe, A. B., T. Day, and W. A. Nelson. 2021. Demystifying individual heterogeneity. Ecology Letters 24:2282–2297.

Gibson, R. J. 2017. Salient needs for conservation of Atlantic Salmon. Fisheries 42:163–174.

Gimenez, O., E. Cam, and J.-M. Gaillard. 2018. Individual heterogeneity and capture–recapture models: what, why and how? Oikos 127:664–686.

Gregory, R., L. Failing, M. Harstone, G. Long, T. McDaniels, and D. Ohlson. 2012. Structured decision making: a practical guide to environmental management choices. John Wiley & Sons, Incorporated, Hoboken, UNITED KINGDOM.

Hamel, S., J.-M. Gaillard, and N. Yoccoz. 2018. Introduction to: Individual heterogeneity – the causes and consequences of a fundamental biological process. Oikos 127:643–647.

Hilderbrand, G. V., C. C. Schwartz, C. T. Robbins, M. E. Jacoby, T. A. Hanley, S. M. Arthur, and C. Servheen. 1999. The importance of meat, particularly salmon, to body size, population productivity, and conservation of North American brown bears. Canadian Journal of Zoology 77:132–138.

Hoekstra, J. M., K. K. Bartz, M. H. Ruckelshaus, J. M. Moslemi, and T. K. Harms. 2007. Quantitative Threat Analysis for Management of an Imperiled Species: Chinook Salmon (oncorhynchus Tshawytscha). Ecological Applications 17:2061–2073.

Keeney, R. L. 2004. Making Better Decision Makers. Decision Analysis 1:193–204.

Kendall, B. E., and G. A. Fox. 2002. Variation among Individuals and Reduced Demographic Stochasticity. Conservation Biology 16:109–116.

National Research Council. 1996. Upstream: salmon and society in the Pacific Northwest. National Academies Press.

Nehlsen, W., J. E. Williams, and J. A. Lichatowich. 1991. Pacific salmon at the crossroads: stocks at risk from California, Oregon, Idaho, and Washington. Fisheries 16:18.

Nel, J. L., D. J. Roux, A. Driver, L. Hill, A. C. Maherry, K. Snaddon, C. R. Petersen, L. B. Smith-Adao, H. Van Deventer, and B. Reyers. 2016. Knowledge co-production and boundary work to promote implementation of conservation plans. Conservation Biology 30:176–188.

Newbold, S. C., and J. Siikamäki. 2009. Prioritizing conservation activities using reserve site selection methods and population viability analysis. Ecological Applications 19:1774–1790.

Plard, F., R. Fay, M. Kéry, A. Cohas, and M. Schaub. 2019. Integrated population models: powerful methods to embed individual processes in population dynamics models. Ecology 100:e02715.

Raffard, A., F. Santoul, J. Cucherousset, and S. Blanchet. 2019. The community and ecosystem consequences of intraspecific diversity: a meta-analysis. Biological Reviews 94:648–661.

Runge, M. C., S. J. Converse, J. E. Lyons, and D. R. Smith. 2020. Structured Decision Making: Case Studies in Natural Resource Management. Johns Hopkins University Press, Baltimore.

Schindler, D. E., R. Hilborn, B. Chasco, C. P. Boatright, T. P. Quinn, L. A. Rogers, and M. S. Webster. 2010. Population diversity and the portfolio effect in an exploited species. Nature 465:609–612.

Servanty, S., S. J. Converse, and L. L. Bailey. 2014. Demography of a reintroduced population: moving toward management models for an endangered species, the Whooping Crane. Ecological Applications 24:927–937.

Slaney, T. L., K. D. Hyatt, T. G. Northcote, and R. J. Fielden. 1996. Status of Anadromous Salmon and Trout in British Columbia and Yukon. Fisheries 21:20–35.

Walsh, J. C., K. Connors, E. Hertz, L. Kehoe, T. G. Martin, B. Connors, M. J. Bradford, C. Freshwater, A. Frid, J. Halverson, J. W. Moore, M. H. H. Price, and J. D. Reynolds. 2020. Prioritizing conservation actions for Pacific salmon in Canada. Journal of Applied Ecology 57:1688–1699.

Werner, E. E., and J. F. Gilliam. 1984. The ontogenetic niche and species interactions in size-structured populations. Annual review of ecology and systematics 15:393–425.

West-Eberhard, M. J. 1989. Phenotypic plasticity and the origins of diversity. Annual review of Ecology and Systematics:249–278.

Zipkin, E. F., and S. P. Saunders. 2018. Synthesizing multiple data types for biological conservation using integrated population models. Biological Conservation 217:240–250.

Chapter 2. EFFECTS OF POPULATION DENSITY AND ENVIRONMENTAL CONDITIONS ON LIFE-HISTORY EXPRESSION IN A MIGRATORY FISH

Publication history: This study was co-authored with Andrew R. Murdoch, Richard W. Zabel, Cory M. Kamphaus, Eric R. Buhle, Mark D. Scheuerell, and Sarah J. Converse. At the time this dissertation was published, this chapter was not in review with a journal.

Open research statement: All data and code are available at https://github.com/Quantitative-Conservation-Lab/Wenatchee-screw-traps.

Abstract: Individual variation in life-history traits can have important implications for the ability of populations to respond to environmental variability and change. In migratory animals, flexibility in the timing of life-history events, such as juvenile emigration from natal areas, can influence the effects of population density and environmental conditions on population dynamics. We evaluated the functional relationships between population density and environmental covariates and the abundance of juveniles expressing different life-history pathways in a migratory fish, Chinook salmon (Oncorhynchus tshawytscha), in a river basin in Washington State, USA. We found that the abundance of younger emigrants from natal streams was best described by an accelerating or near-linear function of spawners, whereas the abundance of older emigrants was best described by a decelerating function of spawners. This supports the hypothesis that emigration timing varies in response to density in natal areas, with younger-emigrating life-history pathways comprising a larger proportion of emigrants when densities of conspecifics are high. We also observed positive relationships between winter stream

discharge and abundance of younger emigrants, supporting the hypothesis that habitat conditions can also influence the expression of different life-history pathways. Our results suggest that early emigration, and a resultant increase in the use of downstream rearing habitats, may increase if winter precipitation increases in the future as is projected due to climate warming. Characterizing relationships between life-history expression and environmental conditions is a necessary first step in understanding the dynamics of species with diverse life-history strategies. As environmental conditions change – due to climate change, management, or other factors – resultant life-history changes are likely to have important demographic implications that will be challenging to predict if life-history diversity is not accounted for in population models.

Keywords: Chinook salmon; density dependence; dispersal; individual heterogeneity; life-history diversity; migration; reproduction

2.1 INTRODUCTION

Genetic, ontogenetic, and behavioral factors interact to shape the expression of life-history traits, such as the timing of breeding and migration (Stearns 1976). Within a population, variation in life-history traits may allow individuals to exploit different niche spaces, thus reducing resource competition and expanding the total niche space exploited by a population (Raffard et al. 2019). This expansion can render populations more capable of coping with environmental variability and change (Conner and White 1999). Furthermore, variability in life-history traits leads to variability in demographic responses to fluctuating environmental conditions, which dampens the variability in populations over time (Schindler et al. 2010).

In migratory animals, individual variability in migratory behavior can mediate the effects of population density and environmental variability on population dynamics (Phillips et al. 2017). Individuals may exhibit variable timing of migration (Brown et al. 2021b) and some individuals

may not migrate at all (Martin et al. 2022). This variability is thought to be influenced by both genetic and environmental factors (Liedvogel et al. 2011, Laforge et al. 2021). In the face of substantial environmental change, diversity and flexibility in migratory behavior may have important implications for species viability (Senner et al. 2020).

Anadromous fish migrate between freshwater spawning habitat and saltwater habitat. These species exhibit considerable diversity in life-history traits as related to the age and extent of downstream and upstream migrations throughout their lives (Thorpe et al. 1998, Bourret et al. 2016). Multiple juvenile life-history pathways (LHPs), defined by use of different freshwater rearing habitats (e.g., natal streams, downstream areas, and lentic habitats) at different times of year and for different durations prior to seaward migration are expressed within species and populations of anadromous salmonids (Bourret et al. 2016). Among anadromous salmonids, diversity in the duration of freshwater and marine residency is negatively associated with variation in population abundance and positively associated with long-term population growth (Greene et al. 2010, Moore et al. 2014). Understanding the factors regulating production of alternative juvenile LHPs in anadromous species is necessary for an understanding of population dynamics.

We hypothesized that the production of juvenile anadromous salmonids exhibiting different LHPs, corresponding to different ages of migration from natal areas, varies in response to the density of conspecifics. Juvenile salmon productivity commonly exhibits density dependence (Einum et al. 2006, Walters et al. 2013). We predicted that we would detect positive density dependence in the production of younger-emigrating LHPs because more individuals should emigrate earlier in the presence of a larger number of conspecifics. We predicted that we would find evidence for negative density dependence in the production of older-emigrating LHPs

because density-dependent emigration from the natal stream and density-dependent mortality within the natal stream should reduce the number of individuals available to emigrate at older ages.

We also hypothesized that the production of different LHPs varies in response to critical environmental drivers. Streamflow has been identified as a driver of juvenile salmon productivity (Apgar et al. 2021), and we hypothesized that flow conditions would affect the production of alternative LHPs. If particular flow conditions are advantageous for growth and survival within natal habitat, fish may respond by choosing to remain for longer, and the number of surviving residents may increase. Furthermore, flow may be a proximate trigger for migration, or may be directly related to a proximate trigger such as growth rate.

We evaluated evidence for our hypotheses by examining relationships between population density, flow patterns, and the abundance of juvenile emigrants across four LHPs that we identified in a semelparous anadromous fish, Chinook salmon (*Oncorhynchus tshawytscha*), in a river basin in Washington State, USA. We found support for our hypotheses that density and flow affect the production of alternative LHPs. Our findings have implications for density-dependent habitat use and population regulation, as well as population responses to environmental variability and change.

2.2 METHODS

2.2.1 *Study System*

The Wenatchee River is a tributary of the Columbia River (river kilometer, rkm, 754) located in Washington State (Figure 2.1), with a drainage area of roughly 3,400 km^2. The Wenatchee River basin supports a population of endangered Chinook salmon that is one of three populations

within the Upper Columbia River Evolutionarily Significant Unit (ESU), one of 49 conservation units considered under the U.S. Endangered Species Act (ESA). Spawning occurs in August–September and juveniles emerge from nests (redds) in winter. Juveniles exhibit a stream-type life history, rearing within the Wenatchee River basin before emigrating to the marine environment in spring just over one year after eggs hatch. While there is little variability in the age of seaward migration, there is individual heterogeneity in age of emigration from natal streams, with some juveniles emigrating at younger ages to rear downstream prior to seaward emigration and others remaining in the natal stream until seaward emigration (Buchanan et al. 2015).

Spawning occurs in five areas in the basin — the Chiwawa River, Nason Creek, the White River, the Little Wenatchee River, and the upper section of the mainstem Wenatchee River below Lake Wenatchee (Figure 2.1). We focused our analysis on monitoring data from three tributaries—the Chiwawa River, Nason Creek, and the White River. The hydrographs in the spawning streams are characterized by a substantial snowmelt-driven spring freshet from April through July followed by summer low flows in August–September and a rainy season from October through December (Appendix S1: Figure S1). Peak water temperatures occur from July through September.

2.2.2 *Data*

Juvenile data — Juvenile outmigrants were monitored with rotary screw traps operated near the mouth of the Chiwawa River (rkm 0.6) in 1997–2018, Nason Creek (rkm 1) in 2004–2018, and the White River (rkm 9) in 2006–2018 (Hillman et al. 2020). Traps were installed in early spring once ice in the river had melted, typically in early March, and were operated as continuously as possible until the river began to freeze again, typically in late November. Outages occurred

periodically during the trapping season due to technical difficulties such as debris jamming the trap, very high discharges, or large releases of hatchery juveniles.

There were two components of the data collected at the rotary screw traps by the Washington Department of Fish and Wildlife and Yakama Nation Fisheries. The first component was the daily numbers of fish captured. During the spring, the traps captured both yearlings en route to the ocean and recently emerged subyearlings (i.e., alevin or fry), while in summer and fall, only subyearlings (i.e., parr) were captured. Subyearlings and yearlings were differentiated in spring based on length and date of capture (Appendix S2). The second component of the trap data was from mark-recapture experiments that were conducted on several days each year to assess capture probabilities in each trap. In these experiments, captured fish >60 mm were marked with passive integrated transponder (PIT) tags and released 0.8–2.6 km upstream of the traps (Hillman et al. 2020). Fish <60 mm, which included most of the subyearling emigrants in spring and a portion of subyearling emigrants in summer, were not large enough to be safely tagged. The numbers of fish released upstream of the traps and the numbers of fish that were recaptured at the traps within 4 days of release were recorded.

Spawner data — The annual abundances of female spawners were estimated by walking spawning streams and counting redds (Hillman et al. 2020). Streams were surveyed every 7–10 days from late July through September, and redds were geo-referenced to avoid double-counting. All known Chinook salmon spawning habitat was surveyed by Washington Department of Fish and Wildlife and Chelan County Public Utility District.

Discharge data — We downloaded daily average stream discharge recorded at the U.S. Geological Survey's Chiwawa River gauge using the *dataRetrieval* package in R (Hirsch et al.

2015). Daily average discharge in Nason Creek and the White River were recorded at Washington Department of Ecology stream gauges (Washington Department of Ecology 2020).

2.2.3 *Modeling framework*

Evaluating environmental effects on juvenile abundance and LHP expression required three steps: 1) estimation of the daily abundance of juvenile emigrants past rotary screw traps, 2) summation of daily emigrant abundances within discrete LHPs delineated based on modes in the time series of average daily emigrants, and 3) fitting models of the annual abundance of each LHP in each stream as a function of spawner abundance and other environmental factors.

2.2.4 *Model of daily juvenile emigrants*

Process component — We modeled the daily abundance of yearling and subyearling emigrants separately, due to the break in the catch data during winter. We also modeled abundance in each natal stream separately because fish behavior and trap efficiency differed among them. We modeled the partially observed true number of daily emigrants $m_{t,y,s,a}$ on day t, year y, stream s, and age a on the log scale (so that abundance remained positive) as a function of a year-specific average, $\mu^{m}_{y,s,a}$, the average day-to-day variation in log emigrant abundance across years, $\delta^{m}_{t,s,a}$, and year-specific daily deviations around those averages, $\epsilon^{m}_{t,y,s,a}$,

$$\log(m_{t,y,s,a}) = \mu^{m}_{y,s,a} + \delta^{m}_{t,s,a} + \epsilon^{m}_{t,y,s,a}. \quad (1)$$

Because the across-year average daily errors, $\delta^{m}_{t,s,a}$, represented seasonality in emigration, which we assumed would be a non-stationary process, we modeled them as a random walk, $\delta^{m}_{0,s,a} = 0$, $\delta^{m}_{t,s,a} \sim \mathrm{N}(\delta^{m}_{t-1,s,a}, \sigma^{\delta}_{s,a})$. In contrast, the year-specific daily errors, $\epsilon_{t,y,s,a}$, represent variation

around the average, which we assumed would be stationary. We therefore modeled them as a stationary first order autoregressive process,

$$\epsilon^{m}_{0,y,s,a} \sim \mathrm{N}\left[0, \sqrt{\frac{\sigma^{\epsilon}_{s,a}}{1-{\rho^{\epsilon}_{s,a}}^{2}}}\right] \qquad (2)$$

$$\epsilon^{m}_{t,y,s,a} = \rho^{\epsilon}\, \epsilon^{m}_{t-1,y,s,a} + \lambda_{t,y,s,a}, \quad \lambda_{t,y,s,a} \sim N(0, \sigma^{\epsilon}_{s,a})$$

with autocorrelation coefficient $\rho^{\epsilon}_{s,a}$ and innovation standard deviation $\sigma^{\epsilon}_{s,a}$.

Observation component — Observed catches $c_{t,y,s,a}$ were assumed to follow a negative binomial distribution, which allows for greater observation error than a Poisson distribution. The expected value of daily catch, $\mu^{c}_{t,y,s,a}$, was equal to the product of the latent daily emigrant abundance and the daily capture probability, $\mu^{c}_{t,y,s,a} = m_{t,y,s,a}\, p_{t,y,s,a}$, with variance equal to $\mu^{c}_{t,y,s,a} + \frac{{\mu^{c}_{t,y,s,a}}^{2}}{\phi_{s,a}}$, which was restricted to be positive and was assumed to be constant across years.

The capture probability of fish emigrating past a trap was modeled on the logit scale as a function of daily discharge:

$$\mathrm{logit}(p_{t,y,s,a}) = \iota_{y,s,a} + \kappa_{y,s,a} D_{t,y,s,a} + \nu_{w(t),s,a} + \xi_{w(t),y,s,a}, \qquad (3)$$

where $\iota_{y,s,a} \sim \mathrm{N}(\beta^{p}_{0,s,a}, \sigma^{\iota}_{s,a})$ is a random intercept for each year, $\kappa_{y} \sim \mathrm{N}(\beta^{p}_{1,s,a}, \sigma^{\kappa}_{s,a})$ is a random effect of Z-scored daily stream discharge ($D_{t,y,s,a}$) in each year, $\nu_{w(t),s,a} \sim \mathrm{N}(0, \sigma^{\nu}_{s,a})$ is a random effect of week (w) that is common across years, and $\xi_{w(t),y,s,a} \sim \mathrm{N}(0, \sigma^{\xi}_{s,a})$ is a random effect of week specific to each year.

The capture probability, $p_{t,y,s,a}$, was informed by the mark-recapture dataset. The number of fish recaptured $k_{t,y,s,a}$ out of the number of marked fish released upstream of the trap $n_{t,y,s,a}$ was assumed to be binomially distributed, $k_{t,y,s,a} \sim \text{Bin}(n_{t,y,s,a}, p_{t,y,s,a})$, with capture probability $p_{t,y,s,a}$. We modeled the capture probability at the screw trap of all marked fish released upstream of the trap based on stream discharge on the day of release. While fish were recaptured up to four days after release, and these fish could have experienced some variability in daily stream discharge between release and recapture, 91.5% of recaptured fish were recaptured on the date that they were released. Therefore, while our assumption may induce some bias in our estimates, this bias is expected to be small, and the simplifying assumption was made to reduce model complexity. We assumed that all fish of a given age and stream had the same capture probabilities on a given day, including those that were too small to be safely tagged.

2.2.1 *Juvenile life-history delineation*

The average time series of the (partially observed) daily emigrant abundances across streams and brood years contained four modes, indicating that emigrants could be categorized into four alternative LHPs of emigration timing from natal streams (Figure 2.2). To delineate the LHPs, we fit a four-component normal mixture distribution to the time series of emigrant abundances, rounded to the nearest integer, from each brood across all years and natal streams using the package mixtools in the R statistical environment (Benaglia et al. 2009, R Core Team 2021). We then determined the days of the year corresponding to local minima between the modes of the mixture distribution components, which were used as cutoffs to delineate the four windows of emigration corresponding to alternative LHPs. Thus, it was assumed that the emigration time windows that defined the LHPs were the same across streams and years. Daily emigrant

abundances were summed within periods to calculate the total number of emigrants ($M_{h,y,s}$) from brood year *y* and stream *s* expressing LHP *h*,

$$M_{h,y,s} = \sum_{t=t_{0,h}}^{t_{f,h}} m_{t,y,s,a}, \quad (4)$$

where $t_{0,h}$ was the first day of the time window corresponding with LHP h and $t_{f,h}$ was the final day. We assumed there was no emigration during the winter period when traps were never operated. While this leads to underestimation of emigrant abundances, we expected the number of emigrants in winter to be relatively small, considering the relatively small number of emigrants observed in late fall prior to trap removal and in early spring just after trap installation.

2.2.2 *Spawner to juvenile emigrant model*

Process component — To model the relationship between the abundance of female spawners and juvenile emigrants in the final step of our analysis, we fit the Myers et al. (1995) version of the classic Beverton-Holt model, which can simultaneously describe positive and negative density dependence,

$$J_{h,y,s} = \frac{\alpha_{h,s} S_{y(h),s}^{\gamma_{h,s}}}{1+\frac{\alpha_{h,s} S_{y(h),s}^{\gamma_{h,s}}}{J_{h,s}^{\max}}} \exp\left(\epsilon_{h,y,s}^{J}\right), \quad (5)$$

where $J_{h,y,s}$ is the abundance of juvenile emigrants expressing LHP *h* produced by female spawners $S_{y(h),s}$ in year $y(h)$, which is one year previous to the emigration year for subyearling emigrants and two years previous for yearling emigrants, and stream *s*. Note that $J_{h,y,s}$ is in theory the same quantity as $M_{h,y,s}$ from the model of daily juvenile abundances. However, we fit the models separately, developing log-normal distributions of $M_{h,y,s}$ with a parametric bootstrap of the model of daily juvenile abundances and using it as a penalty in the spawner-recruit model (see "Observation component" below). Spawner and juvenile abundance were scaled by the

length (km) of spawning habitat in each stream to facilitate comparison across streams. In the modified Beverton-Holt model, $\alpha_{h,s}$ cannot be interpreted as the maximum productivity, as it can in the classic Beverton-Holt, whereas $J_{h,s}^{\max}$ retains its interpretation as the maximum expected juvenile emigrant abundance. The generalized model includes positive density dependence when $\gamma_{h,s}$ >1.0 and negative density dependence when $\gamma_{h,s}$ <1.0. We allowed for multiplicative log-normal residual error $\epsilon_{h,y,s}^{J}$, which we modeled using a latent variable model described below.

The three shape parameters of the modified Beverton-Holt model (Equation 5) were not well informed by the data for all LHPs and streams, so we modeled them hierarchically across streams for each LHP. We modeled $\alpha_{h,s}$, $\gamma_{h,s}$, and $J_{h,s}^{\max}$ hierarchically such that $\alpha_{h,s} \sim \text{logNormal}(\mu_h^{\alpha}, \sigma_h^{\alpha})$, with equivalent expressions for $\gamma_{h,s}$ and $J_{h,s}^{\max}$. Because there were only three streams available to estimate the hyperdistribution standard deviations, σ_h^{α}, we applied exponential regularizing penalties [e.g., $\sigma_h^{\alpha} \sim exp(\lambda)$] (Simpson et al. 2017). We applied the same amount of penalization (i.e., common λ) for the three different parameters and four LHPs.

To make inference about density dependence, we penalized deviations of the log means of the hyperdistributions of $\gamma_{h,s}$ and $J_{h,s}^{\max}$ from values that would result in density-independent production. The modified Beverton-Holt model simplifies to a density-independent model when $\gamma = 1$ and $J^{\max} \to \infty$. Therefore, we applied the following penalties on the log means of the hyperdistributions of these parameters:

$$\mu_h^{\gamma} \sim N\left(0, \tau_h^{\gamma}\right), \quad \tau_h^{\gamma} \sim \exp(\lambda^{\gamma}), \tag{6}$$

$$\mu_h^{J^{\max}} \sim N\left(\log\left(\nu^{J^{\max}}\right), \tau_h^{J^{\max}}\right), \quad \tau_h^{J^{\max}} \sim \exp\left(\lambda^{J^{\max}}\right)$$

which puts weight on a model with minimal density dependence when $\nu^{J^{\max}}$ is large. We set $\nu^{J^{\max}}$ at 1.5e4, which was greater than the upper limit of the 95% confidence interval of the largest observed abundance of emigrants in the dataset (1.26e4). We applied the same penalty rates (i.e., $\lambda^{\gamma}$and $\lambda^{J^{\max}}$) for all LHPs.

We allowed for correlated process errors to account for the structural relationship whereby the number of emigrants expressing each LHP will affect the number of juveniles available to emigrate in subsequent periods. Correlated errors also account for variability in survival within the natal stream affecting the abundance of multiple LHPs. To do so, residual process errors $\epsilon^{J}_{h,y,s}$, were modeled using a latent variable model (Warton et al 2015),

$$\epsilon^{J}_{h,y,s} = \boldsymbol{x}'_{h,y,s}\boldsymbol{\beta}^{\epsilon}_{h} + \omega_{y} l_{h,s} + \eta_{h,y,s}, \quad (7)$$

where $\boldsymbol{x}_{h,y,s}$ are environmental covariates, $\boldsymbol{\beta}^{\epsilon}_{h}$ are regression coefficients, $\omega_y \sim \mathrm{N}(0,1)$ is a latent variable, $l_{h,s}$ are life-history- and stream-specific coefficients for the latent variable (i.e., a factor loading), and $\eta_{h,y,s} \sim \mathrm{N}(0, \sigma^{\eta}_{h,s})$ is an idiosyncratic error. We placed a regularizing penalty on the idiosyncratic error standard deviations, $\sigma^{\eta}_{h,s} \sim exp(\lambda^{\eta})$, to help with convergence.

To assess how interannual variability in flow patterns affected survival and movement, we evaluated the effect of stream discharge on process errors (Equation 7). We included the log maximum of daily average stream discharge within each stream during a brood year's first winter (November–February) as a covariate on process errors in the production of each LHP. The mean of daily discharge during summer (June–September) was included as a covariate on each LHP except spring subyearling emigrants, which emigrate before summer. Finally, we included log maximum winter discharge during the second winter of a year class as a covariate on the spring yearling LHP only. Relationships between process errors and environmental

covariates ($\boldsymbol{\beta}_h^{\epsilon}$) were assumed to be the same for a given LHP across streams. That is, we assumed that deviations from average discharge within a given stream affected fish expressing a specific LHP in the same way across streams. We *Z*-scored the discharge covariates for each stream using the stream-specific mean and standard deviation, such that we were modeling the effects of standardized annual deviations from within-stream average discharge.

Observation component — For computational efficiency, the models of daily juvenile abundance (informed by screw-trap data) and the spawner-recruit models (informed by the summed estimates of juvenile abundance) were fitted in two stages. Data on the abundance of juvenile emigrants and spawners entered the likelihood as log-normal penalties. The estimates of log-mean emigrant abundance for a given LHP, stream, and brood year, $\overline{M^*_{h,y,s}}$, were developed from the model of daily juvenile emigrants via a parametric bootstrap described below, and were assumed to be normally distributed around the log of the latent emigrant abundance in the model of LHP abundance (Equation 5),

$$\overline{M^*_{h,y,s}} \sim \mathrm{N}\left(\log(J_{h,y,s}), \sigma^{\overline{M^*}}_{h,y,s}\right), \quad (8)$$

with observation error $\sigma^{\overline{M^*}}_{h,y,s}$ equal to the standard deviation from the parametric bootstrap of the daily juvenile abundance model.

To conduct the parametric bootstrap, we drew 10,000 parameter sets from a multivariate normal distribution defined by maximum likelihood estimates of parameters and their covariance matrix obtained by inversion of the Hessian matrix calculated using Template Model Builder (TMB) (Kristensen et al. 2016) in R. For each bootstrap sample, we calculated values of $M_{h,y,s}$ using Equations 1 and 4, and calculated their log-mean, $\overline{M^*_{h,y,s}}$, and log-standard deviation, $\sigma^{\overline{M^*}}_{h,y,s}$.

The observed redd counts were assumed to be log-normally distributed around the true female spawner abundances, with standard deviation equal to 0.1 :

$$S_{y,s}^{obs} \sim \text{logNormal}\left(log(S_{y,s}),\ 0.1\right). \quad (6)$$

The observation standard deviation of 0.1 was chosen based on information from Murdoch et al. (2019) and equates to a coefficient of variation of approximately 10%.

2.2.3 *Parameter estimation*

Parameters in all models were estimated using a mixed-effects framework. Specifically, parameters were estimated by expectation maximization where marginal likelihoods were calculated by TMB using Laplace approximation to integrate over random effects. Optimization was carried out using the *TMBhelper* package in R (Thorson 2020). The daily errors δ_t^m and $\epsilon_{t,y}^m$ in the daily-emigrant model, and $\iota_y,\ \kappa_y, \nu_{w(t)}$ and $\xi_{w(t,y)}$ in the capture-probability model were treated as random effects. The fixed effects were $\mu_y^m, \rho^\epsilon, \sigma^\epsilon$ and σ^δ in the daily-emigrant model and $\boldsymbol{\beta}^p, \sigma^\nu, \sigma^\xi,$ and ϕ in the observation model. In the spawner-recruit model, the log-transformed spawner abundances $\log(S_{y,s})$, latent variables ω_y, idiosyncratic errors $\eta_{h,y,s}$, log means of the shape-parameter hyperdistributions μ_h^γ and $\mu_h^{J^{\max}}$, and stream-specific shape parameters $\alpha_{h,s}, \gamma_{h,s},$ and $J^{\max}{}_{h,s}$ were treated as random effects. The fixed effects were μ_h^α, $\sigma_h^\alpha, \sigma_h^\gamma, \sigma_h^{J^{\max}}, \lambda, \tau_h^\gamma, \tau_h^{J^{\max}}, \lambda^\gamma, \lambda^{J^{\max}}, \boldsymbol{\beta}_h^\epsilon, l_{h,a}, \sigma_{h,s}^\eta,$ and λ^η .

2.3 RESULTS

Across streams and years, there were four largely distinct modes of juvenile emigration from each brood, although certain modes were less pronounced in individual streams (Figure 2.2). These four modes included: (1) subyearling emigrants during the ascending limb of the spring

freshet in March–April (hereafter *spring subyearlings*), (2) subyearling emigrants in May–September as flows were declining and water temperatures increasing (*summer subyearlings*), (3) subyearling emigrants from October-November coinciding with decreasing water temperature and rain-driven increases in discharge (*fall subyearlings*), and (4) yearlings emigrating in March–June, on the ascending limb of the spring freshet (*spring yearlings*) en route to the marine environment.

Based on estimates of the γ and J^{max} parameters, there was evidence of positive density dependence in the production of spring subyearling production and to a lesser degree in summer subyearling production (Figure 2.3, Table A1). There was little evidence of negative density dependence in either of these LHPs. The mean γ parameter for spring subyearlings was 1.51 (95% CI = 1.03, 2.23), suggesting positive density dependence. All three streams had mean γ values that were greater than one, but confidence intervals overlapped one in two of three streams (Table A1). For summer subyearling emigrants, the mean γ parameter was 1.09 (0.80, 1.47), providing little evidence of density dependence. The γ parameters for summer subyearlings suggested positive density dependence in one stream, but not in the other two (Table A1). In all streams, the J^{max} parameters for spring and summer subyearlings were similar to the expectation based on the penalty, providing no evidence of negative density dependence.

Negative density dependence was evident in fall subyearling and spring yearling emigrants, whereas there was little evidence of positive density dependence (Figure 2.3). The mean estimate of γ for fall subyearlings was 1.03 (0.73, 1.45), providing little evidence of density dependence. However, the mean estimate of J^{max} for fall subyearlings was only 1,480 (597, 3,706), much less than expected based on the penalty, suggesting negative density dependence. For spring yearling emigrants, negative density dependence was evident based on the average γ parameter of 0.37

(0.17, 0.79). As a result of the positive density dependence in younger-emigrating LHPs, and negative density dependence in older-emigrating LHPs, younger-emigrants comprised a greater proportion of all emigrants as spawner density increased (Figure A2).

The three streams differed in their total productivity and in the proportions of each LHP that they produced (Figure A2). The Chiwawa River produced the most emigrants per spawner, whereas the White River produced the fewest. Spring yearling emigrants made up a larger proportion of emigrants from the Chiwawa and White Rivers compared to Nason Creek, whereas Nason Creek produced higher proportions of fall subyearling emigrants.

Effects of stream discharge on process errors in abundance were variable among LHPs (Figure A3). Maximum daily stream discharge during each brood year's first winter was positively associated with process errors in the abundance of spring (0.37; 0.04, 0.69) and summer (0.10; -0.03, 0.23) subyearling emigrants, and negatively associated with the abundance of fall subyearling (-0.13; -0.28, 0.02) and spring yearling (-0.22; -0.37, -0.08) emigrants. Average stream discharge during the summer was negatively associated with process error in fall subyearling emigrant abundance (-0.14; -0.33, 0.04).

2.4 DISCUSSION

We tested the hypothesis that population density influences the relative expression of alternative LHPs in an anadromous salmonid and found support for this hypothesis. We found evidence of positive density dependence in the production of younger emigrants and negative density dependence in the production of older emigrants. This suggests that some combination of negative density-dependent survival and positive density-dependent emigration occurs in natal streams, resulting in a greater proportion of younger emigrants as population size increases. Our evidence for negative density dependence in older emigrants and positive density dependence in

younger emigrants is consistent with previous studies of juvenile salmon (Einum et al. 2006, Walters et al. 2013, Thorson et al. 2014, Apgar et al. 2021). As the proportions of younger emigrants increase at higher population densities, the fate of younger emigrants should have a greater effect on overall population productivity. Furthermore, because younger emigrants spend more time rearing in downstream habitats, survival in downstream habitats should have a greater effect on population productivity as population densities increase.

We also found support for the hypothesis that environmental factors affect the production of alternative LHPs. We found evidence that the abundance of younger emigrants was positively associated with stream flow during their first winter, prior to when most individuals emerge from the gravel, whereas the abundance of older emigrants was negatively associated with first-winter stream flow. Higher winter flows are associated with warmer winters (Mantua et al. 2010), which are in turn associated with earlier emergence and faster growth rates in juvenile salmonids (Beer and Steel 2018). Fast growth at very young ages has been shown to induce dispersal at younger ages (Bradford and Taylor 1997), which may have driven the pattern that we observed. Winter temperature and discharge are projected to increase with climate change (Mantua et al. 2010), suggesting that younger emigrating LHPs may comprise a greater proportion of total emigrants in the future, based on the observed relationship between winter discharge and process errors.

We also found that summer stream flow was negatively associated with the production of fall subyearling emigrants. One explanation is that higher summer flows are associated with greater snowpack and lower stream temperatures (Mantua et al. 2010), which generally decrease growth rates and may negatively affect the propensity of individuals to disperse from the natal stream in fall (Bradford and Taylor 1997). Nason Creek had warmer average summer temperatures (Isaak

et al. 2016) and produced higher proportions of fall subyearling emigrants relative to the Chiwawa River and White River. Snowpack is projected to decrease and summer stream temperatures to increase in the future (Mantua et al. 2010), which could lead to increased expression of the fall subyearling LHP.

With the data available, we were not able to separate survival and emigration, which simultaneously contribute to the abundance of each LHP. Separating these processes would require direct information on survival within natal streams across time. Therefore, our model is not mechanistic in modeling the multiple demographic processes that generate emigrant abundances. Rather, our model of the emergent patterns provides insights into possible survival and emigration dynamics and has value for understanding drivers of population dynamics and population responses to environmental change.

This study furthers our understanding of how population density affects life-history variability within populations. Similar to our finding that early migration increases at higher densities, Martin et al. (2022) found that a partially migratory population of elk conformed to Ideal Free Distribution theory, where animals select habitats that maximize individual fitness. According to this theory, as densities in the natal stream increase, juvenile salmonids should increasingly select habitats with lower densities to access the resources they need for growth prior to migration. Beyond migration, population density has been shown to affect many other life-history traits that exhibit intraspecific variation, including growth rate, age at first reproduction, and birth rate (Frances et al. 2021). In addition to density dependence, interspecific predatory (Kvile et al. 2021) and competitive (Montorio et al. 2018) interactions can also affect life-history trait expression. Furthermore, the effects of population density on life-history traits can be mediated by environmental factors (Brown et al. 2021, Diez et al. 2021), and the effects

of environmental drivers on life-history traits may increase near carrying capacity (Jesmer et al. 2021).

Environmental variability is also recognized as an influence on life-history variability in a variety of taxa. Lundblad and Conway (2021) found that nest microclimate drove tradeoffs between clutch size, timing of incubation, hatch synchrony, and offspring survival, which helped explain intraspecific diversity in avian life histories. Luevano et al. (2022) found that the occurrence of hurricanes during early life delayed reproductive debut but was associated with higher mean fertility during prime reproductive years for individuals within a population of rhesus macaques (*Macaca mulatta*). In plants, gradients in light availability, soil PH, and herbivore pressure across the landscape are associated with variation in growth, survival, and herbivore resistance among individuals (Hahn and Maron 2016, Jansen et al. 2017). As a result of the interaction between environmental factors and life-history traits, warming and other effects of climate change are expected to impact the relative expression of alternative life histories considerably (Post et al. 2001).

Identifying drivers of life-history variability improves understanding of critical factors regulating population dynamics (Raffard et al. 2019) and may help predict responses to environmental change (Berger et al. 2017). Intraspecific diversity in life-history traits has been shown to mediate the effects of competition and environmental variability on population vital rates like growth, survival, and reproduction (Duffy 2010, Jenouvrier et al. 2015, Zaiats et al. 2021), contributing to population stability and resiliency (Schindler et al. 2010). Characterizing these interactions therefore contributes to understanding dynamics of populations exhibiting life-history diversity. Furthermore, accounting for life-history diversity in population models should

improve predictions of the demographic effects of life-history change driven by climate change, management, and other factors (Phillips et al. 2017, Cunningham et al. 2020).

2.5 ACKNOWLEDGEMENTS

Funding for this research was provided by the National Oceanographic and Atmospheric Administration Northwest Fisheries Science Center, the Washington Cooperative Fish and Wildlife Research Unit, and the Northwest Climate Adaptation Science Center. Data was provided by Grant County Public Utilities District, Chelan County Public Utilities District, the Washington Department of Fish and Wildlife, Yakama Nation Fisheries, Washington Department of Ecology, the U.S. Geological Survey, and the U.S. National Weather Service. We thank Jeffrey Jorgensen, Tracy Hillman, and Tom Cooney for helpful discussion about the analysis. Any use of trade, firm, or product names is for descriptive purposes only and does not imply endorsement by the U.S. Government. The authors have no conflicts of interest to declare.

2.6 FIGURES

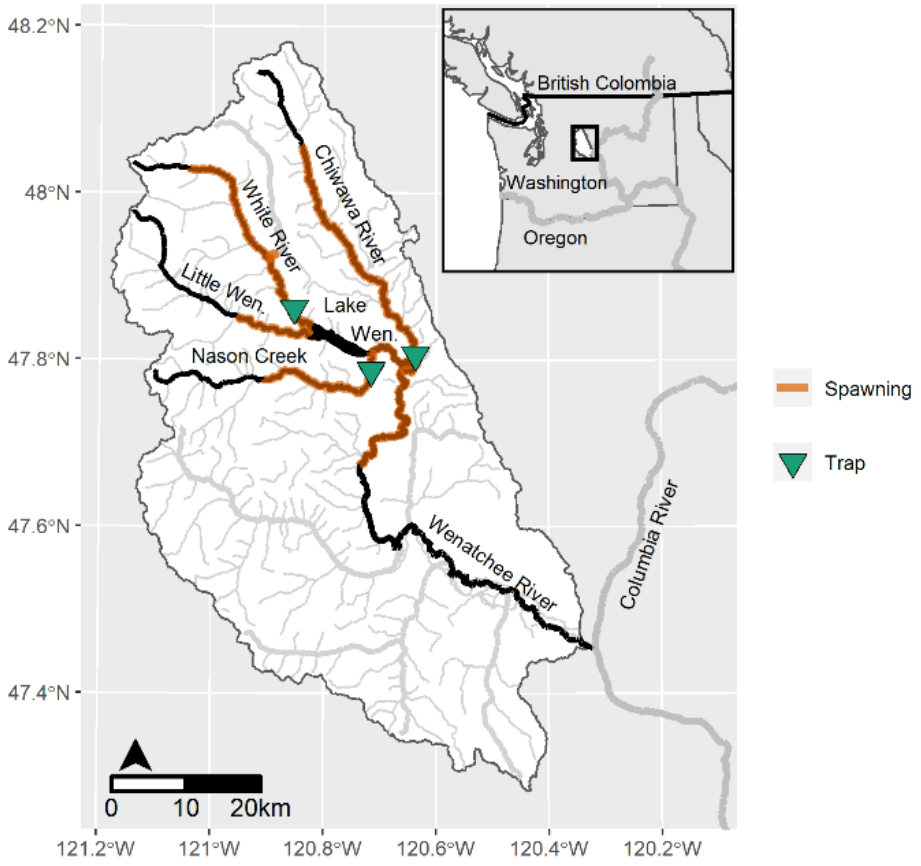

Figure 2.1: Wenatchee River basin, showing Chinook salmon spawning habitat in orange and locations of rotary screw traps where out-migrating juveniles were sampled as green triangles. Little Wen. = Little Wenatchee River; Lake Wen. = Lake Wenatchee.

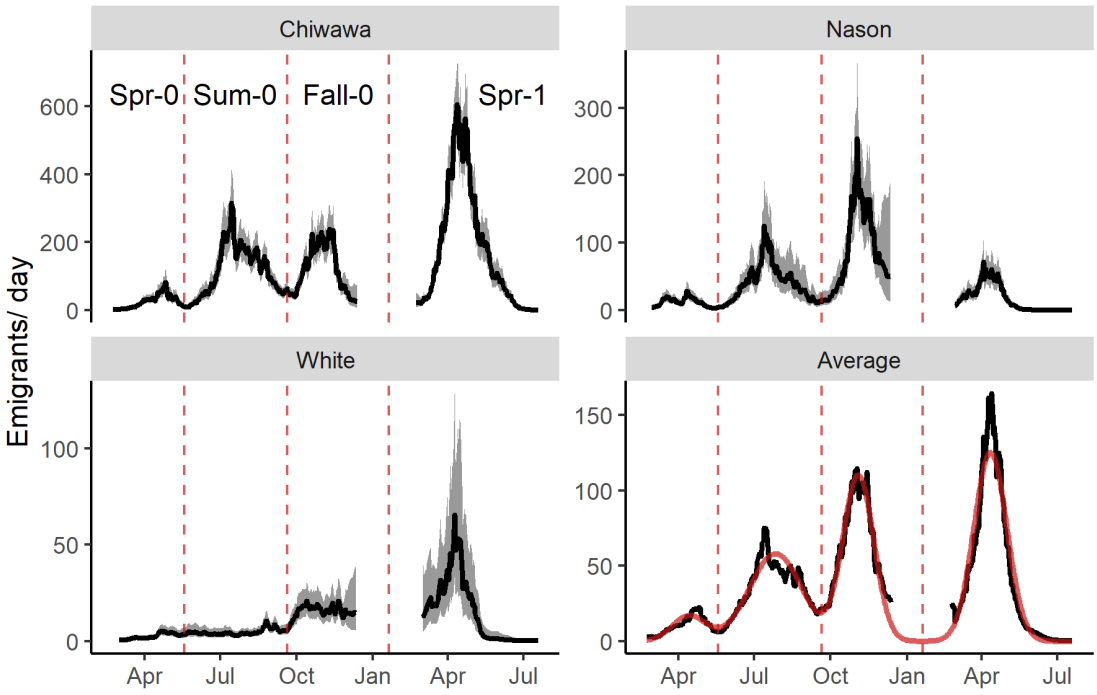

Figure 2.2: Mean daily numbers of emigrants across years in three natal streams. Gray shaded area is the 95% confidence interval. The red solid line is a mixture distribution used to identify breakpoints between juvenile life histories. The red dashed lines delineate the juvenile life-history pathways, defined by emigration day of year: *Spr-0* = spring subyearling, *Sum-0* = summer subyearling, *Fall-0* = fall subyearling, and *Spr-1* = spring yearling emigrants. The gap in outmigrant estimates is the period when no trapping was conducted due to ice in the river.

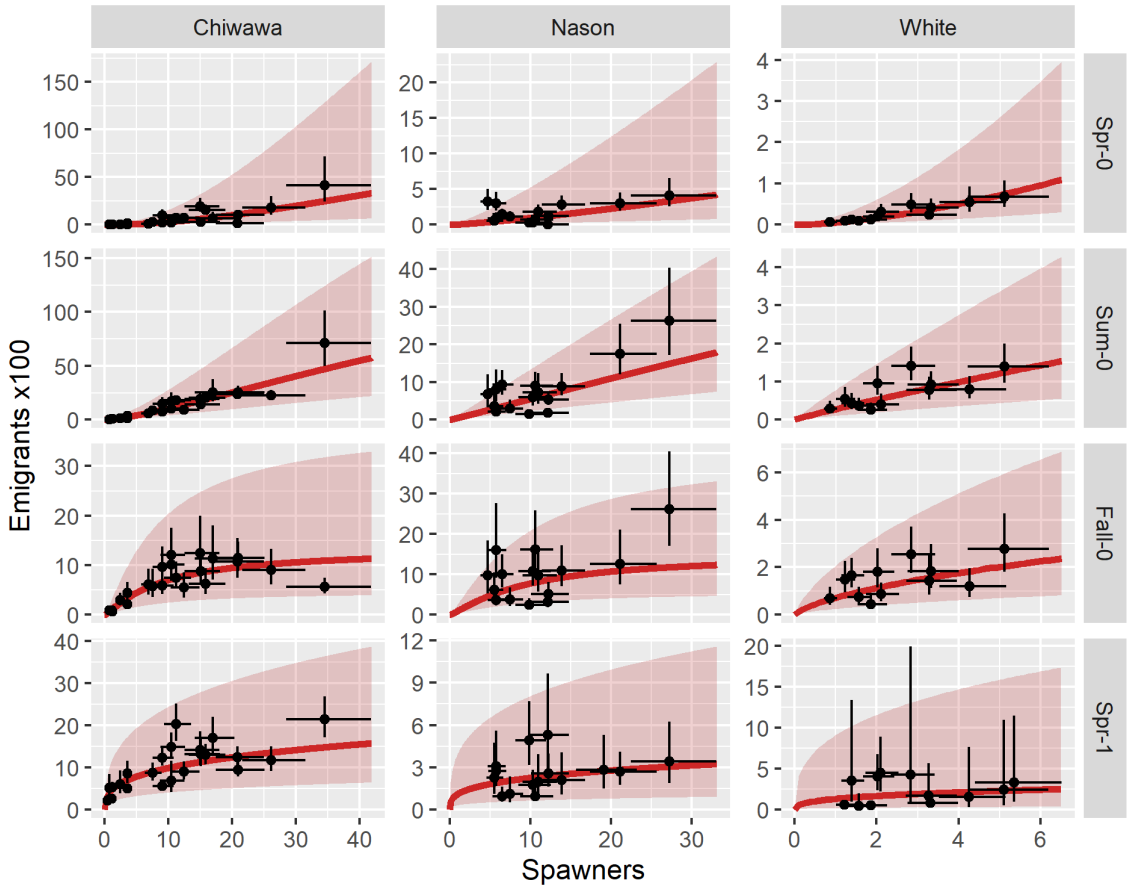

Figure 2.3. Functional relationships between spawner and juvenile emigrant abundances per kilometer of spawning habitat by natal stream and juvenile life history. The functional form is a modified Beverton-Holt model. Points represent estimates of spawner and juvenile emigrant abundances with 95% confidence intervals. The red lines represent the expected number of juvenile emigrants for a given spawner abundance. The red envelope is the 95% prediction interval representing process error. Predictions were made with standardized streamflow covariates set to 0.0.

2.7 REFERENCES

Apgar, T. M., J. E. Merz, B. T. Martin, and E. P. Palkovacs. 2021. Alternative migratory strategies are widespread in subyearling Chinook salmon. Ecology of Freshwater Fish 30:125–139.

Beer, W. N., and E. A. Steel. 2018. Impacts and implications of temperature variability on Chinook salmon egg development and emergence phenology. Transactions of the American Fisheries Society 147:3–15.

Benaglia, T., D. Chauveau, D. R. Hunter, and D. Young. 2009. mixtools: An R package for analyzing finite mixture models. Journal of Statistical Software 32:1–29.

Berger, D., J. Stångberg, K. Grieshop, I. Martinossi-Allibert, and G. Arnqvist. 2017. Temperature effects on life-history trade-offs, germline maintenance and mutation rate under simulated climate warming. Proceedings of the Royal Society B: Biological Sciences 284:20171721.

Bourret, S. L., C. C. Caudill, and M. L. Keefer. 2016. Diversity of juvenile Chinook salmon life history pathways. Reviews in Fish Biology and Fisheries 26:375–403.

Bradford, M. J., and G. C. Taylor. 1997. Individual variation in dispersal behaviour of newly emerged Chinook salmon (Oncorhynchus tshawytscha) from the Upper Fraser River, British Columbia. Canadian Journal of Fisheries and Aquatic Sciences 54:1585–1592.

Brown, A. J., P. S. White, and R. K. Peet. 2021a. Environmental context alters the magnitude of conspecific negative density dependence in a temperate forest. Ecosphere 12:e03406.

Brown, J. M., E. E. van Loon, W. Bouten, K. C. J. Camphuysen, L. Lens, W. Müller, C. B. Thaxter, and J. Shamoun-Baranes. 2021b. Long-distance migrants vary migratory behaviour as much as short-distance migrants: An individual-level comparison from a seabird species with diverse migration strategies. Journal of Animal Ecology 90:1058–1070.

Buchanan, R. A., J. R. Skalski, G. Mackey, C. Snow, and A. R. Murdoch. 2015. Estimating cohort survival through tributaries for salmonid populations with variable ages at migration. North American Journal of Fisheries Management 35:958–973.

Conner, M. M., and G. C. White. 1999. Effects of individual heterogeneity in estimating the persistence of small populations. Natural Resource Modeling 12:109–127.

Cunningham, G. D., G. M. While, M. Olsson, G. Ljungström, and E. Wapstra. 2020. Degrees of change: between and within population variation in thermal reaction norms of phenology in a viviparous lizard. Ecology 101:e03136.

Diez, J. M., R. Boone, T. Bohner, and O. Godoy. 2021. Frequency-dependent tree growth depends on climate. Ecology 102:e03284.

Duffy, M. A. 2010. Ecological consequences of intraspecific variation in lake Daphnia. Freshwater Biology 55:995–1004.

Einum, S., L. Sundt-Hansen, and K. H. Nislow. 2006. The partitioning of density-dependent dispersal, growth and survival throughout ontogeny in a highly fecund organism. Oikos 113:489–496.

Frances, D. N., A. J. Barber, and C. M. Tucker. 2021. Trait–density relationships explain performance in cladoceran zooplankton. Ecology 102:e03294.

Greene, C. M., J. E. Hall, K. R. Guilbault, and T. P. Quinn. 2010. Improved viability of populations with diverse life-history portfolios. Biology Letters 6:382–386.

Hahn, P. G., and J. L. Maron. 2016. A Framework for Predicting Intraspecific Variation in Plant Defense. Trends in Ecology & Evolution 31:646–656.

Hillman, T. W., M. Miller, M. Hughes, C. Moran, W. Williams, M. Tonseth, C. Willard, S. Hopkins, J. Caisman, T. N. Pearsons, and P. Graf. 2020. Monitoring and evaluation of the Chelan and Grant County PUD s hatchery programs: 201 9 annual report. Report to the HCP and PRCC Hatchery Committees. Wenatchee and Ephrata, WA.

Hirsch, R., L. DeCicco, and D. Lorenz. 2015. User guide to Exploration and Graphics for RivEr Trends (EGRET) and dataRetrieval: R packages for hydrologic data. U.S. Geological Survey.

Isaak, D. J., S. J. Wenger, E. E. Peterson, J. M. Ver Hoef, S. W. Hostetler, C. H. Luce, J. B. Dunham, J. L. Kershner, B. B. Roper, D. E. Nagel, and others. 2016. NorWeST modeled summer stream temperature scenarios for the western US.

Jansen, M., N. P. R. Anten, F. Bongers, M. Martínez-Ramos, M. E. Gavito, and P. A. Zuidema. 2017. Explaining long-term inter-individual growth variation in plant populations: persistence of abiotic factors matters. Oecologia 185:663–674.

Jenouvrier, S., C. Péron, and H. Weimerskirch. 2015. Extreme climate events and individual heterogeneity shape life-history traits and population dynamics. Ecological Monographs 85:605–624.

Jesmer, B. R., M. J. Kauffman, A. B. Courtemanch, S. Kilpatrick, T. Thomas, J. Yost, K. L. Monteith, and J. R. Goheen. 2021. Life-history theory provides a framework for detecting resource limitation: a test of the Nutritional Buffer Hypothesis. Ecological Applications 31:e02299.

Kristensen, K., A. Nielsen, C. Berg, H. Skaug, and B. Bell. 2016. TMB: automatic differentiation and Laplace approximation. Journal of Statistical Software, 70(5), 1-21.

Kvile, K. Ø., D. Altin, L. Thommesen, and J. Titelman. 2021. Predation risk alters life history strategies in an oceanic copepod. Ecology 102:e03214.

Laforge, M. P., M. Bonar, and E. Vander Wal. 2021. Tracking snowmelt to jump the green wave: phenological drivers of migration in a northern ungulate. Ecology 102:e03268.

Liedvogel, M., S. Åkesson, and S. Bensch. 2011. The genetics of migration on the move. Trends in Ecology & Evolution 26:561–569.

Luevano, L., C. Sutherland, S. J. Gonzalez, and R. Hernández-Pacheco. 2022. Rhesus macaques compensate for reproductive delay following ecological adversity early in life. Ecology and Evolution 12:e8456.

Lundblad, C. G., and C. J. Conway. 2021. Nest microclimate and limits to egg viability explain avian life-history variation across latitudinal gradients. Ecology 102:e03338.

Mantua, N., I. Tohver, and A. Hamlet. 2010. Climate change impacts on streamflow extremes and summertime stream temperature and their possible consequences for freshwater salmon habitat in Washington State. Climatic Change 102:187–223.

Martin, H. W., M. Hebblewhite, and E. H. Merrill. 2022. Large herbivores in a partially migratory population search for the ideal free home. Ecology n/a:e3652.

Montorio, L., G. Evanno, and M. Nevoux. 2018. Intra- and interspecific densities shape life-history traits in a salmonid population. Oecologia 188:451–464.

Moore, J. W., J. D. Yeakel, D. Peard, J. Lough, and M. Beere. 2014. Life-history diversity and its importance to population stability and persistence of a migratory fish: steelhead in two large North American watersheds. Journal of Animal Ecology 83:1035–1046.

Murdoch, A. R., C. H. Frady, M. S. Hughes, and K. See. 2019. Estimating population size and observation bias for spring Chinook Salmon. Conservation Science and Practice 1:e120.

Myers, R. A., N. J. Barrowman, J. A. Hutchings, and A. A. Rosenberg. 1995. Population dynamics of exploited fish stocks at low population levels. Science 269:1106–1108.

Phillips, R. A., S. Lewis, J. González-Solís, and F. Daunt. 2017. Causes and consequences of individual variability and specialization in foraging and migration strategies of seabirds. Marine Ecology Progress Series 578:117–150.

Post, E., M. C. Forchhammer, N. Chr. Stenseth, and T. V. Callaghan. 2001. The timing of life–history events in a changing climate. Proceedings of the Royal Society of London. Series B: Biological Sciences 268:15–23.

R Core Team. 2021. R: a language and environment for statistical computing. R Foundation for Statistical Computing, Vienna, Austria.

Raffard, A., F. Santoul, J. Cucherousset, and S. Blanchet. 2019. The community and ecosystem consequences of intraspecific diversity: a meta-analysis. Biological Reviews 94:648–661.

Schindler, D. E., R. Hilborn, B. Chasco, C. P. Boatright, T. P. Quinn, L. A. Rogers, and M. S. Webster. 2010. Population diversity and the portfolio effect in an exploited species. Nature 465:609–612.

Senner, N. R., Y. E. Morbey, and B. K. Sandercock. 2020. Editorial: Flexibility in the Migration Strategies of Animals. Frontiers in Ecology and Evolution 8.

Simpson, D., H. Rue, A. Riebler, T. G. Martins, and S. H. Sørbye. 2017. Penalising model component complexity: a principled, practical approach to constructing priors. Statistical Science 32:1–28.

Stearns, S. C. 1976. Life-history tactics: a review of the ideas. The Quarterly Review of Biology 51:3–47.

Thorpe, J. E., M. Mangel, N. B. Metcalfe, and F. A. Huntingford. 1998. Modelling the proximate basis of salmonid life-history variation, with application to Atlantic salmon, Salmo salar L. Evolutionary Ecology 12:581–599.

Thorson, J. 2020. TMBhelper: Package for basic helper functions that are not worth putting in a specialized contributed package. manual.

Thorson, J. T., M. D. Scheuerell, E. R. Buhle, and T. Copeland. 2014. Spatial variation buffers temporal fluctuations in early juvenile survival for an endangered Pacific salmon. Journal of Animal Ecology 83:157–167.

Walters, A. W., T. Copeland, and D. A. Venditti. 2013. The density dilemma: limitations on juvenile production in threatened salmon populations. Ecology of Freshwater Fish 22:508–519.

Washington Department of Ecology. 2020. Flow Monitoring Network. https://fortress.wa.gov/ecy/eap/flows/regions/state.asp.

Zaiats, A., M. J. Germino, M. D. Serpe, B. A. Richardson, and T. T. Caughlin. 2021. Intraspecific variation mediates density dependence in a genetically diverse plant species. Ecology 102:e03502.

Chapter 3. JUVENILE LIFE HISTORY DIVERSITY IS ASSOCIATED WITH LIFETIME DEMOGRAPHIC HETEROGENEITY IN A MIGRATORY FISH

Publication history: This study was co-authored with Andrew R. Murdoch, Richard W. Zabel, Jeffrey C. Jorgensen, Corey M. Kamphaus, and Sarah J. Converse. At the time this dissertation was published, a version of this chapter was in review at *Ecosphere*.

Open research statement: All data and code are available at https://github.com/Quantitative-Conservation-Lab/Wenatchee-survival

Abstract: Differences in the life history pathways of juvenile animals are often associated with differences in demographic rates in later life stages. For migratory animals, different life-history pathways often result in animals from the same population occupying distinct habitats subjected to different environmental drivers. Understanding how demographic rates differ among animals expressing different life history pathways may reveal fitness tradeoffs that drive the expression of alternative life history pathways and enable better prediction of population dynamics in a changing environment. To understand how demographic outcomes and their relationships with environmental variables differ among animals with different life history pathways, we analyzed a long-term (2006–2021) mark-recapture dataset for Chinook salmon (*Oncorhynchus tshawytscha*) from the Wenatchee River, Washington, USA. Distinct life history pathways represented in this population include either remaining in the natal stream until emigrating to the ocean as a one-year-old (*natal-reach rearing*) or emigrating from the natal stream and rearing in downstream

habitats for several months before completing the emigration to the ocean as a one-year-old (*downstream rearing*). We found that downstream-rearing fish emigrated to the ocean 19 days earlier on average and returned as adults from the ocean at higher rates. We detected a positive correlation between rate of return from the ocean by downstream-rearing fish and coastal upwelling in their spring of outmigration, whereas for natal-reach-rearing fish we detected a positive correlation with sea surface temperature during their first marine summer. Different responses to environmental variability should lead to asynchrony in adult abundance among juvenile life history pathways. A higher proportion of downstream-rearing fish returned at younger ages compared to natal-reach-rearing fish, which contributed to more variability in age at reproduction and greater mixing across generations. Our results provide an example of how diversity in juvenile life history pathways is associated with heterogeneity in demographic rates during subsequent life stages. This demographic heterogeneity can in turn affect variance in the aggregate population abundance and population response to environmental change. Our findings underscore the importance of considering life history diversity in demographic analyses and lay the foundation for the development of population models that account for different life history pathways.

Keywords: Individual heterogeneity; carry-over effects; individual stochasticity; multi-state model; synchrony; survival; maturation age; Chinook salmon; mark recapture; response diversity; static heterogeneity; endangered species

3.1 INTRODUCTION

Individual heterogeneity in life history traits is often associated with individuals occupying distinct habitats and consequently experiencing differences in demographic rates throughout the

life cycle. This heterogeneity can result in important consequences for population dynamics and fitness (Kendall and Fox 2002, Vindenes et al. 2008, Forsythe et al. 2021). Animals exhibiting alternative life history pathways (LHPs) may have different survival rates, which may have different environmental drivers. The resulting asynchrony in LHP abundance dampens variability in total population abundance and may confer a level of resilience to environmental change (Elmqvist et al. 2003) known as the portfolio effect (Schindler et al. 2010). Life history diversity also contributes to population stability through variability in age at maturity and longevity (Lewin et al. 2017).

Tradeoffs exist when life history events have both costs and benefits to fitness (Stearns 1989). For example, reproduction increases immediate fitness, but may reduce survival, and therefore reproduction over an organism's lifetime (Oosthuizen et al. 2021). Thus, a tradeoff exists between immediate and lifetime reproductive output. Such tradeoffs are believed to play a primary role in the evolution of life histories (Stearns 1989). Furthermore, tradeoffs can lead to heterogeneity within populations when multiple viable life history tactics exist or when an organism's state determines which life history tactic will confer the greatest fitness (e.g., Oosthuizen et al. 2019).

A better understanding of how demographic rates differ among animals within populations that express different LHPs could help elucidate the tradeoffs that maintain life history diversity within populations (Salguero-Gómez et al. 2018), while a better understanding of diversity in response to environmental variables could inform how life history diversity contributes to population stability (Hamel et al. 2018). Furthermore, information regarding how demographic rates and responses to environmental variability differ among organisms expressing alternative LHPs could benefit conservation and management efforts by informing predictions of how

populations will respond to management actions, climate change, and other sources of environmental change that may differentially affect LHPs (e.g., Lok et al. 2019). However, the lifetime demographic consequences of alternative LHPs, especially alternative pathways exhibited by young animals, are poorly studied because it is difficult to track individuals throughout their life cycles (Clutton-Brock and Sheldon 2010). Above a certain age, it becomes difficult to distinguish individuals that exhibited different juvenile LHPs, yet those pathways may have lifetime effects on demographic rates and fitness.

Anadromous salmonids (Salmonidae Spp.) exhibit considerable diversity of LHPs related to freshwater habitat use during juvenile life stages, and this diversity is associated with greater population stability (Schroeder et al. 2015, Bourret et al. 2016). However, the degree to which lifetime demographic rates and demographic responses to environmental conditions vary among juvenile LHPs within populations is not well understood (Braun et al. 2016, Bourret et al. 2016). To determine how lifetime demographic outcomes differ among animals with different juvenile LHPs, we analyzed a long-term (2006–2021) mark-recapture dataset for >150,000 Chinook salmon (Oncorhynchus tshawytscha) with known juvenile LHPs from a population in the Columbia River Basin listed under Endangered Species Act. Fish were marked as juveniles when emigrating from their natal stream, the timing of which defined their juvenile LHP (Chapter 2). They were subsequently detected when passing dams during their juvenile downstream and adult upstream migrations, allowing for estimation of survival, return rates from the ocean (reflecting at-sea survival and return age), and maturation age of fish expressing alternative juvenile LHPs. We identified differences in the rates and ages of return from the ocean as well as diversity in responses to environmental variables across LHPs. These results provide insights into the effects

of life history diversity on population dynamics and tradeoffs that may contribute to the maintenance of life history diversity.

3.2 METHODS

3.2.1 *Study system*

The Wenatchee River Basin lies in central Washington State, USA (Figure 3.1 b) and supports a population of federally endangered spring Chinook salmon. As is common among Chinook salmon, juveniles exhibit a two-stage emigration from natal streams (Copeland and Venditti 2009, Schroeder et al. 2015, Bourret et al. 2016); stage-one emigration is to downstream freshwater rearing areas and occurs at variable times but by their second spring, while stage-two emigration is to the ocean and occurs in the second spring (Buchanan et al. 2015, Favrot and Jonasson 2020). One LHP is characterized by fish remaining in the natal stream until their second spring and initiating stage-two emigration directly after stage one (natal-reach rearing). Other LHPs are characterized by fish carrying out stage-one emigration from natal streams in spring, summer, or fall of their first year of life, and rearing and overwintering in downstream reaches prior to initiating stage-two emigration the following spring (downstream rearing). Adults return from the ocean in spring at age three, four, or five, reside within the Wenatchee River Basin over summer, and spawn in late summer.

3.2.2 *Data*

From 2006 through 2017, juvenile spring Chinook salmon were sampled with rotary screw traps during stage-one emigration from three natal streams – the Chiwawa River, Nason Creek, and the White River (Figure 3.1a). The traps were installed in early spring and operated continuously through late fall. Captured juveniles > 60 mm were implanted with passive integrated

transponder (PIT) tags within their peritoneal cavity using a syringe. PIT tags transmitted a unique radio-frequency identification (RFID) code when triggered by an electromagnetic pulse from an RFID reader such that encounter histories unique to each tagged individual could be constructed. The dates and locations that marked fish were released and subsequently detected were downloaded from the Columbia Basin PIT Tag Information System (www.ptagis.org).

We categorized fish in our dataset into three distinct juvenile LHPs based on their date and age of emigration (corresponding to their date and age of first capture). LHPs were delineated based on the seasonality in average daily emigrant abundances (Sorel et al., *in review*; Ch. 2): (1) summer subyearlings; (2) fall subyearlings; and (3) spring yearlings. Summer subyearlings were the youngest fish that were large enough to be marked with PIT tags. They emigrated between day of year (DOY) 141 and 262. Fall subyearlings emigrated between DOY 263 and when the traps were removed in early winter ($\leq$ DOY 345). Spring yearlings emigrated in spring, between when traps were installed ($\geq$ DOY 53) and DOY 179 and were distinguished from subyearlings based on a previously developed length-date cutoff rule (Sorel et al., *in review*; Ch. 2).

Following initial capture, the first opportunity for detection (constituting the second capture occasion) occurred at a rotary screw trap operated near the confluence of the Wenatchee River and the Columbia River (*lower Wenatchee screw trap*) (Figure 1a).This trap was only operated from late winter through summer, but we assumed that downstream-rearing fish remained within the Wenatchee River Basin until their second spring of life, at which point surviving individuals could be recaptured when passing the lower Wenatchee screw trap during stage-two emigration. It is possible that some fish passed the lower Wenatchee screw trap in late fall through winter prior to trap operations, which could introduce bias into survival estimates if these fish had different survival rates than fish that migrated during trap operations.

Subsequent detection occasions occurred as fish transited downstream on their way to the ocean and when they traveled back upstream as adults prior to spawning. The third and fourth detection occasions occurred at juvenile bypass systems at the McNary and Bonneville Dams within the Columbia River seaward migration corridor (Figure 3.1). Only juveniles that passed dams via the juvenile fish bypass systems were detected as there were no RFID readers in other passageways (i.e., spillways or turbines). After passing Bonneville Dam as juveniles, fish entered the marine environment and could not be detected until they returned to Bonneville Dam as adults one to three years later.

The fifth and sixth detection occasions occurred as returning adult fish ascended fish ladders at Bonneville and McNary Dams, which are the only passage routes upstream through these dams. The seventh and final capture occasion occurred at the fish ladder at Tumwater Dam on the mainstem of the Wenatchee River, which all fish must transit to return to their natal streams.

We used data on several environmental variables as covariates in our analysis. Wenatchee River discharge data were recorded at USGS gauge 12459000 and obtained using the dataRetrieval package in R version 4.0.4 (De Cicco et al. 2018, R Core Team 2021). Air temperature data were recorded at Wenatchee Pangborn Airport and obtained from the National Weather Service using the NOWData webtool (https://w2.weather.gov/climate/xmacis.php?wfo=otx). Data on discharge and spill percentage at mainstem Columbia River Dams were obtained using the Columbia Basin Research Data Access in Real Time webtool (http://www.cbr.washington.edu/dart/query/river_graph_text). Processed data on seasonal sea surface temperature (https://www1.ncdc.noaa.gov/pub/data/cmb/ersst/v5/netcdf/) and coastal upwelling anomalies

(https://www.pfeg.noaa.gov/products/PFELData/upwell/monthly/upanoms.mon) were obtained from the github repository (bchasco/SAR_paper) associated with Chasco et al. (2021).

3.2.3 *Model description*

We used a multi-state mark-recapture model to estimate downstream survival and marine-return rate ($\phi_{t,l,s,y}$) by interval (t), juvenile LHP (l), natal stream (s), and year (y); upstream adult survival ($\phi_{t,y,a}$) by interval, year, and age (a); and maturation probabilities ($\psi_{l,y,a}$) by juvenile LHP, year, and age (Arnason 1973, Brownie et al. 1993). Here, an *interval* refers to a stretch of river or ocean located between two detection points. Because fish could not be observed after passing downstream of Bonneville Dam unless they returned to Bonneville Dam one to three years later (detection occasion five), annual marine survival and maturation (i.e., marine return) probabilities were confounded and not separately identifiable without making assumptions such as constant annual survival. Instead, we modeled the probability of marine return, at any age, for all fish entering the ocean each year, and conditional on marine return, the probabilities of fish spending one, two, or three years at sea (Buhle et al. 2018).

Survival and marine-return rates — Juvenile survival and marine-return rates (ϕ) were modeled as:

$$\begin{aligned} \text{logit}\left(\phi_{t,l,s,y}\right) &= \alpha_t + \boldsymbol{x}_{t,l,s,y}\boldsymbol{\beta} + \delta_{t,y} + \epsilon_{t,l,y} \\ \delta_{t,y} &\sim N(0, \sigma_t) \\ \epsilon_{t,l,y} &\sim \text{N}\left(0, \tau_{t,l}\right) \end{aligned} \qquad (1)$$

where α_t is an interval-specific intercept, $\boldsymbol{x}_{t,l,s,y}$ is a row of the design matrix coding covariates and categorical effects, $\boldsymbol{\beta}$ is a vector of coefficients, $\delta_{t,y}$ are random effects of year specific to each interval, and $\epsilon_{t,y,l}$ are random effects of year specific to each interval and LHP (where

certain LHPs were grouped in some intervals). The reasons for including the synchronous random effect of year, $\delta_{t,y}$, that affected all LHPs was so that the model could be used for prospective simulations that account for synchrony, and to provide information about the degree of synchrony. The random effects of year were assumed to be normally distributed around zero with standard deviation σ_t for effects modeled as synchronous across LHPs, and $\tau_{t,l}$ for effects modeled as asynchronous across individual LHPs. We did not include random effects of year that were specific to individual natal streams due to small sample sizes for some streams.

To improve parameter identifiability and increase model parsimony, we applied penalized-complexity priors (Simpson et al. 2017) on coefficients $\boldsymbol{\beta}$ and random effects of year. Each coefficient (β_n) was assumed to be drawn from a zero-centered normal distribution, $\beta_n \sim \mathrm{N}(0, \upsilon_{\beta_n})$, with a standard deviation (υ_{β_n}) that was unique to each coefficient in the model. An exponential penalty was applied on each standard deviation, $\upsilon_{\beta_n} \sim \exp(\lambda_t)$, where the rate parameter (λ_t) determined the strength of the penalty and was applied to all υ_{β_n} within a given interval. In addition, to help with model fitting, a penalty rate parameter ($\lambda_t^{\mathrm{rand}}$) was fit and applied for random effect standard deviations, $\sigma_t \sim \exp(\lambda_t^{\mathrm{rand}})$, and $\tau_{t,l} \sim \exp(\lambda_t^{\mathrm{rand}})$, in each interval *t*. We used a prior for the penalty rate parameters, e.g., $\lambda_t \sim \mathrm{half-normal}(0, SD = 50)$, to constrain those that were not well informed by the data. The covariates and categorical effects included in each interval are presented in Table 3.1 and random-effects structures are presented in Table B1. We used sum-constraint coding for all categorical variables in the design vectors ($\boldsymbol{x}_{t,l,s,y}$) so that we penalized deviations from across-group averages.

During the first interval (from first capture to passage of the screw trap at the confluence of the Wenatchee and Columbia Rivers), we fit penalized effects of juvenile LHP, natal stream, and

their interaction. In the second through fourth intervals, we grouped the two downstream-rearing LHPs (summer and fall subyearling emigrants; *downstream rearing*), to increase statistical power considering the relatively small sample size of summer subyearling emigrants. This decision was also supported by our observation that the two downstream-rearing LHPs had similar detection timing on detection occasions two through four (Figure C2). In contrast, natal-reach-rearing emigrants had different detection timing on these detection occasions. Therefore, during the second through fourth intervals, we modeled penalized effects of grouped LHP (downstream vs. natal-reach reach rearing), natal stream, and their interaction.

During the first interval, we included effects of average annual winter (November–February) air temperature and Wenatchee River discharge on survival of summer sub-yearling and fall subyearling LHPs (Favrot and Jonasson 2020), allowing for separate effects by LHP but assuming common effects across natal streams. Based on relationships between Chinook salmon marine-return rates and environmental covariates reported by Crozier et al. (2021), we evaluated the effects of three covariates on marine-return rates (fourth interval): sea surface temperature in an arc of the northeast Pacific Ocean defined by Johnstone and Mantua (2014) during the winter prior to the spring when fish entered the marine environment, coastal upwelling anomalies off the coast of Washington State in the spring when fish entered the ocean, and sea surface temperature off the coast of Washington State during the summer after fish entered. Coefficients for all environmental covariates on survival during intervals two through four were allowed to vary between natal-reach and downstream-rearing LHPs but were assumed to be common across natal streams to increase statistical power to detect relationships. All environmental covariate values were *Z*-score transformed prior to inclusion in the analysis.

In the fifth and sixth intervals, representing adult upstream migration, we did not model effects of juvenile LHPs nor natal streams on survival, assuming that carryover effects from the juvenile life stage would be diminished by adulthood and due to the smaller numbers of detections of returning adults (Table 3.1). Instead, we modeled effects of marine-return age (*a*) on survival, as might result from age-specific migration timing differences and seasonality in fisheries or physical conditions in the river. Adult survival was modeled as:

$$\begin{aligned} \text{logit}\left(\phi_{t,y,a}\right) &= \alpha_t + \boldsymbol{x}_{t,y,a}\boldsymbol{\beta} + \delta_{t,y} \\ \delta_{t,y} &\sim \text{N}(0, \sigma_t) \end{aligned} \qquad (2)$$

where α_t is a detection occasion-specific intercept, $\boldsymbol{x}_{t,y,a}$ is a row of the design matrix coding age effects, $\boldsymbol{\beta}$ is a vector of coefficients, and $\delta_{t,y}$ are random effects of year specific to each interval. No asynchronous year effects were included for upstream adult survival, due to the lower statistical power given the smaller number of adult detections.

Return ages — The conditional probabilities ($\boldsymbol{\psi}_{l,y}$) of returning at ages three, four, or five given that a fish returned from the ocean were modeled using a multinomial logit link,

$$\begin{aligned} \text{mlogit}\left(\boldsymbol{\psi}_{l,y}\right) &= \boldsymbol{\alpha}^{\psi} + \boldsymbol{x}_{l,y}^{\psi}\boldsymbol{\beta}^{\psi} + \boldsymbol{\delta}_{y}^{\psi} \\ \boldsymbol{\delta}_{y}^{\psi} &\sim \text{N}\left(0, \boldsymbol{\Sigma}^{\psi}\right) \end{aligned} \qquad (3)$$

where $\boldsymbol{\alpha}^{\psi}$ represents intercepts for ages three and five in multinomial logit space, the intercept for age four is fixed at 0.0, $\boldsymbol{x}_{l,y}^{\psi}$ is a row of the design matrix coding effect of natal-reach and downstream-rearing LHP, and $\boldsymbol{\beta}^{\psi}$ is a vector of coefficients. These differences were penalized in the same fashion as coefficients in the model of survival, with penalty rate parameter λ^{ψ}. We modeled only random effects of year that were synchronous across LHPs ($\boldsymbol{\delta}_{y}^{\psi}$) for marine-return

age probabilities due to limited power to fit asynchronous random effects of year. The synchronous random effects of year for each return age were bivariate normally distributed with covariance matrix $\mathbf{\Sigma}^{\psi}$ to account for the inherent correlation in the proportions of the population that returned at different ages each year (Buhle et al. 2018). The marginal standard deviations of the random effects of year, $\boldsymbol{\sigma}^{\psi} = \text{diag}\left(\mathbf{\Sigma}^{\psi}\right)^{0.5}$, were penalized as described above for the random effect standard deviations in the survival model, $\boldsymbol{\sigma}^{\psi} \sim \exp\left(\lambda^{\psi^{\text{rand}}}\right)$.

Detection — Detection probabilities were modeled in logit space using the same specification of categorical effects (Table 3.1) and random effects of year (Table B1) as for survival. However, different covariates were used. Coefficients and random effects of year were penalized in the same way as for survival, with unique penalty rate parameters λ_t^p and $\lambda_t^{p^{\text{rand}}}$ for each detection occasion.

On the third and fourth detection occasions (juvenile detection at McNary and Bonneville Dams), we included effects of average daily discharge and spill percentage in May–June at McNary and Bonneville Dams, as these could affect the proportion of fish going through the juvenile bypass systems, spillways, or turbines. Just as for survival probabilities, we allowed for different effects of environmental covariates – flow and spill – on detection probabilities of natal-reach and downstream-rearing LHPs, because of their different migration timing, but assumed common effects across natal streams.

Detection probability on the final occasion (Tumwater Dam) was fixed at 1.0, which ensured identifiability of the final interval-specific survival rate. This detection probability was supported by the auxiliary observation that out of 465 fish that were known to have passed Tumwater Dam

as adults because they were detected at downstream dams on the mainstem Columbia River and then on PIT detection arrays in natal tributaries upstream of Tumwater Dam, 464 (99.78%) were detected in adult fish ladders in Tumwater Dam.

3.2.4 *Model fitting*

The likelihood of the data for a given set of parameters was calculated using the forward algorithm (Zucchini et al. 2016, McClintock et al. 2020) and the Laplace approximation of the marginal log-likelihood integrated over random effects by the package TMB in R (Kristensen et al. 2016, R Core Team 2021). We fit the model by minimizing the negative marginal log-likelihood, which was conducted in R using the TMBhelper::fit_tmb function, which relies on the base::nlminb optimization algorithm (Gay 1990, Thorson 2020). Fixed effects were intercepts, standard deviations, covariance, and penalty-rate parameters. The random effects were the regression coefficients and all random effects of year. To calculate confidence intervals for derived quantities, we conducted a parametric bootstrap where we sampled 10,000 fixed and random effects from a multivariate normal distribution defined by the maximum marginal likelihood estimates and the inverse Hessian matrix returned by TMB, then calculated derived quantities with each sample parameter set and found the quantiles corresponding with the confidence interval.

3.2.5 *Goodness of fit*

We assessed goodness of fit by examining scaled quantile residuals (Dunn and Smyth 1996, Gelman and Hill 2006). We simulated 250 datasets of the same size as the observed data by sampling from binomial distributions for survival and detection, and multinomial distributions for marine-return age, conditional on the marginal maximum likelihood estimates (MLEs) of

parameters. Conditional simulations were conducted using the MLEs of model parameters and random effects of year, while marginal simulations were conducted using the MLEs of model parameters (including coefficients) but sampling random effects of year from their hyper-distributions. We summarized simulated and observed datasets by the numbers of detections on each occasion from each release group (LHP by stream by year) and adult age for adult detection occasions. We used the DHARMa package (Hartig 2021) to calculate scaled quantile residuals for the summarized numbers of detections and to interrogate the residuals for outliers and departures from uniformity.

In addition, we calculated *P* values by sampling 500 parameter sets from the multivariate normal distribution defined by the MLEs and inverted Hessian matrix and calculating the Freeman-Tukey fit statistic, $\sum_t \sum_l \sum_s \sum_y \sum_a \left(\sqrt{d_{t,l,s,y,a}} - \sqrt{E\left[d_{t,l,s,y,a}\right]}\right)^2$ for observed and simulated data generated with each parameter set (Conn et al. 2018). Here, $d_{t,l,s,y,a}$ is the summarized number of detections at a given occasion for fish of a given juvenile LHP, natal stream, year, and age, and $E\left[d_{t,l,s,y,a}\right]$ is the expectation of that number of detections given the model and a particular parameter set. The *P* value was then calculated as the proportion of parameter sets in which the Freeman-Tukey fit statistic for the simulated data was greater than the statistic for the observed data. We calculated *P* values either conditionally given the fitted random effects of year or marginally by sampling random effects of year from their hyper-distributions (Conn et al. 2018).

3.3 RESULTS

Average survival of fish from the White River during the first interval was lower than the average across all three natal streams (effect size = -0.786; 95% confidence interval (CI) = -1.117, -0.451) (Figure 3.2, Table B2). Here and in the remainder of the Results section, *effect size* refers to the magnitude of the effect on the logit-scale parameter estimate. Winter air temperature was negatively associated with survival of summer (-0.435; CI = -0.641, -0.228) and fall (-0.289; CI = -0.511, -0.068) subyearling LHPs (Figure C1).

Both the timing of detection on the second occasion (the mouth of the Wenatchee River) and third occasion (McNary Dam), and survival of fish during the interval between, differed between natal-reach and downstream-rearing life histories. The median detection day at the mouth of the Wenatchee River was 19 days earlier for downstream-rearing fish than natal-reach-rearing fish across natal streams, and 9 days earlier at McNary Dam (Figure C2). Between the mouth of the Wenatchee River and McNary Dam (second survival interval), there was some evidence that downstream-rearing fish from the Chiwawa River had lower survival than natal-stream rearing fish (-0.367; CI = -0.539, 0.139), whereas there was little evidence of this for fish from Nason Creek (-0.033; CI = -0.295, 0.220) or the White River (0.286; CI = -0.272, 0.520; Figure 3.3, Table B2). We did not detect survival differences among LHPs during the third interval, which represented the second stretch of the downstream migration (B2).

We identified differences among LHPs in timing of ocean entry, marine-return rates, and relationships between marine-return rates and covariates. Downstream-rearing fish passed Bonneville Dam 10 days earlier as juveniles on average than natal-reach-rearing fish and returned at a higher rate on average than natal-reach-rearing fish (0.597; CI = 0.117, 1.078;

Figure 3.3, Table B2). Marine-return rates of downstream-rearing fish were positively associated with coastal upwelling in spring (0.327; CI = 0.080, 0.574), but we did not detect the same relationship for natal-reach-rearing fish (-0.001; CI = -0.133, 0.131; Figure C1). Instead, return rates of natal-reach-rearing fish were negatively correlated with sea surface temperature off the coast of Washington State during summer (-0.311; CI = -0.554, -0.069). There was relatively little evidence of such a correlation for downstream-rearing fish (-0.119; CI = -0.329, 0.092). Spring upwelling and summer sea surface temperature were not meaningfully correlated with each other (0.25 Pearson correlation).

Most adult fish returned at four years of age in both natal-reach (0.739 probability of returning at age 4; CI = 0.660, 0.801) and downstream-rearing fish (0.750; CI = 0.680, 0.803), but there were differences between LHPs in proportions returning at ages three and five (Figure 3.4, Table B3). The proportion of age-three returning adults was higher among downstream-rearing fish (0.123; CI = 0.075, 0.192) than natal-reach-rearing fish (0.065; CI = 0.035, 0.117). The proportion of age-five returning adults was lower among downstream-rearing fish (0.126; CI = 0.078, 0.193) than natal-reach-rearing fish (0.195; CI = 0.131, 0.277).

Goodness of fit indicated that the model adequately fit the data. Scaled quantile residuals were approximately uniformly distributed based on examination of Q-Q plots and plots of simulated residuals vs. observations, and the numbers of outliers did not exceed the range of expectations (Figures B8–B10). The *P* value conditional on the fitted random effects of year was 0.312 and when we sampled the random effects of year from their hyper-distributions it was 0.700, neither of which indicated a lack of fit.

3.4 DISCUSSION

We found that marine-return rates of the distinct life history types (defined by their behavior as juveniles) responded to different environmental drivers in the marine environment. These results are an example of response diversity among LHPs within populations, which should dampen the variance in return rates of the aggregate population (Kendall and Fox 2002, Elmqvist et al. 2003). This is akin to response diversity that has previously been observed among populations of Chinook salmon (Braun et al. 2016) and sockeye salmon (*Onchorhynchus nerka*) (Freshwater et al. 2017) that exhibit different juvenile LHPs and behave differently upon ocean entry. The different relationships between marine-return rates and environmental variables that we identified may have been facilitated in part by differences in ocean-entry timing that we observed. Additionally, differences among LHPs in habitat use and feeding behavior in the ocean, or body condition might have contributed to different relationships with environmental variables.

We found that downstream-rearing fish entered the marine environment earlier and returned from the ocean at a higher rate than natal-reach rearing fish. Earlier marine entry timing has been associated with higher rates of return from the ocean in multiple populations and species of salmon in the Columbia River basin (Scheuerell et al. 2009, Crozier et al. 2021, Wilson et al. 2021), suggesting that earlier downstream migration may have contributed to the higher return rates of downstream-rearing LHPs. The downstream-rearing LHPs were detected entering the downstream-migration corridor 19 days earlier than natal-reach-rearing LHPs but were detected only 10 days earlier on the final detection occasion before ocean entry, suggesting that migration was slower for downstream-rearing LHPs. This suggests a potential survival tradeoff wherein earlier seaward departure is associated with slower migration and potentially lower migration

survival for downstream-rearing LHPs but confers the benefit of earlier ocean entry and higher marine survival. However, our analysis provided evidence of lower downstream-migration survival in downstream-rearing LHPs from only one of three natal streams.

We also observed that downstream-rearing LHPs returned from the ocean at younger ages on average, reducing time at sea to grow but also reducing exposure to marine mortality. This likely contributed to the higher return rates of downstream rearing LHPs. Females that return at younger ages are generally smaller and have fewer eggs (Healey and Heard 1984), and the smaller size of early-returning males makes them less effective at competing for mates (Berejikian et al. 2010). Thus, there is a tradeoff between return rate and fecundity or fertility (Gross 1985), which the alternative LHPs navigate differently. The differences in return ages between LHPs should contribute to population stability by spreading the reproductive effort of each individual generation more uniformly across future generations (Schindler et al. 2010).

The younger return age of downstream rearing LHPs relative to natal-reach rearing LHPs may be influenced by both environmental and genetic factors (Waters et al. 2021). Tréhin et al. (2021) found that marine growth rates during the first year at sea were positively associated with the probability of maturation after one only year at sea in Atlantic salmon (*Salmo salar*). A number of studies have found that larger salmon smolts tend to return at younger ages (Scheuerell 2005, Tattam et al. 2015, Gregory et al. 2019). Additionally, genetic and environmental factors experienced early in life may have set downstream-rearing fish on a trajectory for a faster life history wherein they initiated emigration from natal streams, seaward migration, and adult return all at younger ages than did natal-reach-rearing fish.

For downstream-rearing LHPs in our system, survival while rearing in downstream habitats of the Wenatchee River basin was negatively associated with winter air temperature. Winters are warming in this region and are projected to continue to do so (Mantua et al. 2010, Masson-Delmotte et al. 2021), suggesting that survival rates of fish overwintering in downstream habitats may decline. Warmer air temperature is associated with warmer water temperature, which may increase metabolic demand during winter when food is scarce. This may lead to starvation or increased time spent foraging and associated predation risk (Favrot and Jonasson 2020). We were not able to estimate the overwinter survival of natal-reach-rearing fish within the natal reach because fish were not tagged until emigration. However, knowing how average overwinter survival differed between natal-reach and downstream-rearing fish, and whether they exhibit different responses to winter air temperature, could reveal further tradeoffs and response diversity among LHPs.

The dataset that we analyzed contained limited information to assess some parameters of interest. It only included fish that were >60 mm upon emigration from the natal stream and therefore excluded a portion of the population that emigrate in spring as subyearlings at lengths < 60 mm. Additionally, recapture probabilities were particularly low during the second capture occasion, which contributed to uncertainty in estimates of survival, especially during the first and second intervals. This limited our ability to identify differences in survival between LHPs during downstream migration.

Combining our model with models of the rest of the salmon life cycle within an integrated population model (Buhle et al. 2018, Plard et al. 2019) would allow for population projection and assessment of the contribution of alternative LHPs to population productivity and stability. Because our multi-state model includes both synchronous and asynchronous variability in

demographic rates as functions of ecological variables and other sources of stochasticity, it can be used to simulate population trajectories that reflect this variability (Kendall and Fox 2002). A population model accounting for differences in demographic rates between LHPs would be able to capture differential effects on LHPs of alternative management strategies such as restoration of habitat in natal streams versus restoration in downstream areas. Lastly, the relationships that we identified between environmental variables and demographic rates could be used to simulate the effects of projected climate change on demographic rates and population trajectories (e.g., Crozier et al. 2021).

Our model allowed us to identify sources of demographic asynchrony and adult life history diversity among fish exhibiting different juvenile LHPs, which have important implications for conservation and natural resource management in a changing world. Population traits that contribute to stability in variable environments may be important for reducing the impact of changing environmental conditions and increasing environmental variability on population dynamics ((Mantua et al. 2010, Moran et al. 2016, Masson-Delmotte et al. 2021). Therefore, conserving juvenile life history diversity is one tool that can be used to conserve populations and the sustainable provisioning of ecosystem services (Cordoleani et al. 2021).

This study adds to a growing list of examples of demographic models that account for individual heterogeneity to gain new insights into drivers of population dynamics (Gimenez et al. 2018). As long-term population monitoring datasets continue to grow and more complex modeling techniques are developed and refined, there should be new opportunities to assess demographic variability across components of structured populations. One advantage of this type of modeling is that it allows partitioning of variance in demographic rates and abundance among population components (Kendall and Fox 2002, van Daalen and Caswell 2020). Further, considering

population components individually allows for the detection of relationships between demographic rates and environmental variables that may not be detectable when considering an entire population in aggregate (Gimenez et al. 2018). These relationships may enable better prediction of population responses to environmental change when that change differentially affects population components (Vindenes et al. 2008, Moran et al. 2016). For these reasons, we see models that account for individual heterogeneity in demographic rates as valuable tools for learning about drivers of population dynamics and effectively managing populations.

3.5 ACKNOWLEDGEMENTS

Funding for this research was provided by the National Oceanographic and Atmospheric Administration Northwest Fisheries Science Center, the Washington Cooperative Fish and Wildlife Research Unit, and the Northwest Climate Adaptation Science Center. Data collection was funded by Grant County Public Utilities District, Chelan County Public Utilities District, the Washington Department of Fish and Wildlife, Yakama Nation Fisheries, Bonneville Power Administration, Washington Department of Ecology, the U.S. Geological Survey, the U.S. National Weather Service, and others. We thank the many biologists and technicians who have tagged juvenile Chinook salmon in the Wenatchee River Basin and who maintain and operate recapture and detection locations on the Columbia River. We also thank the organizations and individuals who maintain databases for accessing data, including the Pacific States Marine Fisheries Commission and Columbia Basin Research. We are grateful for helpful reviews of previous versions of this manuscript by Abby Bratt and Brielle Thompson. Any use of trade, firm, or product names is for descriptive purposes only and does not imply endorsement by the U.S. Government. The authors have no conflicts of interest to declare.

3.6 TABLES & FIGURES

Table 3.1: Variables included in models of: survival probabilities (ϕ) following each detection occasion, conditional probabilities of age at return from the ocean given survival (ψ), and detection probabilities (p) on each occasion. *LHP* = juvenile life history pathway, *DS* = downstream rearing LHPs (only summer and fall subyearlings), *NR.DS* = juvenile life history pathways where summer and fall subyearlings are grouped (i.e., natal-reach vs. downstream rearing), *Ad.age* = adult age, *Stream* = natal stream, *Win.flow* = winter discharge in the Wenatchee River, *Win.air* = winter air temperature in the Wenatchee Basin, *SST.Arc.Win* = sea surface temperature in a broad area in the northeast Pacific ocean defined by Johnstone and Mantua (2014) in winter, *CUI.Spr* = coastal upwelling off of the coast of Washington State in spring, *SST.WA.Sum* = sea surface temperature off the coast of Washington State in summer, *Flow* = discharge measured at a dam of detection, and *Spill* = percentage of water spilled at dam of detection. Detection probability at Tumwater Dam for adults was assumed to be 1.0.

Occasion/interval	Variables
ϕ	
1-Natal emigration	LHP + Stream + LHP*Stream + DS*Win.flow + DS*Win.air
2-Lower Wenatchee	NR.DS + Stream + NR.DS*Stream
3-McNary.juv	NR.DS + Stream + NR.DS*Stream
4-Bonneville.juv	NR.DS + Stream + NR.DS*Stream + NR.DS*SST.Arc.Win + NR.DS*CUI.Spr + NR.DS*SST.WA.Sum
5-Bonneville.ad	Ad.age
6-McNary.ad	Ad.age
ψ	
4-Bonneville	NR.DS
p	
2-Lower Wenatchee	LHP + Stream + LHP*Stream
3-McNary.juv	NR.DS + Stream + NR.DS*Stream + NR.DS*Flow + NR.DS*Spill
4-Bonneville.juv	NR.DS + Stream + NR.DS*Stream + NR.DS*Flow + NR.DS*Spill
5-Bonneville.ad	Ad.age
6-McNary.ad	Ad.age
7-Tumwater.ad	-

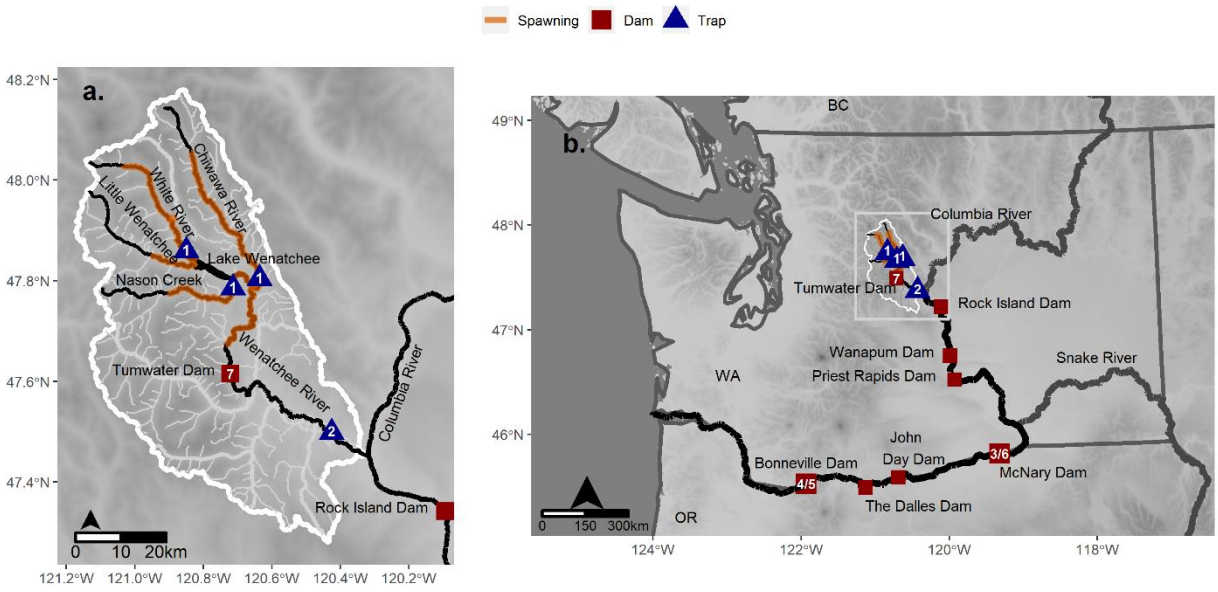

Figure 3.1: Maps of the Wenatchee River Basin (a) and the Columbia River migration corridor (b). The numbers on dams and traps represent the detection occasions corresponding with fish passing each location.

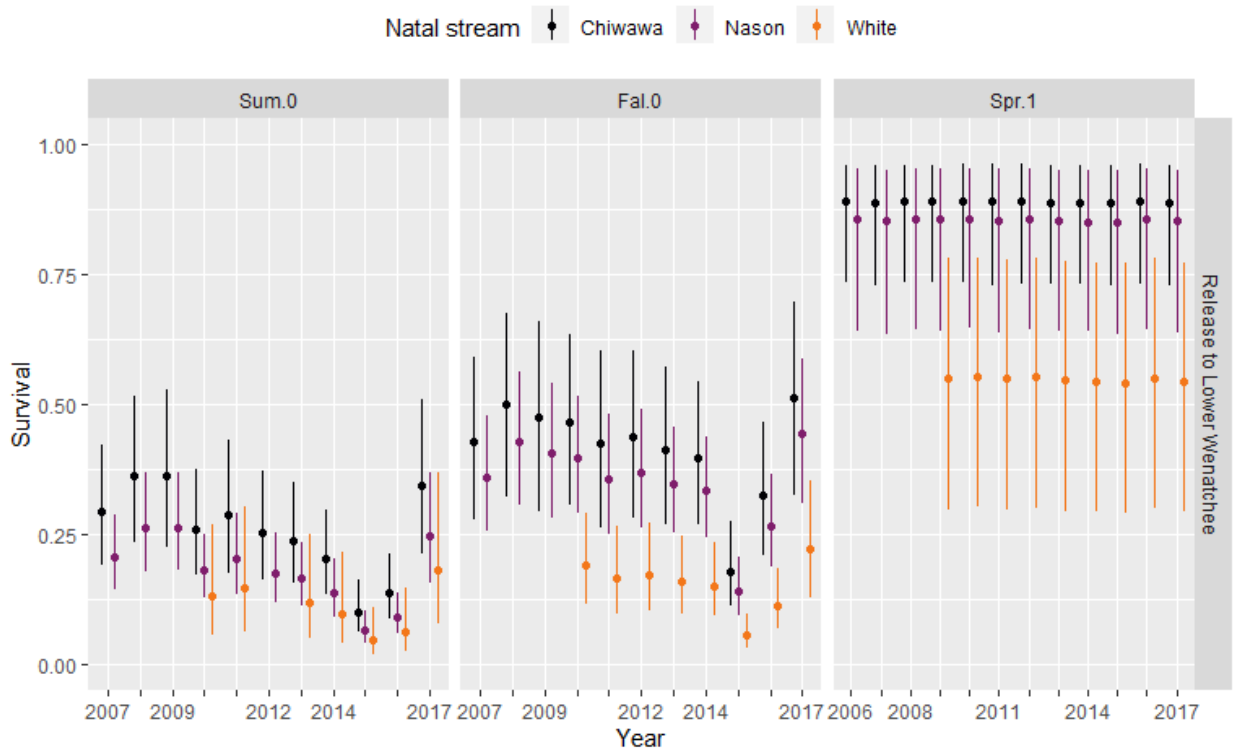

Figure 3.2: Annual survival estimates between release near the mouths of three natal streams – Chiwawa River, Nason Creek, and White River – and passing the mouth of the Wenatchee River en route to the ocean, for fish expressing three different juvenile life history pathways. The three juvenile life history pathways are fish that emigrated from their natal stream as subyearlings in summer (*Sum.0*) or fall (*Fal.0*), or as yearlings in spring (*Spr.1*). Points represent mean estimates and lines span 95% confidence intervals.

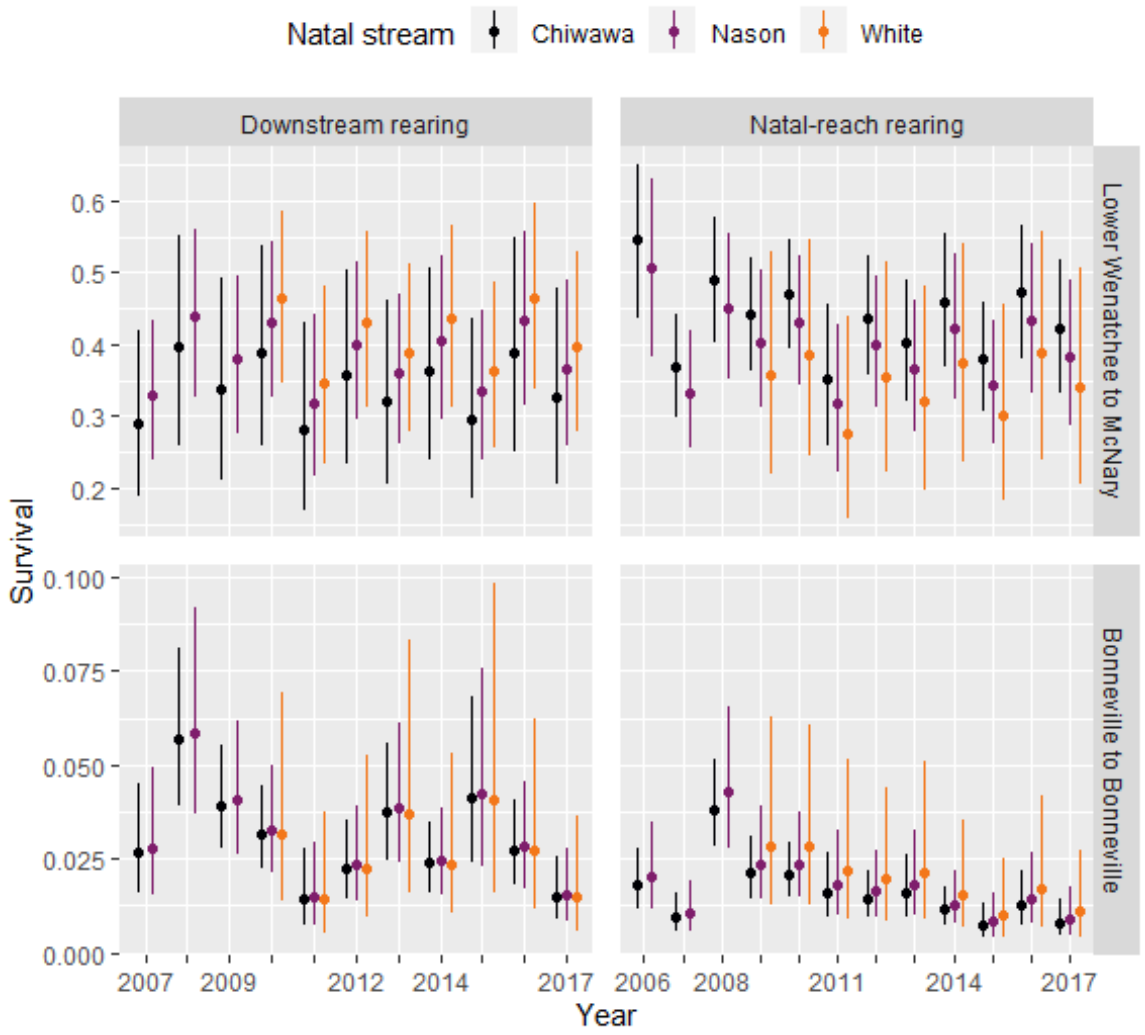

Figure 3.3: Annual survival estimates between the mouth of the Wenatchee River and McNary Dam (top row) and marine-return rates between passing downstream of Bonneville Dam as a juvenile and returning from the ocean to Bonneville Dam as an adult between one and three years later (bottom row). Different juvenile life history pathways are shown in different columns of panels and natal streams are indicated by color. Points represent mean estimates and lines span 95% confidence intervals

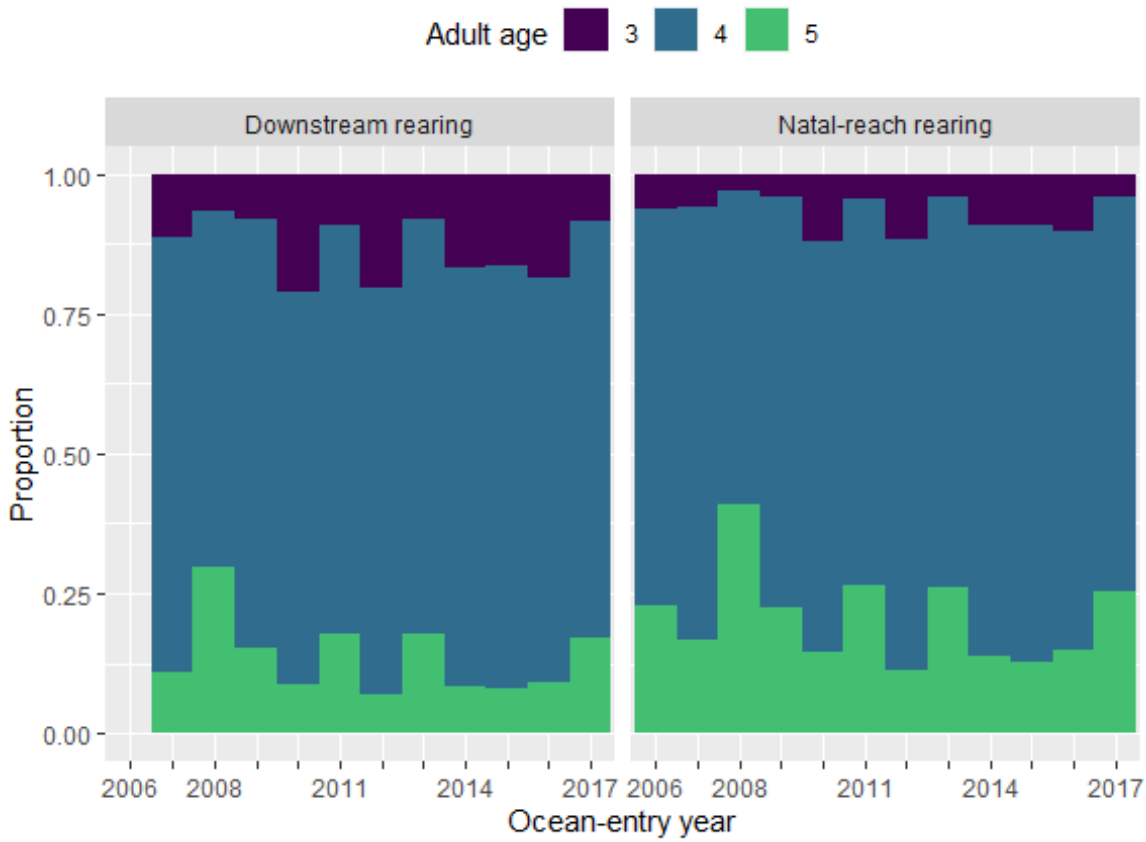

Figure 3.4: Maximum likelihood estimates of age proportions of returning adult salmon from the ocean by juvenile life history pathway year.

3.1 REFERENCES

Arnason, A. N. 1973. The estimation of population size, migration rates and survival in a stratified population. Researches on population ecology 15:1–8.

Berejikian, B. A., D. M. Van Doornik, R. C. Endicott, T. L. Hoffnagle, E. P. Tezak, M. E. Moore, and J. Atkins. 2010. Mating success of alternative male phenotypes and evidence for frequency-dependent selection in Chinook salmon, Oncorhynchus tshawytscha. Canadian Journal of Fisheries and Aquatic Sciences 67:1933–1941.

Bourret, S. L., C. C. Caudill, and M. L. Keefer. 2016. Diversity of juvenile Chinook salmon life history pathways. Reviews in Fish Biology and Fisheries 26:375–403.

Braun, D. C., J. W. Moore, J. Candy, and R. E. Bailey. 2016. Population diversity in salmon: linkages among response, genetic and life history diversity. Ecography 39:317–328.

Brownie, C., J. E. Hines, J. D. Nichols, K. H. Pollock, and J. B. Hestbeck. 1993. Capture-Recapture Studies for Multiple Strata Including Non-Markovian Transitions. Biometrics 49:1173–1187.

Buchanan, R. A., J. R. Skalski, G. Mackey, C. Snow, and A. R. Murdoch. 2015. Estimating cohort survival through tributaries for salmonid populations with variable ages at migration. North American Journal of Fisheries Management 35:958–973.

Buhle, E. R., M. D. Scheuerell, T. D. Cooney, M. J. Ford, R. W. Zabel, and J. T. Thorson. 2018. Using integrated population models to evaluate fishery and environmental impacts on Pacific salmon viability. NOAA Technical Memorandum.

Chasco, B., B. Burke, L. Crozier, and R. Zabel. 2021. Differential impacts of freshwater and marine covariates on wild and hatchery Chinook salmon marine survival. PLOS ONE 16:e0246659.

Clutton-Brock, T., and B. C. Sheldon. 2010. Individuals and populations: the role of long-term, individual-based studies of animals in ecology and evolutionary biology. Trends in Ecology & Evolution 25:562–573.

Conn, P. B., D. S. Johnson, P. J. Williams, S. R. Melin, and M. B. Hooten. 2018. A guide to Bayesian model checking for ecologists. Ecological Monographs 88:526–542.

Copeland, T., and D. A. Venditti. 2009. Contribution of three life history types to smolt production in a Chinook salmon (Oncorhynchus tshawytscha) population. Canadian Journal of Fisheries and Aquatic Sciences 66:1658–1665.

Cordoleani, F., C. C. Phillis, A. M. Sturrock, A. M. FitzGerald, A. Malkassian, G. E. Whitman, P. K. Weber, and R. C. Johnson. 2021. Threatened salmon rely on a rare life history strategy in a warming landscape. Nature Climate Change 11:982–988.

Crozier, L. G., B. J. Burke, B. E. Chasco, D. L. Widener, and R. W. Zabel. 2021. Climate change threatens Chinook salmon throughout their life cycle. Communications Biology 4:1–14.

van Daalen, S., and H. Caswell. 2020. Variance as a life history outcome: Sensitivity analysis of the contributions of stochasticity and heterogeneity. Ecological Modelling 417:108856.

De Cicco, L. A., D. Lorenz, R. M. Hirsch, and W. Watkins. 2018. dataRetrieval: R packages for discovering and retrieving water data available from U.S. federal hydrologic web services. manual, U.S. Geological Survey / U.S. Geological Survey, Reston, VA.

Dunn, P. K., and G. K. Smyth. 1996. Randomized Quantile Residuals. Journal of Computational and Graphical Statistics 5:236–244.

Elmqvist, T., C. Folke, M. Nyström, G. Peterson, J. Bengtsson, B. Walker, and J. Norberg. 2003. Response diversity, ecosystem change, and resilience. Frontiers in Ecology and the Environment 1:488–494.

Favrot, S. D., and B. C. Jonasson. 2020. Fall and Winter Movement Dynamics of Naturally Produced Spring Chinook Salmon Parr in Two Neighboring Interior Pacific Northwest Natal Rivers. Transactions of the American Fisheries Society 149:532–551.

Forsythe, A. B., T. Day, and W. A. Nelson. 2021. Demystifying individual heterogeneity. Ecology Letters 24:2282–2297.

Gay, D. M. 1990. Usage summary for selected optimization routines. Computing Science Technical Report 153. AT&T Bell Laboratories, Murray Hill.

Gelman, A., and J. Hill. 2006. Data analysis using regression and multilevel/hierarchical models. Cambridge university press.

Gimenez, O., E. Cam, and J.-M. Gaillard. 2018. Individual heterogeneity and capture–recapture models: what, why and how? Oikos 127:664–686.

Gregory, S. D., A. T. Ibbotson, W. D. Riley, M. Nevoux, R. B. Lauridsen, I. C. Russell, J. R. Britton, P. K. Gillingham, O. M. Simmons, and E. Rivot. 2019. Atlantic salmon return rate increases with smolt length. ICES Journal of Marine Science 76:1702–1712.

Gross, M. R. 1985. Disruptive selection for alternative life histories in salmon. Nature 313:47–48.

Hamel, S., J.-M. Gaillard, and N. Yoccoz. 2018. Introduction to: Individual heterogeneity – the causes and consequences of a fundamental biological process. Oikos 127:643–647.

Hartig, F. 2021. DHARMa: Residual diagnostics for hierarchical (multi-level / mixed) regression models. manual.

Healey, M., and W. R. Heard. 1984. Inter-and intra-population variation in the fecundity of chinook salmon (Oncorhynchus tshawytscha) and its relevance to life history theory. Canadian journal of fisheries and aquatic sciences 41:476–483.

Johnstone, J. A., and N. J. Mantua. 2014. Atmospheric controls on northeast Pacific temperature variability and change, 1900–2012. Proceedings of the National Academy of Sciences 111:14360–14365.

Kendall, B. E., and G. A. Fox. 2002. Variation among Individuals and Reduced Demographic Stochasticity. Conservation Biology 16:109–116.

Kristensen, K., A. Nielsen, C. Berg, H. Skaug, and B. Bell. 2016. TMB: automatic differentiation and Laplace approximation. Journal of Statistical Software, 70(5), 1-21.

Lewin, N., E. M. Swanson, B. L. Williams, and K. E. Holekamp. 2017. Juvenile concentrations of IGF-1 predict life-history trade-offs in a wild mammal. Functional Ecology 31:894–902.

Lok, T., C. J. Hassell, T. Piersma, R. Pradel, and O. Gimenez. 2019. Accounting for heterogeneity when estimating stopover duration, timing and population size of red knots along the Luannan Coast of Bohai Bay, China. Ecology and Evolution 9:6176–6188.

Mantua, N., I. Tohver, and A. Hamlet. 2010. Climate change impacts on streamflow extremes and summertime stream temperature and their possible consequences for freshwater salmon habitat in Washington State. Climatic Change 102:187–223.

Masson-Delmotte, V., P. Zhai, A. Pirani, S. L. Connors, C. Péan, S. Berger, N. Caud, Y. Chen, L. Goldfarb, M. I. Gomis, M. Huang, K. Leitzell, E. Lonnoy, J. B. R. Matthews, T. K. Maycock, T. Waterfield, O. Yelekçi, R. Yu, and B. Zhou. 2021. Summary for policymakers. In: Climate change 2021: The physical science basis. Contribution of working group I to the sixth assessment report of the intergovernmental panel on climate change.

McClintock, B. T., R. Langrock, O. Gimenez, E. Cam, D. L. Borchers, R. Glennie, and T. A. Patterson. 2020. Uncovering ecological state dynamics with hidden Markov models. Ecology letters 23:1878–1903.

Moran, E. V., F. Hartig, and D. M. Bell. 2016. Intraspecific trait variation across scales: implications for understanding global change responses. Global Change Biology 22:137–150.

Oosthuizen, W. C., G. Péron, R. Pradel, M. N. Bester, and P. J. N. de Bruyn. 2021. Positive early-late life-history trait correlations in elephant seals. Ecology 102:e03288.

Oosthuizen, W. C., M. Postma, R. Altwegg, M. Nevoux, R. Pradel, M. N. Bester, and P. J. N. de Bruyn. 2019. Individual heterogeneity in life-history trade-offs with age at first reproduction in capital breeding elephant seals. Population Ecology 61:421–435.

Plard, F., R. Fay, M. Kéry, A. Cohas, and M. Schaub. 2019. Integrated population models: powerful methods to embed individual processes in population dynamics models. Ecology 100:e02715.

R Core Team. 2021. R: A Language and Environment for Statistical Computing. R Foundation for Statistical Computing, Vienna, Austria.

Salguero-Gómez, R., C. Violle, O. Gimenez, and D. Childs. 2018. Delivering the promises of trait-based approaches to the needs of demographic approaches, and vice versa. Functional Ecology 32:1424–1435.

Scheuerell, M. D. 2005. Influence of juvenile size on the age at maturity of individually marked wild Chinook salmon. Transactions of the American Fisheries Society 134:999–1004.

Scheuerell, M. D., R. W. Zabel, and B. P. Sandford. 2009. Relating juvenile migration timing and survival to adulthood in two species of threatened Pacific salmon (Oncorhynchus spp.). Journal of Applied Ecology 46:983–990.

Schindler, D. E., R. Hilborn, B. Chasco, C. P. Boatright, T. P. Quinn, L. A. Rogers, and M. S. Webster. 2010. Population diversity and the portfolio effect in an exploited species. Nature 465:609–612.

Schroeder, R. K., L. D. Whitman, B. Cannon, and P. Olmsted. 2015. Juvenile life-history diversity and population stability of spring Chinook salmon in the Willamette River basin, Oregon. Canadian Journal of Fisheries and Aquatic Sciences 73:921–934.

Sorel, M. H., A. R. Murdoch, R. W. Zabel, C. M. Kamphaus, E. R. Buhle, M. D. Scheuerell, and S. J. Converse. *in review*. Effects of population density and environmental conditions on life-history expression in a migratory fish.

Stearns, S. C. 1989. Trade-offs in life-history evolution. Functional ecology 3:259–268.

Tattam, I. A., J. R. Ruzycki, J. L. McCormick, and R. W. Carmichael. 2015. Length and Condition of Wild Chinook Salmon Smolts Influence Age at Maturity. Transactions of the American Fisheries Society 144:1237–1248.

Thorson, J. 2020. TMBhelper: Package for basic helper functions that are not worth putting in a specialized contributed package. manual.

Tréhin, C., E. Rivot, L. Lamireau, L. Meslier, A.-L. Besnard, S. D. Gregory, and M. Nevoux. 2021. Growth during the first summer at sea modulates sex-specific maturation schedule in Atlantic salmon. Canadian Journal of Fisheries and Aquatic Sciences 78:659–669.

Vindenes, Y., S. Engen, and B. Sæther. 2008. Individual Heterogeneity in Vital Parameters and Demographic Stochasticity. The American Naturalist 171:455–467.

Waters, C. D., A. Clemento, T. Aykanat, J. C. Garza, K. A. Naish, S. Narum, and C. R. Primmer. 2021. Heterogeneous genetic basis of age at maturity in salmonid fishes. Molecular Ecology 30:1435–1456.

Wilson, S. M., T. W. Buehrens, J. L. Fisher, K. L. Wilson, and J. W. Moore. 2021. Phenological mismatch, carryover effects, and marine survival in a wild steelhead trout Oncorhynchus mykiss population. Progress in Oceanography 193:102533.

Zucchini, W., I. L. MacDonald, and R. Langrock. 2016. Hidden Markov models for time series: An introduction using R, second edition. Chapman and Hall/CRC.

Chapter 4. INTEGRATING INDIVIDUAL HETEROGENEITY INTO AN INTEGRATED POPULATION MODEL TO INFORM VIABILITY ANALYSIS

Publication history: This study was co-authored Jeffrey C. Jorgensen, Richard W. Zabel, Andrew R. Murdoch, Corey M. Kamphaus, and Sarah J. Converse. At the time this dissertation was published, this chapter was not in review with a journal.

Abstract: Individual heterogeneity within a population can have important effects on population dynamics. For example, heterogeneity in individual response to environmental variability can dampen temporal variability in abundance, a phenomenon known as the portfolio effect, which can in turn reduce risk to populations. To understand the role that individual heterogeneity plays in population trajectories, population models can account for individual heterogeneity. Integrated population modeling (IPM) is an approach to population modeling that offers a variety of benefits for information sharing and uncertainty propagation across data sets, but relatively few examples exist in which individual heterogeneity has been integrated into these models. We developed an IPM for an endangered population of Chinook salmon (Oncorhynchus tshawytscha) in Washington State, USA, which accounts for individual heterogeneity in juvenile life history, spawning location, and return age, allowing us to quantify and account for portfolio effects in population projections. In population projections, the year to year variability in adult abundance was reduced by 17% due to portfolio effects of juvenile life history diversity. Diversity in juvenile life history, spawning location, and return age have been identified as viability metrics for endangered salmon populations, and our work provides an empirical link between these metrics and population viability. We found that one of three studied spawning

aggregations had a 98% probability of dropping below a low-abundance threshold associated with increased extirpation risk, and that abundance criteria for recovery of the population were unlikely to be met in the next 50 years. These results suggest that management intervention may be necessary if recovery goals are to be achieved. We conclude that IPMs hold substantial promise for more thoroughly integrating individual heterogeneity into population viability analyses and predictions of management and environmental effects on populations.

Keywords: Portfolio effects; synchrony; life cycle model; data integration; Chinook salmon; endangered species; population projection; hatchery supplementation

4.1 INTRODUCTION

Individual heterogeneity, while often ignored or regarded as a nuisance in demographic parameter estimation, is an important biological phenomenon that influences and is influenced by life history trajectories, demography, and eco-evolutionary dynamics (Hamel et al. 2018). Individual heterogeneity can contribute to population stability when it results in asynchronous variability among individuals with different traits, a phenomenon known as the portfolio effect (Kendall and Fox 2002; Schindler et al. 2010). Some of this asynchrony may result from different demographic responses to environmental variability through time among individuals with unique traits (Gimenez et al. 2018; Forsythe et al. 2021). Furthermore, the distribution of heterogeneous life history traits such as growth, survival, and movement within a population may respond to population states (e.g., density dependence), which can in turn affect population trajectories (e.g., Martin et al. 2022). Therefore, considering individual heterogeneity may be key to understanding population-scale phenomena such as habitat use, population regulation, and response to environmental factors like anthropogenic climate change (Armstrong et al. 2021).

Increasingly, examples exist of ways in which individual heterogeneity can be accounted for in population models (Plard et al. 2019a). Matrix population models often include effects of discrete traits (e.g., natal habitat patch, resident vs. migrant) on demographic rates, while integral projection models include effects of continuous traits (e.g., natal latitude/longitude, migration timing) on demographic rates (Doak et al. 2021). Models can account for different traits being favored under different habitat conditions or population states, which may affect the fitness of individuals and the relative expression of different traits in the population through time (e.g., Reid et al. 2020). Furthermore, individual heterogeneity that is not tied to a particular trait can be accounted for, such as by using individual random effects (Gimenez et al. 2018). An array of modeling techniques accounting for different aspects of individual heterogeneity is being developed and applied to answer fundamental questions of population biology and to guide management in a changing world, resulting in more accurate and informative predictions of population dynamics (Forsythe et al. 2021).

In the past 20 years, integrated population models (IPMs) have become a critical tool for improving the accuracy and precision of population models (Besbeas et al. 2002). IPMs, which link multiple data sets through a common population process model via a joint likelihood, provide a framework for estimating population parameters from multiple data sources and are increasingly used in population management (Maunder and Punt 2013; Zipkin and Saunders 2018). While IPMs have greatly expanded our capabilities in population modeling, there have been relatively few examples illustrating how to effectively include individual heterogeneity in IPMs, and how those models can be applied to assess the effects of individual heterogeneity on population dynamics, and the effects of management actions and environmental variability on population trajectories (though see Plard et al. 2019a).

Endangered spring Chinook salmon in the Wenatchee River Basin of Washington, USA, exhibit multiple dimensions of individual heterogeneity, with important potential effects on population dynamics. First, each individual is hatched in, and as an adult, returns to one of several distinct spawning areas, and most but not all fish return to the same area where they were hatched (Honea et al. 2009). Second, individuals express different juvenile life history pathways (LHPs), determined by the timing of migration from the natal area; some juveniles rear within their natal tributary throughout their first year of life while others disperse to downstream-rearing habitat at a few distinct points (Buchanan et al. 2015). After a full year in freshwater, all juveniles embark on a migration to the marine environment. A third dimension of heterogeneity is the number of years spent at sea, which varies between one and three years in this population, before returning to freshwater to spawn and then die. Multiple datasets exist from several long-running monitoring programs to inform IPMs for these and other salmon in the Columbia River Basin (Hillman et al. 2020), including data on spawner abundance, juvenile abundance, and survival through the dammed mainstem Columbia River migration corridor (Ford et al. 2013; Buchanan et al. 2015; Murdoch et al. 2019). Managers need tools to evaluate the effects of hatchery supplementation, habitat modification, hydroelectric dams, and fisheries on population status of spring Chinook salmon and other endangered salmonids in the Columbia River Basin.

We developed an IPM for spring Chinook salmon in the Wenatchee River Basin of Washington, USA. Our model accounts for individual heterogeneity in spawning location, juvenile LHP, and return age. We used the model to evaluate population viability and the effect of individual heterogeneity on temporal variance in abundance (portfolio effects), while also providing a template for IPMs of other populations exhibiting important forms of individual heterogeneity. We found that juvenile life history diversity and the existence of multiple spatially distinct

spawning aggregations contribute to population stability. The risk of falling below 15 female spawners on average over a four-year period was low at the population level, but smaller spawning aggregations were at high risk. Furthermore, abundance did not meet recovery goals in projections. Our population viability analysis accounted for parametric uncertainty, environmental and demographic stochasticity, and density-dependent survival and life history expression. The model we developed provides a basis for evaluation of management scenarios in future work.

4.2 METHODS

4.2.1 *Study Species*

The Wenatchee River drains from the east side of the Cascade Mountain Range in central Washington state and meets the Columbia River at river kilometer 754 (Figure 4.1). Adult spring Chinook salmon return from the ocean to the Wenatchee River Basin in spring and spawn in autumn. Our model considers fish that spawn in three tributaries of the Wenatchee River — the Chiwawa River, Nason Creek, and the White River —which comprise approximately 90% of the population and which have been monitored for juvenile abundance as part of a hatchery-effectiveness monitoring program (Figure 4.1; Hillman et al. 2020). Juveniles emerge from nests in late winter and spend just over a year rearing within the Wenatchee River Basin before migrating to the ocean in their second spring of life. However, juveniles exhibit life history diversity: a portion rear within their natal tributary for the entirety of their freshwater juvenile rearing period, while others emigrate to downstream rearing areas at various times during their first year of life (Buchanan et al. 2015). Specifically, we consider the four juvenile LHPs identified in Sorel et al. (*in review a*; Ch. 2): three LHPs emigrate during their first year of life

(*downstream-rearing LHPs*) in spring (*spr.0*), summer (*sum.0*), and fall (*fal.0*), and one LHP emigrates at age 1 (*natal-reach-rearing LHP*) in spring (*spr.1*).

After migrating downstream through the mainstem Columbia River, which requires individuals to pass seven hydroelectric dams, fish enter the northeast Pacific Ocean where they typically rear for one to three years before maturing and returning through the Columbia River back to the Wenatchee River Basin to spawn. The population is supplemented by two integrated-conservation hatchery programs, which use natural-origin fish in their broodstock to keep the hatchery population more genetically related to the natural population. The programs release hatchery-origin juveniles in the Chiwawa River and Nason Creek, and a portion of returning adults from the hatchery population are allowed to pass upstream of Tumwater Dam to spawn with the natural population in the tributaries, contributing to natural production.

The population of spring Chinook salmon that spawn in the Wenatchee River Basin are part of the Upper Columbia River spring-run Evolutionarily Significant Unit (ESU), designated as endangered under the U.S. Endangered Species Act (ESA) in 1999. This ESU is one of 29 threatened or endangered salmon and steelhead conservation units listed under the ESA.

4.2.1 *Data sources*

We used several data sources to develop our IPM (Figure 4.2), including data from juvenile-migrant trapping to inform the abundance of juveniles expressing different LHPs, and mark-recapture data to inform juvenile survival rates, rates of return from the ocean (a function of survival and return age) and adult survival rates. We used data from surveys of the spawning grounds to inform female spawner abundance and the proportions of hatchery-origin spawners,

and auxiliary data on the number of fish collected for hatchery broodstock and adult sex ratios. We also used information from literature to develop informed priors on certain parameters.

Screw traps — We used estimates of the abundance of emigrants expressing different juvenile life history strategies generated from data collected at screw traps (Sorel et al. *in review* a; Ch. 2). A sample of juvenile emigrants from natal tributaries was captured in rotary screw traps operated downstream of spawning habitat. To estimate capture probability in the traps, mark-recapture trials were conducted wherein tagged fish were released upstream of traps and recaptures were recorded. The catch and mark-recapture data were used to estimate the abundance of daily emigrants (Sorel et al. *in review* a; Ch. 2).

Daily emigrant abundance estimates of each age were summed within discrete time periods each year that represented the four distinct juvenile LHPs – the three downstream-rearing LHPs (*spr.0*, *sum.0*, and *fal.0*) and the natal-reach-rearing LHP (*spr.1*; Sorel et al. *in review* a; Ch. 2). To account for uncertainty in estimates of the abundance of emigrants from each natal stream expressing each LHP each year, lognormal distributions were developed using a parametric bootstrap of daily abundance (Sorel et al. *in review* a; Ch. 2).

Mark-recapture data — A subset of emigrants captured in the screw traps that were >60 mm was marked with passive integrated transponder (PIT) tags prior to release (Figure 4.1). These fish could be recaptured at a screw trap near the confluence of the Wenatchee River and the Columbia River and could be detected in PIT-tag detection arrays when passing McNary and Bonneville Dams as juveniles and again as adults. Fish that survived to return to the Wenatchee River were detected when passing Tumwater Dam, just below the spawning grounds.

Hatchery removals and sex ratios — Some returning natural-origin adults were collected at Tumwater Dam and at weirs within spawning tributaries to serve in conservation hatchery broodstocks. Two conservation hatchery programs operate in the basin, in the Chiwawa River and Nason Creek, to supplement natural production. Both programs use natural-origin fish (born in the wild) as part of their broodstock to minimize genetic effects of allowing hatchery-origin fish (born in hatcheries) to spawn in the natural environment. The abundance and age composition of natural-origin adults collected for broodstock were recorded. Age was determined using the presence of a PIT tag that the fish received as a juvenile or, in the absence of a tag, by analysis of scales (Hillman et al. 2020). The sex of fish that were handled at Tumwater Dam and weirs was determined by examining external features visually and internal anatomy with a portable ultrasound.

Spawning-ground surveys — All known spawning habitat was walked by surveyors from the Washington Department of Fish and Wildlife and Chelan County Public Utilities Districts at 7- to 10-day intervals in August–September each year. Redds (nests) were counted and marked with flagging to avoid double-counting in subsequent surveys. In addition, the origin (hatchery vs. natural) of salmon carcasses recovered by surveyors was determined based on the presence of coded wire tags and clipped fins in hatchery-origin fish.

4.2.2 *Population process model*

The population process model consisted of the following components: functions for density-dependent juvenile production, survival rates, return rates from the ocean, return ages from the ocean, adult sex ratios, proportions of hatchery- and natural-origin spawners, a scalar for the number of eggs in five-year old females relative to four-year old females, and a scalar for the

production of juveniles by hatchery-origin spawners relative to natural-origin spawners (Figure 4.2). Environmental covariates were included on some demographic parameters to account for environmental variability that affects the population.

Juvenile production — The abundance of juvenile emigrants, $Juv_{h,y,s}$, expressing LHP *h* and emigrating in year *y* from stream *s* was calculated as a function of the effective number of female spawners, $S_{y(h),s}$ (defined in equation 8 below), in year y_h, which is one year before the emigration year for downstream-rearing LHPs and two years previous for natal-reach-rearing LHPs emigrants. To allow for both positive and negative density-dependence in the production of juvenile emigrants, we modeled juvenile production using the modified Beverton-Holt model of Myers et al. (1995),

$$Juv_{h,y,s} = \frac{\alpha_{h,s} S_{y_h,s}^{\gamma_{h,s}}}{1 + \frac{\alpha_{h,s} S_{y_h,s}^{\gamma_{h,s}}}{J_{h,s}^{\max}}} \exp\left(\epsilon_{h,y,s}\right) \quad (1)$$

with shape parameters $\alpha_{h,s}$, $\gamma_{h,s}$, and $J_{h,s}^{\max}$, specific to each LHP *h* and stream *s*, and process error $\epsilon_{h,y,s}$ specific to each LHP, stream, and year *y* (Sorel et al. *in review* a; Ch. 2). This model simplifies to the traditional Beverton-Holt model when $\gamma_{h,s}$ is equal to one, in which case $\alpha_{h,s}$ is interpretable as the asymptotic maximum production rate. However, when $\gamma_{h,s}$ is greater than one, it induces positive density dependence, and when it is less than one it induces negative density dependence. In either case, $\alpha_{h,s}$ is no longer interpretable as the asymptotic maximum juvenile production rate when $\gamma_{h,s} \neq 1$, but does affect productivity. As in the traditional

Beverton-Holt model, the $J_{h,s}^{\max}$ parameter is the asymptotic maximum expected juvenile abundance.

The shape parameters of the modified Beverton-Holt function were modeled hierarchically across streams, and penalties were applied to avoid overfitting (Sorel et al. *in review* a; Ch. 2). The lognormal process errors in juvenile abundance, $\epsilon_{h,y,s}$, for each LHP *h*, year *y*, and stream *s*, were modeled as a function of annual streamflow covariates, a latent variable that each LHP and stream loaded onto uniquely, and random effects of year that were unique to each LHP and stream. A detailed description of the juvenile production model is in Appendix D and Sorel et al. (*in review* a; Ch. 2).

4.2.3 *Survival and adult return*

The abundance of juvenile smolts (two-year olds) passing Bonneville Dam, $Smolts_{h,y,s}$ in year *y* from steam *s* that had expressed LHP *h* was the product of the number of emigrants and their survival rates $\phi_{h,y,s}^{r}$ over three intervals, *r*, between release and passing Bonneville Dam,

$$Smolts_{h,y,s} = Juv_{h,y,s} \prod_{r=1}^{3} \phi^{r}{}_{h,y,s} \,. \quad (2)$$

The three intervals were: 1) from release to the lower Wenatchee River screw trap, 2) from the lower Wenatchee to McNary Dam, and 3) from McNary Dam to Bonneville Dam (Figure 4.1). For downstream-rearing LHPs the year of smolting was the year following emigration whereas the natal-reach-rearing LHP initiated seaward migration in the same year as emigration.

During the first three survival intervals, we fit unique average survival rates for each LHP in each stream, synchronous random effects of year that were common to all LHPs and stream, and

asynchronous random effects that were unique to LHPs but common across streams (Appendix S.2). In the first survival interval, we included effects of winter air temperature on the survival of downstream-rearing LHPs. In the second and third survival intervals, we assumed that the three downstream-rearing LHPs had common survival rates within streams but allowed this to differ from the natal-reach-rearing LHP.

The number of adults $Ad.Bon_{h,y,s}$ that had expressed each LHP h from stream s returning to Bonneville Dam from the ocean in year y at adult age a was a product of smolt abundance, smolt-to-adult return rate, $\phi^{\mathrm{SAR}}{}_{h,y-a,s}$, and the conditional probability, $\psi_{h,y-a,s,a}$, of a smolt that entered the ocean in year y-a returning at age a, given that it returned:

$$Ad.Bon_{h,y,s,a} = Smolts_{h,y-a,s}\ \phi^{\mathrm{SAR}}{}_{h,y-a,s}\psi_{h,y-a,s,a} \quad (3)$$

We modeled ϕ^{SAR} similarly to survival during the third and fourth survival intervals, such that downstream-rearing LHPs were assumed to have common rates that differed from the natal-reach-rearing LHP, and we included random effects of year that were both synchronous and asynchronous between LHP types (Appendix S.2). We included effects of upwelling during the spring of ocean entry and sea surface temperature during fish's first marine summer as covariates on ϕ^{SAR}, allowing for unique effects on each LHP type (downstream- and natal-reach-rearing) but assuming common effects across streams. We allowed for different average $\psi_{h,y-a,s,a}$ parameter values for LHP types and fit random effects of year that were synchronous across LHPs and streams (Appendix S.2).

4.2.4 *Abundance of female spawners*

The abundance of adults returning to Tumwater Dam, $Ad.Tum_{h,y,s,a}$, was the product of the number of adults returning to Bonneville Dam and their upstream survival rates,

$$Ad.Tum_{h,y,s,a} = Ad.Bon_{h,y,s,a} \prod_{r=4}^{5} \phi_{y,a}^{r} \quad (4)$$

where the two upstream survival occasions, *r*, were 4) from Bonneville Dam to McNary Dam, and 5) from McNary Dam to Tumwater Dam. We allowed upstream survival to vary by adult age but assumed that it was common across LHPs and natal streams (Appendix E). We included random effect of year that were synchronous across all fish for upstream survival.

The total number of natural-origin adults returning to Tumwater Dam, $Ad.Tum_{y,s}$, from stream *s* in year *y*, was the sum of returning adults across ages *a* and juvenile LHPs *h*: $Ad.Tum_{y,s} = \sum_{a=3}^{5} \sum_{h} Ad.Tum_{h,y,s,a}$. The abundance of natural-origin female spawners, $S.NO_{y,s}$, was the abundance of adults that returned to Tumwater Dam less fish removed for hatchery broodstock, $B_{y,s,a}^{\mathrm{Rem}}$ multiplied by the proportion of returning adults that were female $p_{y,s}^{\mathrm{F}}$ and survived from Tumwater Dam to spawning, ϕ^{PS}.

$$S.NO_{y,s} = p_{y,s}^{F} \phi^{\mathrm{PS}} \quad (5)$$

Fish are collected for the Chiwawa River hatchery broodstock either at a weir in the Chiwawa River or at Tumwater Dam if they can be identified as having originated from the Chiwawa River based on PIT tags inserted as juveniles, so all fish for the Chiwawa Broodstock originate in

the Chiwawa River (NMFS 2015). However, for the Nason Creek broodstock, natural-origin fish of unknown origin are collected at Tumwater Dam because of the difficulty of trapping fish in Nason Creek and the small number of marked fish returning to Nason Creek. Fish from the White River are not collected because they can be differentiated based on genetics. To reflect this in the model, the broodstock for the Nason Creek supplementation program was composed of fish originating from the Chiwawa River and Nason Creek in proportion to their abundance. The abundance of natural-origin returns collected for the Nason Creek program broodstock that originated from Nason Creek, $B^{\text{Nason}}_{y,a,\text{Nason}}$, was calculated as

$$B^{\text{Nason}}_{y,a,\text{Nason}} = B^{\text{obs}}_{y,a,\text{Nason}}\, Ad.Tum_{y,\text{Nason}} / \left(Ad.Tum_{y,\text{Chiwawa}} - B^{\text{obs}}_{y,a,\text{Chiwawa}} + Ad.Tum_{y,\text{Nason}}\right) \quad (6)$$

where $B^{\text{obs}}_{y,a,\text{Nason}}$ is the observed total number of fish of age *a* collected for the Nason Creek program broodstock from both streams, $Ad.Tum_{y,\text{Nason}}$ is the latent abundance of adults from Nason Creek returning to Tumwater Dam, $Ad.Tum_{y,\text{Chiwawa}}$ is the latent abundance of adults from the Chiwawa River returning to Tumwater Dam, and $B^{\text{obs}}_{y,a,\text{Chiwawa}}$ is the observed abundance of adults returning from the Chiwawa River collected for the Chiwawa River hatchery program broodstock. The abundance of natural-origin returns from the Chiwawa River collected for the Nason Creek hatchery broodstock was, $B^{\text{Chiwawa}}_{y,a,\text{Nason}} = B^{\text{obs}}_{y,a,\text{Nason}} - B^{\text{Nason}}_{y,a,\text{Nason}}$. The total number of adults from the Chiwawa River collected for broodstock, $B^{\text{rem}}_{y,a,\text{Chiwawa}}$, (used in equation 5) was therefore $B^{\text{obs}}_{y,a,\text{Chiwawa}} + B^{\text{Chiwawa}}_{y,a,\text{Nason}}$ and for Nason Creek it was simply $B^{\text{Nason}}_{y,a,\text{Nason}}$

The number of female spawners of hatchery origin that spawned in the wild in year *y* and stream *s*, $S.HO_{y,s}$, was calculated based on the number of natural-origin spawners, $S.NO_{y,s}$, and the proportion of hatchery-origin spawners, $p_{y,s}^{\mathrm{HO}}$,

$$S.HO_{y,s} = \frac{S.NO_{y,s}\, p_{y,s}^{\mathrm{HO}}}{1 - p_{y,s}^{\mathrm{HO}}}. \quad (7)$$

To calculate the effective number of female spawners, $S_{y,s}$, used in equation 1, we weighted the numbers of spawners to account for the greater number of eggs in older natural-origin fish relative to younger natural origin fish (we did not model the age structure of hatchery-origin fish) and the lower production of juvenile emigrants by hatchery-origin relative to natural-origin spawners (relative reproductive success; Ford et al. 2013):

$$S_{y,s}^{\mathrm{f}} = \left[S.NO_{y,s}\left(1 + \frac{Ad.Tum_{h,y,s,5}}{Ad.Tum_{h,y,s,4} + Ad.Tum_{h,y,s,5}}\delta\right)\right] + S.HO_{y,s}p^{\mathrm{RRS}} \quad (8)$$

where δ is the percent difference between the productivity of five- and four-year-old natural origin spawners and is restricted to be positive, and p^{RRS} is the productivity of hatchery-origin female spawners relative to four-year old natural-origin females and is restricted to be between 0 and 1. We assumed that all three-year-old spawners were male, whereas all female spawners are either four-year-olds or five-year-olds (Hillman et al. 2020). We assumed that the sex ratios for four- and five-year-old adults were the same as one another.

To initialize the model, we fit parameters for natural-origin female spawner abundance in the first five years. We assumed that the population age structure in the first five years was equal to the expected value of the age structure of adults returning from the ocean across downstream-

and natal-reach-rearing LHPs, which was necessary to calculate the effective number of spawners in equation 8. The abundances of spawners in the sixth year and beyond were calculated from the effective number of spawners in the first five years and the population process model.

4.2.5 *Joint likelihood*

The observed abundances of juvenile emigrants and total female-spawners were assumed to be lognormally distributed around the latent values from the population model,

$$\begin{gathered}\overline{M^*_{h,y,s}} \sim N\left(\log\left(Juv_{h,y,s}\right), \sigma^{\overline{M^*}}_{h,y,s}\right), \\ \log\left(S.obs_{\,y,s}\right) \sim N\left(log\left(S.NO_{y,s} + S.HO_{y,s}\right), \sigma_S\right),\end{gathered} \tag{9}$$

where $\overline{M^*_{h,y,s}}$ and $\sigma^{\overline{M^*}}_{h,y,s}$ are the log mean and standard deviation, respectively, of juvenile abundance in LHP *h*, year *y*, and natal stream *s* estimated from a model of daily abundance fit to screw-trap data (Sorel et al. *in review* a; Ch. 2), $S.obs_{\,y,s}$ is the observed count of redds, and σ_S is the observation standard error for redd counts. We applied an informed lognormal prior on the observation standard error for redd counts, $\log(\sigma_S) \sim N(log(0.10), 0.25)$ based on estimates from studies of observation error in redd counts (Chasco et al. 2014; Murdoch et al. 2019).

The multistate-model likelihood for each PIT-tagged fish released from a rotary screw trap was calculated with the forward algorithm (see Zucchini et al. 2016, McClintock et al. 2020), while accounting for imperfect detection. Details of the observation model for the multistate model are included in Appendix S.2 and Sorel et al. (*in review* b; Ch. 3). We did not have data to directly inform the survival of spr.0 emigrants, because they were almost all too small to be tagged

(<60mm) upon emigration. We therefore used a relationship between fork length at emigration and survival during the first interval for sum.0 emigrants, as well as the average fork lengths of the spr.0 and sum.0 emigrants, to estimate the difference in survival between the spr.0 and sum.0 LHPs during the first interval (Appendix E). All downstream-rearing LHPs were assumed to have common demographic rates after the first interval.

Data on the sex ratio of adults came from an examination of a composite of fish from all spawning areas upstream of Tumwater dam, including those not considered in the IPM. We therefore assumed that observations of the proportion of adults that were female, $p_{\mathrm{y}}^{\mathrm{F_{obs}}}$, in year *y* were a noisy measure of the true proportion of adults that were female within each stream *s* and year *y*, $\mathrm{logit}\left(p_y^{\mathrm{F_{obs}}}\right) \sim N\left(\mathrm{logit}\left(p_{s,y}^{\mathrm{F}}\right), 0.25\right)$, with an observation SE of 0.25. We also assumed that the annual proportions of returning adults that were female were normally distributed on the logit scale, $\mathrm{logit}\left(p_{s,t}^{\mathrm{F}}\right) \sim N\left(\mu_{p^{\mathrm{F}}}, \sigma_{p^{\mathrm{F}}}\right)$, with average $\mu_{p^{\mathrm{F}}}$ and standard deviation $\sigma_{p^{\mathrm{F}}}$ across streams and years.

We did not have data on the pre-spawn survival rates between when fish pass Tumwater Dam as adults and when they spawn. We therefore assumed a constant rate, ϕ^{PS} across years and streams, which was informed by a prior: $\mathrm{logit}(\phi^{\mathrm{PS}}) \sim N(\mathrm{logit}(0.85), 0.50)$, with parameters based on a meta-analysis of pre-spawn survival rates (Bowerman et al. 2016).

The percent difference in the number of eggs between four- and five-year old females, δ, was based on counts of eggs within natural-origin females used in hatchery broodstock between 1997 and 2020. The average fecundity of natural-origin four-year-old spawners was 4,437 eggs (n = 519, sd = 682), and for five-year-old females it was 5,507 (n = 133, sd = 897) (Hillman et al.

2020). Based on this information, we applied an informative prior on δ,

$$\log(\delta) \sim \mathrm{N}\left(\log\left(\frac{5{,}507}{4{,}437} - 1\right), 0.1\right).$$

The proportion of hatchery-origin spawners, $p_{y,s}^{\mathrm{HO}}$, was informed by the numbers of hatchery-origin carcasses recovered on the spawning grounds, $C_{y,s}^{\mathrm{H}}$, out of the total number of carcasses, $C_{y,s}$, recovered. However, Murdoch et al. (2010) found that carcass-recovery probabilities were affected by fish length, which induced observation error in the proportion of hatchery-origin carcasses recovered above that of a binomial sample. We therefore modeled the number of hatchery-origin carcasses as Poisson distributed, with rate equal to the product of the total number of carcasses and the proportion of hatchery origin spawners, $C_{y,s}^{\mathrm{H}} \sim \mathrm{Poisson}\left(C_{y,s}\, p_{y,s}^{\mathrm{HO}}\right)$. To regularize $p_{y,s}^{\mathrm{HO}}$ values away from boundaries at 0 and 1, we assumed that they were normally distributed around a mean, $\mu_{p^{\mathrm{HO}}}$, on the logit scale, $\mathrm{logit}\left(p_{y,s}^{\mathrm{HO}}\right) \sim \mathrm{N}\left(\mu_{p^{\mathrm{HO}}}, \sigma_{p^{\mathrm{HO}}}\right)$ with standard deviation $\sigma_{p^{\mathrm{HO}}}$. We applied an informative prior on the relative reproductive success of hatchery-origin spawners, $\mathrm{logit}(p^{\mathrm{RRS}}) \sim \mathrm{N}(\mathrm{logit}(0.53), 1.0)$ based on the results of Ford et al. (2013).

4.2.6 *Posterior sampling*

The model was developed in Template Model Builder (Kristensen et al. 2016) in R version 4.1.2 (R Core Team 2021), and posterior samples were generated using the No-U-Turn Sampler (NUTS) in Stan (Carpenter et al. 2017), implemented with the tmbstan package (Monnahan and Kristensen 2018). Uniform priors were applied for all model parameters for which a prior is not described above or in Appendices S.1 and S.2. We sampled the posterior distributions of model parameters using three Markov chains with 2,000 posterior draws each, using the first 500

iterations for warmup. To evaluate whether the chains had converged, we confirmed that potential scale reduction factors (i.e., $\hat{R}$) were less than 1.02 and that Monte Carlo standard errors were < 5% of posterior standard errors. We ensured that there were no divergent transitions in any of the chains, which would indicate a failure of the NUTS algorithm.

4.2.7 *Population viability analysis*

To evaluate population viability, we projected the population into the future for 50 years. Future demographic rates were based on realizations of random processes (i.e., random effects of year), environmental covariates, and hatchery management decisions. All random effects of year other than $p_{y,s}^{\mathrm{HO}}$ were sampled from their hyper-distributions when simulating demographic rates for projections. Rather than calculating the number of hatchery-origin spawners based on $p_{y,s}^{\mathrm{HO}}$, as we did when fitting the model (equation 7), the number of hatchery-origin spawners in projections was determined by an abundance-based control rule designed to meet the constraints in the hatchery genetic management plans (HGMPs; Appendix F; Chelan PUD and WDFW 2009, Grant PUD et al. 2009). Management decisions about the abundance of natural-origin returns to collect for hatchery broodstock in projections also followed abundance-based control rules defined in the HGMPs.

Environmental covariate simulation — To generate future times series of environmental covariates with similar temporal and among-variable correlation structure as the historical covariate values, we fit models to the historical time series of the environmental covariates used in the IPM, which we then sampled from to simulate covariates to calculate demographic parameters during the projection period. We used longer times series of covariates to fit the models than were used to estimate demographic parameters to maximize the information used to

inform future covariate trajectories. We assessed whether there were trends in the historical time series of covariates, which might reflect climate change. Covariate model fitting and simulation were conducted using the MARSS package in R (Holmes et al. 2012). Additional details on covariate modeling and simulation are provided in Appendix G.

Hatchery supplementation — Management decisions regarding hatchery supplementation were simulated based on control rules that satisfied the constraints outlined in HGMPs (Chelan PUD and WDFW 2009, Grant PUD et al. 2009) and the biological opinion (NMFS 2015) for the programs (Appendix F). The two decisions that were made annually in the model for each program were the number of natural-origin adults collected for hatchery broodstock and the number of hatchery-origin adults released to spawn in the natural environment. Each of these decisions was made based on the forecasted number of natural-origin adults returning to Tumwater Dam, because no more than 30% of forecasted natural-origin returns were collected for broodstock and the number of hatchery-origin adults released onto the spawning grounds decreases with increasing natural-origin adult abundance. Details of the implementation of hatchery management rules in the model are in Appendix F.

Population viability metrics — To account for parametric uncertainty and stochasticity, we simulated 100 prospective population trajectories for each of 500 parameter sets (every 9th posterior sample, randomly selecting one of 1,500 simulated multivariate environmental-covariate time series for each projection. We characterized future abundance based on the geometric mean of natural-origin female spawner abundance over the 50 projected years (2020-2069). Another dimension of viability is a population having a low probability of declining to low abundance, where risks of inbreeding depression and reduced mate finding success increase. This has often been referred to as the probability of falling below a quasi-extinction threshold

(p $^{\mathrm{QET}}$; e.g., Buhle et al. 2018; Crozier et al. 2021). We defined p^{QET} as the probability of the four-year mean natural-origin female spawner abundance falling below 15. To evaluate parametric uncertainty around p^{QET}, we calculated the proportion of the 100 simulations conducted with each parameter set in which the four-year mean fell below 15 spawners. As a metric to describe the genetic effects of introgression with the hatchery population, we calculated the across-year average Proportionate Natural Influence (PNI; Paquet et al. 2011), $\mathrm{PNI}_{y,s} = p_{y,s}^{\mathrm{NOB}}/(p_{y,s}^{\mathrm{NOB}} + p_{y,s}^{\mathrm{HO}})$, where $p_{y,s}^{\mathrm{NOB}}$ is the proportion of the broodstock for the hatchery program in stream *s* in year *y* composed of natural-origin spawners, and $p_{y,s}^{\mathrm{HO}}$ is the proportion of fish spawning in the natural-environment that are of hatchery origin. Higher PNI is associated with a lower effect of hatchery supplementation on the natural adaptations of fish to their environment (Paquet et al. 2011). We conducted a sensitivity analysis to evaluate the effect of parametric uncertainty on projected abundance. Detailed methods and results of the sensitivity analysis are included in Appendix H.

Portfolio effects — We calculated portfolio effects attributable to asynchrony among LHPs and natal streams. To do so, we calculated the CV of natural-origin adults returning to Tumwater Dam for each juvenile LHP and natal stream as well as for the total spawner abundance across LHPs within each natal stream and for the total spawner abundance across natal streams and LHPs. We calculated portfolio effects as $1 - \frac{CV^{\mathrm{Total}}}{CV^{\mathrm{Mean}}}$ where CV^{Total} was the CV of the aggregate return across LHPs or natal streams and CV^{Mean} was the average of the CVs of individual LHPs or natal streams, weighted by their relative abundance (Schindler et al. 2010; Carlson and Satterthwaite 2011).

4.3 RESULTS

The median across simulations of the geometric mean abundance of projected natural-origin female spawners was 80 (90% quantile range = 46 – 229) in the Chiwawa River, 26 (14 – 74) in Nason Creek, 10 (2 – 40) in the White River, and 128 (73 – 378) in total across all three streams (Figure 4.3). The probability that the four-year running mean of natural-origin female spawner abundance dropped below 15 in the projection was 0.00 (0.00 – 0.09) in the Chiwawa River, 0.77 (0.07 – 1.00) in Nason Creek, 1.00 (0.77 – 1.00) in the White River, and 0.00 (0.00 – 0.00) for the three streams combined (Figure 4.4).

The average projected proportion of hatchery-origin spawners (p^{HOS}) was 0.41 (90% quantile range = 0.11 – 0.62) in the Chiwawa River, 0.43 (0.12 – 0.66) in Nason Creek, and 0.17 (0.03 – 0.50) in the White River (Figure I1). The average proportion of broodstock that was of natural-origin (p^{NOB}) was 0.64 (0.43 – 0.91) in the Chiwawa River and 0.14 (0.01 – 0.60) in Nason Creek (Figure I2). The average PNI for the Chiwawa River supplementation program was 0.61 (0.41 – 0.90) and for the Nason Creek program it was 0.18 (0.03 – 0.64); Figure I3).

The average proportion of projected natural-origin adults returning to Tumwater that had expressed the natal-reach-rearing LHP (*spr.1*) as juveniles was 0.58 (90% quantile = 0.44–0.70) in the Chiwawa River, 0.32 (0.15–0.51) in Nason Creek, 0.72 (0.40–0.88) in the White River, and 0.54 (0.37–0.68) across all three streams (Figure 4.5). The remaining adults had expressed downstream-rearing LHPs (*spr.0*, *sum.0*, and *fal.0*) as juveniles. Of the three downstream rearing LHPs, the *fal.0* LHP was the most abundant, followed by the *sum.0* LHP, and the *spr.0* LHP contributed a considerably smaller amount toward total abundance.

On average across simulations, the CV of projected natural-origin adult returns to Tumwater Dam was 16% (90% quantile = 8–27%) lower than the weighted average of CVs across LHPs in the Chiwawa River, 20% (7–32%) lower in Nason Creek, 9% (2–22%) lower in the White River, and 17% (7–28%) lower for the aggregate abundance across streams (Figure 4.6). The CV of the aggregate abundance across LHPs and streams was 27% (15–39%) lower than the weighted average of CVs across individual LHPs and natal streams, and 7% (2–15%) lower than the weighted average of the CVs of the total returns to individual streams. Returns of fish that had expressed the *fal.0* LHP had the lowest CV in each stream (Figure I4).

4.4 DISCUSSION

While the productivity of this endangered salmon population did not appear sufficient to meet recovery goals for abundance, the risk of falling below the quasi-extinction threshold was low at the full population scale. By accounting for individual heterogeneity in juvenile LHPs in our model we were able to identify that asynchronous variability among LHPs dampened the variance in overall abundance, which reduced the risk of it falling below a quasi-extinction threshold. Our model provides an example of how individual heterogeneity influences populations due to the differential effects of environmental conditions on demographic performance of different traits (i.e., LHPs) and density dependence in the relative frequency of alternative traits.

In our population projections, the average abundance of wild female spawners was considerably less than half of the recovery goal of 2,000 adults in the Wenatchee River Basin (UCSRB and NMFS 2007). There is some production from spawning habitat that we did not model, but the unmodeled production generally only makes up about 10% of the population (Hillman et al.

2020). Considerable numbers of hatchery-origin fish also spawned in the wild in our simulations. The average projected PNI of both supplementation programs were below the 0.67 minimum level suggested in the Biological Opinions for the programs (NMFS 2015), indicating a higher than preferred effect of supplementation on the genetic adaptations of the population to its habitat.

In our projections, the probability of the population dropping below the quasi-extinction threshold, p^{QET}, was 0.0 at the scale of the entire basin over a 50-year interval but was non-negligible in two of three spawning streams, which also had lower average spawner abundances. The differences in p^{QET} among natal streams raises the question of how demographically isolated these spawning aggregations truly are, because the exchange of individuals could reduce the risks of smaller populations falling below the quasi-extinction threshold, and the risks if they were too. Previous studies have found that stray rates of natural-origin adults are relatively low (2-7%) in this population (Ford et al. 2015; Pearsons and O'Connor 2020), but straying could be accounted for in future population models.

We also examined the role of individual heterogeneity in dampening population variability (i.e., portfolio effects). Intuitively, abundance in natal streams that had more juvenile life history diversity, measured as having more similar proportions of natal-reach- and downstream-rearing LHPs, had the greatest dampening in variability attributable to life history diversity. Abundance of the *fal.0* LHP was the least variable through time of the four LHPs but was the numerically dominant LHP in only one of three natal streams. We also documented portfolio effects of multiple distinct spawning aggregations, although the structure of the model, wherein random effects of year on survival and return were assumed to be synchronous among natal streams, somewhat limited our ability to fully evaluate these portfolio effects. It may be possible to

effectively estimate random effects of year on survival unique to each stream, but that would likely require more years of data. The maintenance of multiple spatially distinct spawning aggregations and life history diversity within the population are commonly considered to be conservation objectives for at-risk salmon populations due to their benefits for population stability (Phillis et al. 2018; Cordoleani et al. 2021), and our results provide a quantitative assessment of this benefit.

Our population viability analysis suggests that management interventions may be necessary to meet recovery goals for abundance, and our model could be used to simulate the outcomes of alternative actions. For example, population trajectories could be simulated under alternative hatchery-control rules and with modified demographic parameters to represent habitat management actions (e.g., Saunders et al. 2018; Nater et al. 2022; Honea et al. 2009). This would provide policy makers with estimates of expected population viability metrics (e.g., abundance, p^{QET}, and PNI) across a range of different management scenarios to help inform decisions. There is also interest in better understanding the effects of climate change on the population under alternative management actions, which could be explored by adding trends to the values of climate-driven covariates used in projections (e.g., Crozier et al. 2021). Our model's accounting for unique effects of environmental conditions and population abundance on the productivity of different population components could improve predictions of responses to management and climate change relative to a model where this heterogeneity is ignored (Plard et al. 2019a; Armstrong et al. 2021). Our projections accounted for trends of decreasing spring upwelling and increasing summer sea surface temperature and their effects on return-rates of fish that express different LHPs.

A challenge of accounting for demographic heterogeneity as a function of individual traits is that it requires fitting more parameters which generally increases parametric uncertainty. But statistical methods are available to efficiently share information about parameter values across discrete (e.g., natal habitat patch, resident vs. migrant) or continuous (e.g., natal latitude/longitude, migration timing) trait values (Schaub and Kéry 2012). Specifically, random effects can be used to leverage shared information across groups or across the range of continuous variables (Pedersen et al. 2019) and can be fit within fully Bayesian or marginal maximum likelihood frameworks (Herliansyah et al. 2022). Our model provides an example of how these techniques can be used to share information about average demographic rates and their variance through time.

A primary goal of accounting for individual heterogeneity in population models is to capture how the distribution of traits within a population interacts with environmental factors to shape population trajectories (Fox and Kendall 2002; Hamel et al. 2018; Plard et al. 2019a). This may include modeling how environmental factors affect the distribution of traits, including both plastic and evolutionary responses to factors like population density and habitat conditions (Vindenes and Langangen 2015; Plard et al. 2019b). Accounting for heterogeneity allows for modeling of different effects of environmental conditions on vital rates among individuals (e.g., Henn et al. 2018), which can help with predicting population responses to climate change, management, and other environmental changes that may favor particular life history traits over others (Vindenes and Langangen 2015; Johnston et al. 2019). Understanding how variability in life history traits translates to reduced variability in population abundance through time provides insights into the implications of the loss of life history diversity for the extinction risk of small

populations and the sustainable provisioning of ecosystem services (Kendall and Fox 2002; Schindler et al. 2010; van Daalen and Caswell 2020; Armstrong et al. 2021).

4.5 ACKNOWLEDGEMENTS

This research was funded by the National Oceanographic and Atmospheric Administration Northwest Fisheries Science Center, the Washington Cooperative Fish and Wildlife Research Unit, and the Northwest Climate Adaptation Science Center. Data was provided by Grant County Public Utilities District, Chelan County Public Utilities District, the Washington Department of Fish and Wildlife, Yakama Nation Fisheries, Bonneville Power Administration, Washington Department of Ecology, the U.S. Geological Survey, the U.S. National Weather Service, and others. This work would not be possible if not for the tremendous efforts of those who monitor Chinook salmon in the Wenatchee River Basin and the Columbia River and maintain databases for storing and accessing data. I thank Abby Bratt for helpful suggestions on a previous version of this chapter. Any use of trade, firm, or product names is for descriptive purposes only and does not imply endorsement by the U.S. Government.

4.6 FIGURES & TABLES

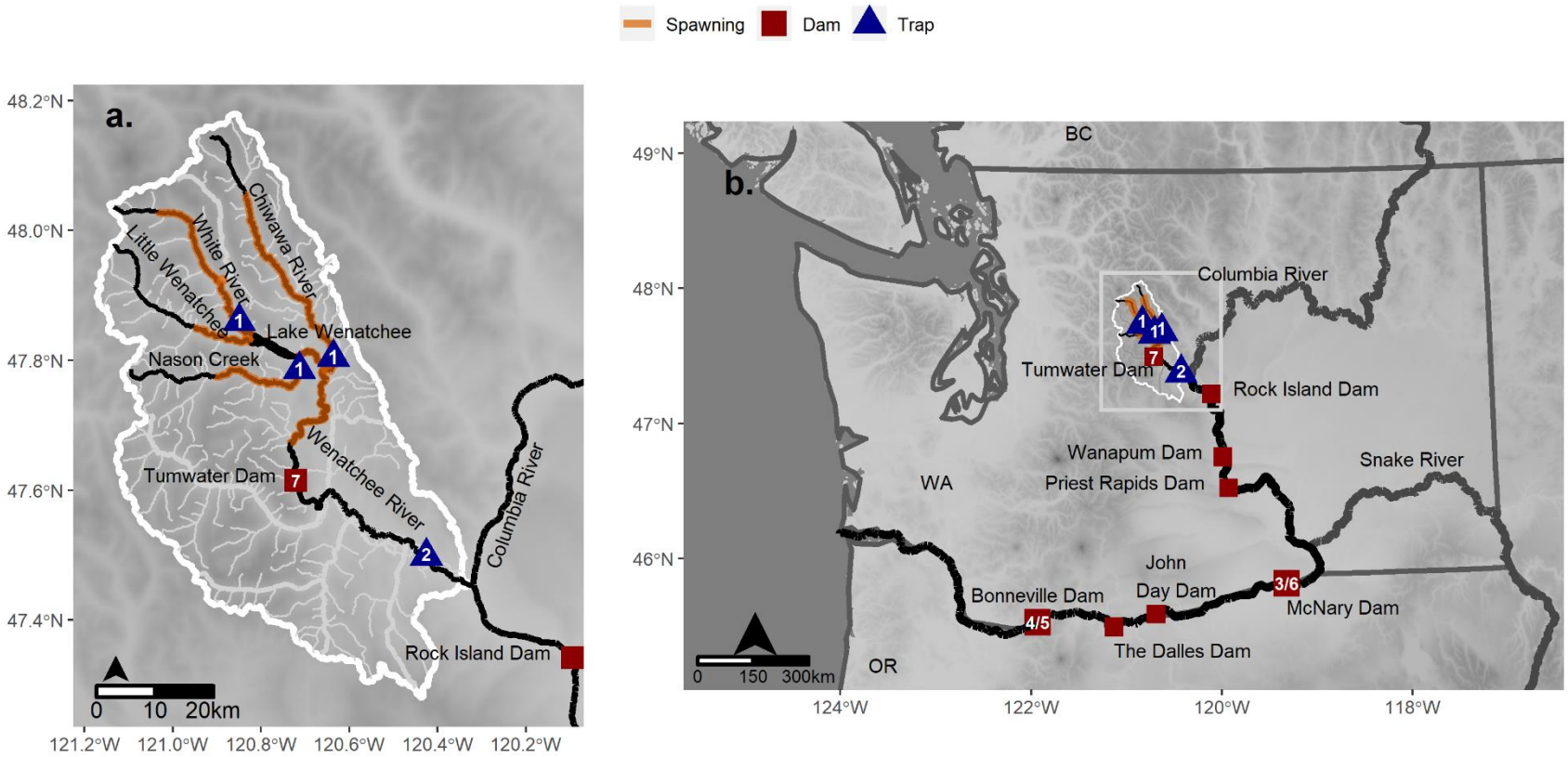

Figure 4.1: Maps of the Wenatchee River Basin (a) and the Columbia River migration corridor (b). The numbers on dams and traps represent the detection occasions corresponding with fish passing each location. Detections of both juveniles moving downstream and adults moving upstream past McNary and Bonneville Dams were used.

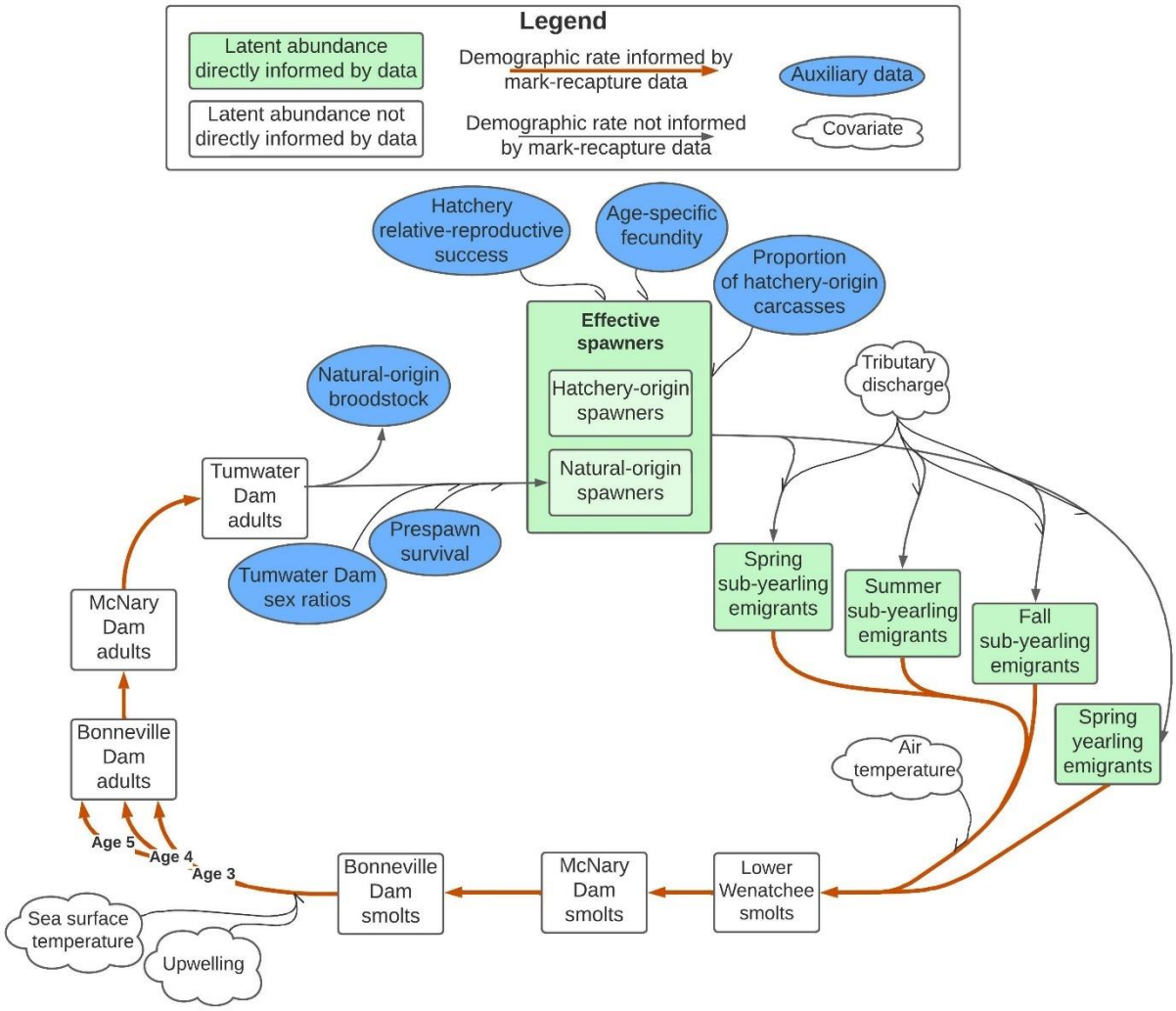

Figure 4.2: Conceptual diagram of population model. Square boxes represent population states (i.e., life stage abundances) and arrows connecting boxes represent demographic rates (i.e., juvenile production, survival, and maturation). Green boxes are directly informed by abundance data, whereas white boxes are not. Orange arrows are directly informed by mark-recapture data whereas black lines are not. Blue ovals represent auxiliary data that inform population states and demographic rates, and white clouds represent environmental covariate data.

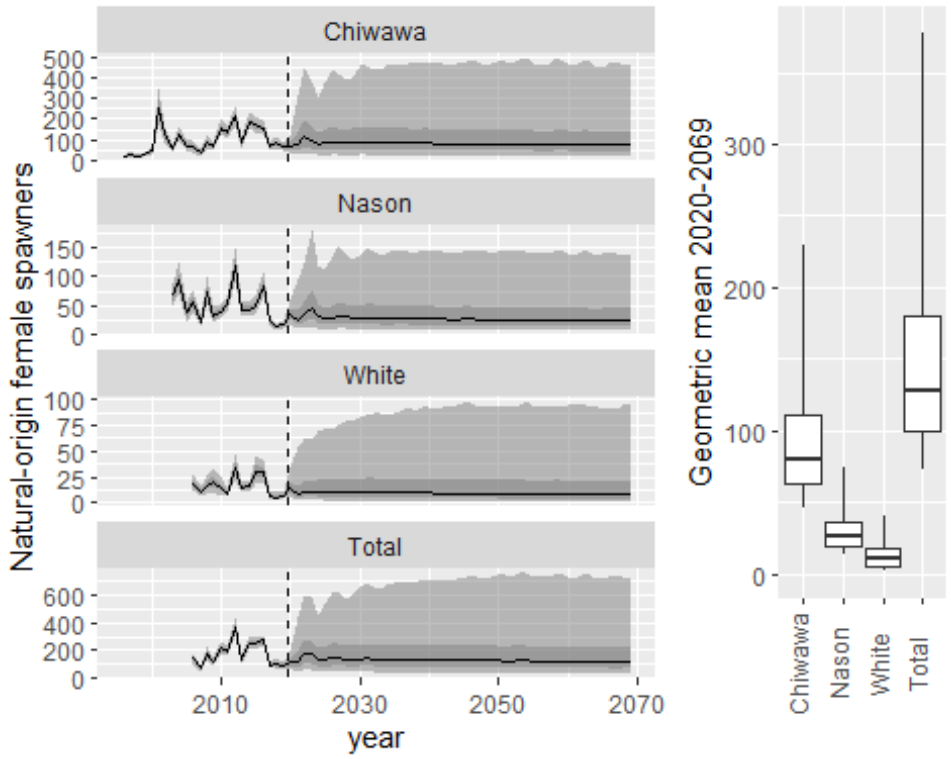

Figure 4.3: *Left panel*: Natural-origin female spawner abundance in three natal streams and the total across streams. Years to the left of the dotted line were fit to data and years to the right of the dotted line were projected. Lines represents medians across simulations, dark shaded envelopes represent interquartile ranges and light shaded envelopes represents 90% quantile ranges. Y-axis scales differ across streams. *Right panel*: Boxplots are of the geometric mean abundance in years 2020-2069 across projections. Horizontal lines represent medians, boxes span interquartile ranges and whiskers span 90% quantile ranges.

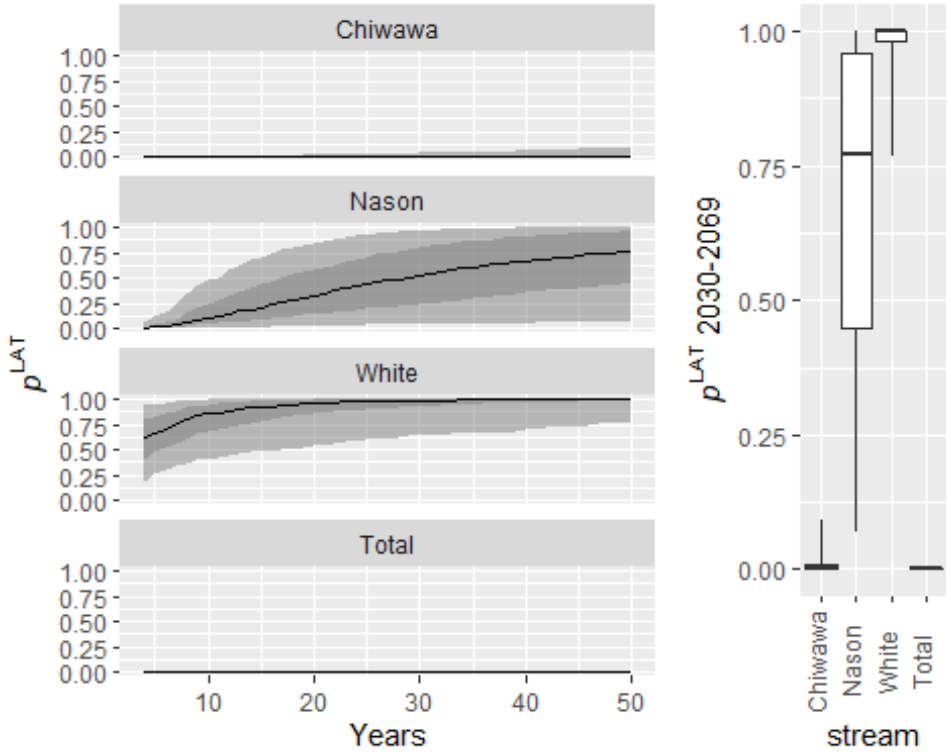

Figure 4.4: *Left panel*: Proportion of projections in which the four-year running mean of natural-origin female spawner abundance fell below a quasi-extinction threshold of 15 (p^{QET}) at least once over periods of increasing numbers of years (x-axis), calculated for projection years 2020–2069. Shaded envelope represents 90% quantiles from a bootstrap. *Right panel*: Boxplots are of the p^{QET} over the full 50-year projection period. Horizontal lines represent medians, boxes span interquartile ranges and whiskers span 90% quantile ranges. The high p^{QET} in the White River indicate considerable demographic risk for that spawning aggregation.

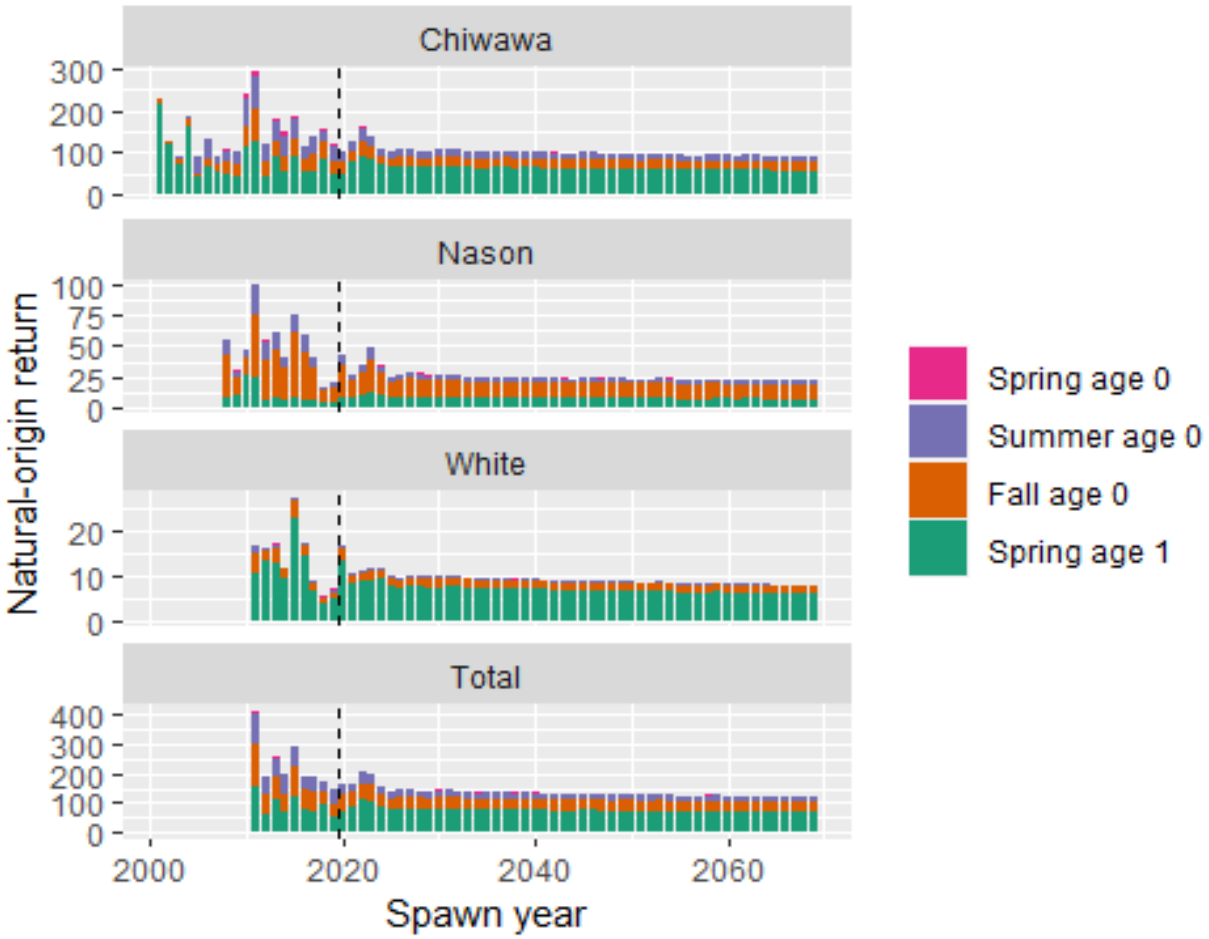

Figure 4.5: Median abundance of natural-origin adults returning to Tumwater Dam by year and juvenile life history pathway (LH; color) for three natal streams and the total across streams. Vertical dashed lines delineate years fit to data from projections.

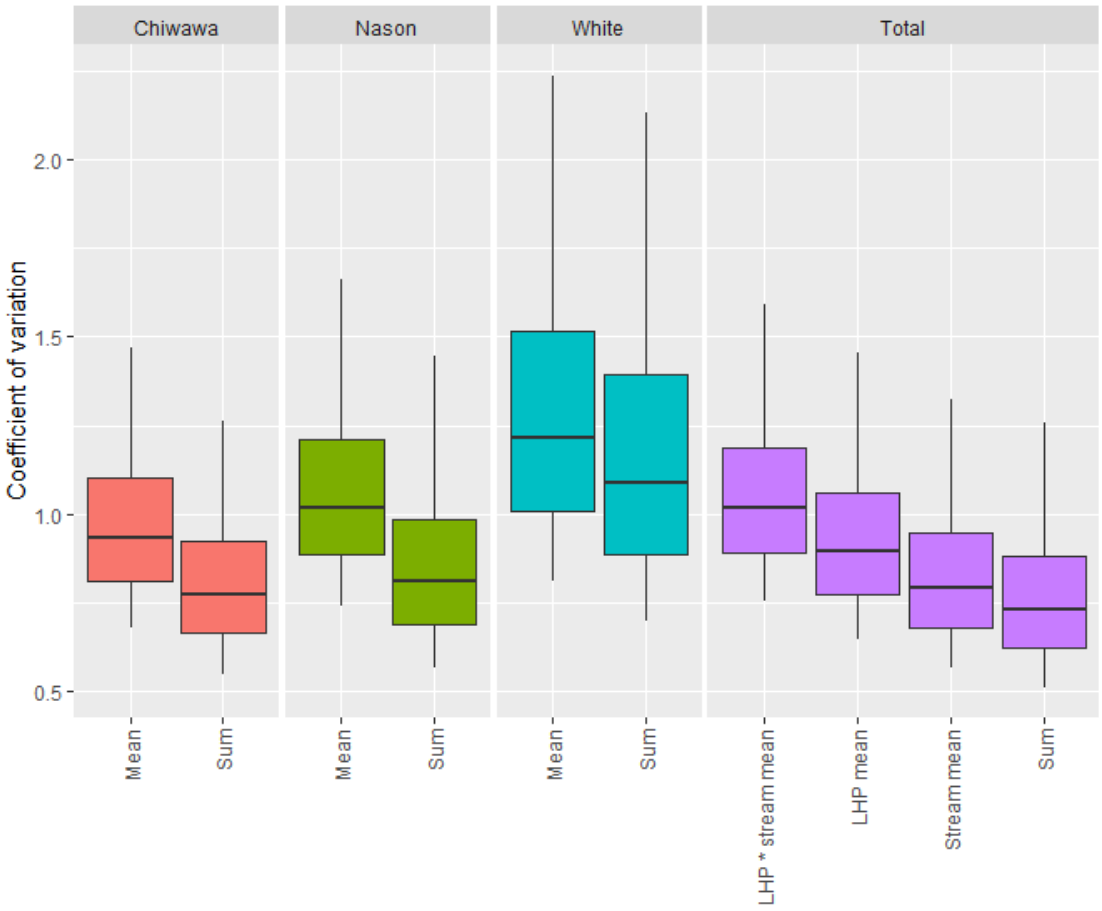

Figure 4.6: Boxplots of the coefficients of variation (CV) of simulated abundance of natural-origin adults returning to Tumwater Dam in 2020-2069. *Means* for Chiwawa, Nason, White, and Total represent average CVs across LHPs within each stream or for the total abundance across streams. *Sums* represent the CV of the sum of returns across LHPs. The *LPH * stream mean* is the average CV across LHPs and natal streams, and the *Stream mean* is the average of the CVs of the total returns (across LHPs) to each stream. *Total sum* is the CV of the aggregate return across streams and LHPs. For each box, the thick line represents the median CV across 50,000 projections, the boxes span the interquartile range, and the whiskers span the 90% quantile range.

4.7 REFERENCES

Armstrong, D. P., E. H. Parlato, and P. G. H. Frost. 2021. Incorporating individual variation in survival, reproduction and detection rates when projecting dynamics of small populations. Ecological Modelling 455:109647.

Besbeas, P., S. N. Freeman, B. J. T. Morgan, and E. A. Catchpole. 2002. Integrating mark–recapture–recovery and census data to estimate animal abundance and demographic parameters. Biometrics 58(3):540–547.

Bowerman, T., M. L. Keefer, and C. C. Caudill. 2016. Pacific salmon prespawn mortality: patterns, methods, and study design considerations. Fisheries 41(12):738–749.

Buchanan, R. A., J. R. Skalski, G. Mackey, C. Snow, and A. R. Murdoch. 2015. Estimating cohort survival through tributaries for salmonid populations with variable ages at migration. North American Journal of Fisheries Management 35(5):958–973.

Buhle, E. R., M. D. Scheuerell, T. D. Cooney, M. J. Ford, R. W. Zabel, and J. T. Thorson. 2018. Using integrated population models to evaluate fishery and environmental impacts on Pacific salmon viability. NOAA Technical Memorandum.

Carlson, S. M., and W. H. Satterthwaite. 2011. Weakened portfolio effect in a collapsed salmon population complex. Canadian Journal of Fisheries and Aquatic Sciences 68(9):1579–1589.

Carpenter, B., A. Gelman, M. D. Hoffman, D. Lee, B. Goodrich, M. Betancourt, M. Brubaker, J. Guo, P. Li, and A. Riddell. 2017. Stan: a probabilistic programming language. Journal of Statistical Software 76(1):1–32.

Chasco, B. E., E. J. Ward, J. A. Hesse, C. Rabe, R. N. Kinzer, J. L. Vogel, and R. Orme. 2014. Evaluating the Accuracy and Precision of Multiple Abundance Estimators Using State-Space Models: A Case Study for a Threatened Population of Chinook Salmon in Johnson Creek, Idaho: North American Journal of Fisheries Management: Vol 34, No 5. https://www.tandfonline.com/doi/full/10.1080/02755947.2014.926302.

Chelan County Public Utility District No. 1 (Chelan PUD), and Washington Department of Fish and Wildlife (WDFW). 2009. Hatchery and genetic management plan: Wenatchee Upper Columbia River spring Chinook: Chiwawa spring Chinook.

Cordoleani, F., C. C. Phillis, A. M. Sturrock, A. M. FitzGerald, A. Malkassian, G. E. Whitman, P. K. Weber, and R. C. Johnson. 2021. Threatened salmon rely on a rare life history strategy in a warming landscape. Nature Climate Change 11(11):982–988.

Crozier, L. G., B. J. Burke, B. E. Chasco, D. L. Widener, and R. W. Zabel. 2021. Climate change threatens Chinook salmon throughout their life cycle. Communications Biology 4(1):1–14.

van Daalen, S., and H. Caswell. 2020. Variance as a life history outcome: Sensitivity analysis of the contributions of stochasticity and heterogeneity. Ecological Modelling 417:108856.

Ford, M. J., S. Howard, A. R. Murdoch, and M. S. Hughes. 2013. Monitoring the reproductive success of naturally spawning hatchery and natural spring Chinook salmon in the Wenatchee River. Page 28. Annual report the Bonneville Power Administration for project 2003-039.

Ford, M. J., A. Murdoch, and M. Hughes. 2015. Using parentage analysis to estimate rates of straying and homing in Chinook salmon (Oncorhynchus tshawytscha). Molecular Ecology 24(5):1109–1121.

Forsythe, A. B., T. Day, and W. A. Nelson. 2021. Demystifying individual heterogeneity. Ecology Letters 24(10):2282–2297.

Fox, G. A., and B. E. Kendall. 2002. Demographic Stochasticity and the Variance Reduction Effect. Ecology 83(7):1928–1934.

Gimenez, O., E. Cam, and J.-M. Gaillard. 2018. Individual heterogeneity and capture–recapture models: what, why and how? Oikos 127(5):664–686.

Hamel, S., J.-M. Gaillard, and N. Yoccoz. 2018. Introduction to: Individual heterogeneity – the causes and consequences of a fundamental biological process. Oikos 127:643–647.

Henn, J. J., V. Buzzard, B. J. Enquist, A. H. Halbritter, K. Klanderud, B. S. Maitner, S. T. Michaletz, C. Pötsch, L. Seltzer, R. J. Telford, Y. Yang, L. Zhang, and V. Vandvik. 2018. Intraspecific Trait Variation and Phenotypic Plasticity Mediate Alpine Plant Species Response to Climate Change. Frontiers in Plant Science 9.

Herliansyah, R., R. King, and S. King. 2022. Laplace Approximations for Capture–Recapture Models in the Presence of Individual Heterogeneity. Journal of Agricultural, Biological and Environmental Statistics.

Hillman, T. W., M. Miller, M. Hughes, C. Moran, W. Williams, M. Tonseth, C. Willard, S. Hopkins, J. Caisman, T. N. Pearsons, and P. Graf. 2020. Monitoring and evaluation of the Chelan and Grant County PUD s hatchery programs: 201 9 annual report. Report to the HCP and PRCC Hatchery Committees. Wenatchee and Ephrata, WA.

Holmes, E. E., E. J. Ward, and K. Wills. 2012. MARSS: multivariate autoregressive state-space models for analyzing time-series data. R journal 4(1).

Honea, J. M., J. C. Jorgensen, M. M. McClure, T. D. Cooney, K. Engie, D. M. Holzer, and R. Hilborn. 2009. Evaluating habitat effects on population status: influence of habitat restoration on spring-run Chinook salmon. Freshwater Biology 54(7):1576–1592.

Johnston, A. S. A., R. J. Boyd, J. W. Watson, A. Paul, L. C. Evans, E. L. Gardner, and V. L. Boult. 2019. Predicting population responses to environmental change from individual-level mechanisms: towards a standardized mechanistic approach. Proceedings of the Royal Society B: Biological Sciences 286(1913):20191916.

Kendall, B. E., and G. A. Fox. 2002. Variation among Individuals and Reduced Demographic Stochasticity. Conservation Biology 16(1):109–116.

Kristensen, K., A. Nielsen, C. Berg, H. Skaug, and B. Bell. 2016. TMB: automatic differentiation and Laplace approximation. Journal of Statistical Software, 70(5), 1-21.

Martin, H. W., M. Hebblewhite, and E. H. Merrill. 2022. Large herbivores in a partially migratory population search for the ideal free home. Ecology n/a(n/a):e3652.

Maunder, M. N., and A. E. Punt. 2013. A review of integrated analysis in fisheries stock assessment. Fisheries Research 142:61–74.

McClintock, B. T., R. Langrock, O. Gimenez, E. Cam, D. L. Borchers, R. Glennie, and T. A. Patterson. 2020. Uncovering ecological state dynamics with hidden Markov models. arXiv:2002.10497 [q-bio, stat].

Monnahan, C. C., and K. Kristensen. 2018. No-U-turn sampling for fast Bayesian inference in ADMB and TMB: Introducing the adnuts and tmbstan R packages. PloS one 13(5):e0197954.

Murdoch, A. R., C. H. Frady, M. S. Hughes, and K. See. 2019. Estimating population size and observation bias for spring Chinook Salmon. Conservation Science and Practice 1(11):e120.

Murdoch, A. R., T. N. Pearsons, and T. W. Maitland. 2010. Estimating the spawning escapement of hatchery-and natural-origin spring Chinook salmon using redd and carcass data. North American Journal of Fisheries Management 30(2):361–375.

Myers, R. A., N. J. Barrowman, J. A. Hutchings, and A. A. Rosenberg. 1995. Population dynamics of exploited fish stocks at low population levels. Science 269(5227):1106–1108.

Nater, C. R., M. W. Stubberud, Ø. Langangen, A. Rustadbakken, S. J. Moe, T. Ergon, L. A. Vøllestad, and Y. Vindenes. 2022. Towards a future without stocking: harvest and river regulation determine long-term population viability of migratory salmonids. Climate Research 86:37–52.

National Marine Fisheries Service (NMFS). 2015. Reinitiation of the Issuance of Three Section 10(a)(1)(A) Permits for the Upper Columbia River: Chiwawa River, Nason Creek, and White River Spring Chinook Salmon Hatchery Programs.

Paquet, P., T. Flagg, A. Appleby, J. Barr, L. Blankenship, D. Campton, M. Delarm, T. Evelyn, D. Fast, J. Gislason, and others. 2011. Hatcheries, conservation, and sustainable fisheries—achieving multiple goals: results of the Hatchery Scientific Review Group's Columbia River basin review. Fisheries 36(11):547–561.

Pearsons, T. N., and R. R. O'Connor. 2020. Stray Rates of Natural-Origin Chinook Salmon and Steelhead in the Upper Columbia River Watershed. Transactions of the American Fisheries Society 149(2):147–158.

Pedersen, E. J., D. L. Miller, G. L. Simpson, and N. Ross. 2019. Hierarchical generalized additive models in ecology: an introduction with mgcv. PeerJ 7:e6876.

Phillis, C. C., A. M. Sturrock, R. C. Johnson, and P. K. Weber. 2018. Endangered winter-run Chinook salmon rely on diverse rearing habitats in a highly altered landscape. Biological Conservation 217:358–362.

Plard, F., R. Fay, M. Kéry, A. Cohas, and M. Schaub. 2019a. Integrated population models: powerful methods to embed individual processes in population dynamics models. Ecology 100(6):e02715.

Plard, F., D. Turek, M. U. Grüebler, and M. Schaub. 2019b. IPM2: toward better understanding and forecasting of population dynamics. Ecological Monographs 89(3):e01364.

Public Utility District No 2 of Grant County(Grant PUD), Washington Department of Fish and Wildlife, and Yakama Nation. 2009. Hatchery and genetic management plan: Upper Columbia River spring-run Chinook salmon – Nason Creek supplementation program.

R Core Team. 2021. R: A Language and Environment for Statistical Computing. R Foundation for Statistical Computing, Vienna, Austria.

Reid, J. M., M. Souter, S. R. Fenn, P. Acker, A. Payo-Payo, S. J. Burthe, S. Wanless, and F. Daunt. 2020. Among-individual and within-individual variation in seasonal migration covaries with subsequent reproductive success in a partially migratory bird. Proceedings of the Royal Society B: Biological Sciences 287(1931):20200928.

Saunders, S. P., F. J. Cuthbert, and E. F. Zipkin. 2018. Evaluating population viability and efficacy of conservation management using integrated population models. Journal of Applied Ecology 55(3):1380–1392.

Schaub, M., and M. Kéry. 2012. Combining information in hierarchical models improves inferences in population ecology and demographic population analyses. Animal Conservation 15(2):125–126.

Schindler, D. E., R. Hilborn, B. Chasco, C. P. Boatright, T. P. Quinn, L. A. Rogers, and M. S. Webster. 2010. Population diversity and the portfolio effect in an exploited species. Nature 465(7298):609–612.

Sorel, M. H., A. R. Murdoch, R. W. Zabel, C. M. Kamphaus, E. R. Buhle, M. D. Scheuerell, and S. J. Converse. *in review*. Effects of population density and environmental conditions on life-history expression in a migratory fish.

Upper Columbia Salmon Recovery Board (UCSRB), and United States National Marine Fisheries Service (NMFS), editors. 2007. Upper Columbia Spring Chinook Salmon and Steelhead Recovery Plan.

Vindenes, Y., and Ø. Langangen. 2015. Individual heterogeneity in life histories and eco-evolutionary dynamics. Ecology Letters 18(5):417–432.

Zipkin, E. F., and S. P. Saunders. 2018. Synthesizing multiple data types for biological conservation using integrated population models. Biological Conservation 217:240–250.

Zucchini, W., I. L. MacDonald, and R. Langrock. 2016. Hidden Markov models for time series: An introduction using R, second edition. Chapman and Hall/CRC.

Chapter 5. INFORMING SALMON HABITAT RESTORATION AND HATCHERY MANAGEMENT WITH MANAGEMENT MODELING

Publication history: This study was co-authored with Richard W. Zabel, Andrew R. Murdoch and Sarah J. Converse. At the time this dissertation was published, this chapter was not in review with a journal.

Abstract: A primary challenge in conservation is optimally allocating resources to achieve desired outcomes. There are a variety of management interventions available for the conservation of imperiled salmonids in North America, and tools are needed to inform the allocation of management effort to activities such as habitat restoration and hatchery management. We convened a workshop of decision makers and experts on Chinook salmon (*Oncorhynchus tshawytscha*) conservation in the Wenatchee River Basin of Washington State. Participants helped define candidate strategies involving habitat restoration and hatchery management. We evaluated the effects of these strategies on a variety of metrics – including persistence and maintenance of wild genetic structure – using simulations built on an integrated population model. Simulations indicated that restoration of natal streams would result in greater natural production than restoration of downstream habitats. However, downstream restoration would benefit fish from multiple natal streams as well as fish that spawn in downstream habitats. Reducing hatchery broodstock sizes from current targets would result in relatively small changes in natural productivity and reduce the risk of the hatchery program affecting adaptations of the

wild population. Using principals of decision analysis and management modeling enabled evaluation of alternative management strategies that are most relevant to conservation decisions.

Keywords: Chinook salmon, habitat restoration, hatchery management, conservation prioritization, decision analysis, integrated population model

5.1 INTRODUCTION

Conservation requires decisions about how to allocate limited resources over space, time, or conservation action type (Runge et al. 2020) to affect desired outcomes. Decision makers need predictions of expected outcomes under different allocation strategies to make optimal decisions. However, predicting the effects of different strategies can be challenging. This is especially true for migratory species that use different habitats at different times of year (Martin et al. 2007) and when individuals within a population respond differently to management actions (Forsythe et al. 2021).

Decision analysis (also known as Structured Decision Making; SDM) is a collaborative and iterative approach that is increasingly applied to conservation (Hemming et al. 2022). SDM emphasizes formal framing of decision problems as a first step toward decision making (Gregory et al. 2012; Runge et al. 2020), wherein decision makers, stakeholders, and scientific experts work together to define the decision problem, identify desired outcomes, and generate alternative management strategies for consideration. The creation of these initial three components of a decision framework can sometimes by itself be enough to allow decision makers to identify preferred actions (*sensu* Keeney 2004). However, in many cases, models may be required to undertake the next phase of SDM, involving explicit prediction of the effects of management strategies in terms of desired outcomes. Quantitative models can efficiently integrate existing

knowledge, while accounting for uncertainty about the expected outcomes of strategies to facilitate their evaluation (Schmolke et al. 2010). The process of evaluating candidate strategies through modeling is known as management modeling (e.g., Servanty et al. 2014).

Migratory salmonids as a taxonomic group are at substantial risk of population extirpation, due to a variety of complex threats across freshwater, marine, and migratory habitats (Nehlsen et al. 1991; Slaney et al. 1996; Gibson 2017). In the Columbia River Basin in the northwest of the contiguous U.S., five evolutionarily significant units (ESUs) of Chinook salmon (*Oncorhynchus tshawytscha*) are listed under the U.S. Endangered Species Act. The commonly cited threats to Columbia River salmonids are habitat degradation, hydropower development, overharvest, and genetic effects of hatcheries in some basins (Ruckelshaus et al. 2002; McClure et al. 2003).

For Columbia River Basin salmonids, there are multiple decision-makers and stakeholders, an array of alternative management actions, and considerable uncertainty about the efficacy of actions to recover threatened salmonid populations (Volkman & McConnaha 1993; Williams et al. 1999). For populations listed as threatened or endangered under the U.S. Endangered Species Act, the U.S. National Oceanic and Atmospheric Administration (NOAA) is the federal agency that oversees recovery. Sovereign Indigenous nations and state governments each have rights to harvest healthy salmon populations, and local governments, non-profits, and other entities are all similarly invested in recovering populations due to their economic, cultural, and ecological value. Finally, organizations participating in actions such as hydroelectric power generation, irrigation, and flood control, which can harm salmon populations, are required to mitigate their impacts by altering their actions and funding mitigation measures such as hatchery supplementation and habitat restoration (Kareiva et al. 2000; Peters & Marmorek 2001). Given the large number of entities with different jurisdictions, aligning conservation actions with the

identified needs of populations has proven challenging (Barnas et al. 2015). To help allocate resources toward multiple different kinds of management actions across space, a framework is needed to integrate what we know to understand how management can have the greatest impact on populations (e.g., Fonner et al. 2021).

Freshwater habitats, where salmon spawn and rear as juveniles, are a large focus of conservation efforts and are managed by a subset of entities working on salmon conservation. Within freshwater habitats, habitat restoration and hatchery supplementation are the two primary management interventions available. Because salmon populations often have multiple spatially distinct spawning aggregations, habitat restoration and hatchery supplementation may target individual spawning aggregations. Juvenile salmonids exhibit individual heterogeneity in life history pathways (LHPs) in terms of habitat used at different life stages (Buchanan et al. 2015; Schroeder et al. 2015), so habitat restoration may target a specific spawning aggregation, life stage, or juvenile LHP. A major question is therefore how to optimally allocate habitat restoration efforts across space to provide the maximum benefit (Scheuerell et al. 2006; Fonner et al. 2021). Hatchery supplementation similarly may target individual spawning aggregations, and a major question is how many fish to collect for use in hatchery broodstock to maximize benefits to wild populations (Naish et al. 2007). Given the complexity of salmon spatial distribution and conservation hatchery management, modeling tools are needed to conceptualize and explicitly evaluate the outcomes of alternative actions.

We convened a workshop with decision makers and scientific experts to define desired outcomes and identify alternative management strategies for endangered spring Chinook salmon in the Wenatchee River Basin of Washington State. The Wenatchee River is a tributary of the Columbia River that hosts an ESU of Chinook salmon that is listed as endangered under the U.S.

Endangered Species Act (UCSRB and NMFS 2007). We then developed a management model, built upon an integrated population model (IPM; Besbeas et al. 2002) framework, to project population trajectories in three spawning aggregations under alternative spatial allocations of habitat restoration effort and hatchery management. For each candidate strategy, we calculated population viability metrics, including abundance, extinction risk, and effects of introgression with hatchery-origin spawners on natural adaptations. Resulting predictions of population response to different allocation strategies can be considered in decision making to conserve this important salmon population. Our approach also provides a framework for similar analyses targeted at a variety of candidate management strategies targeted at threatened salmonid populations.

5.2 METHODS

5.2.1 *Study System*

The Wenatchee River Basin drains approximately 3,400 km^2 of the eastern slope of the Cascade Mountain Range in central Washington State before meeting the Columbia River at river km 754 (Jorgensen et al. 2009). The environment in the basin transitions from high alpine in the headwaters to forested in the middle elevations to arid shrub-steppe in the lower elevations. The spring Chinook salmon population in the Wenatchee River spawns in tributaries of the mainstem Wenatchee River and Lake Wenatchee as well as the upper portion of the mainstem Wenatchee River below Lake Wenatchee (Figure 5.1). We considered fish that spawn in three tributaries – the Chiwawa River, Nason Creek, and the White River – which together account for roughly 90% of the population (Hillman et al. 2020).

The return of adult spring Chinook salmon from the ocean to the Wenatchee River Basin begins in April, and fish hold within the basin until spawning begins in August (UCSRB and NMFS

2007). Eggs develop for several months before hatching in late winter. Juveniles rear within the basin for a full year prior to migrating to the marine environment; however, juveniles exhibit life history diversity in their freshwater habitat use. Some juveniles leave their natal stream at various times of year as subyearlings and spend several months in downstream rearing areas within the basin before migrating to sea (*downstream-rearing LHPs*), while some fish remain within their natal stream until commencing seaward migration as yearlings (*natal reach-rearing LHPs*; Buchanan et al. 2015). The three downstream-rearing LHPs considered in this study are comprised of fish that emigrate as subyearlings in spring, summer, and fall, whereas all natal reach-rearing emigrants leave the natal stream in spring (Sorel et al. *in review* a; Ch. 2). Fish spend one to three years at sea before returning to the basin to spawn.

Conservation hatchery programs are operated in the Chiwawa River and Nason Creek to supplement natural production. These programs use an integrated broodstock, composed mostly of natural-origin fish, to keep the hatchery line genetically similar to the natural line. Juveniles are reared in the hatchery for several months before being released into acclimation facilities in natal tributaries in the fall, where they imprint on the olfactory signature of the stream before being released and migrating to the ocean the following spring. Hatchery-origin adults returning to the spawning tributaries are intercepted at Tumwater Dam, where a portion are allowed to pass upstream to spawn with natural-origin fish, a portion are removed for hatchery broodstock, and the remainder are removed and used for food or nutrient supplementation in natal streams (NMFS 2015).

Spring Chinook salmon in the upper Columbia River Basin declined in abundance during the latter half of the 20th Century, leading to their designation as an endangered ESU under the U.S. Endangered Species Act (ESA) in 1999 (UCSRB and NMFS 2007). The population of spring

Chinook salmon that spawn in the Wenatchee River Basin comprise one of three extant Major Population Groups within the listed Upper Columbia River spring-run ESU. The responsibility to administer ESA protections for this ESU falls on NOAA, and they work with several other entities on this endeavor. The development of the most recent Recovery Plan for the Upper Columbia River spring Chinook salmon ESU was led by the Upper Columbia Salmon Recovery Board (UCSRB), who worked in collaboration with NOAA and several other entities (UCSRB and NMFS 2007). Recovery criteria for the Wenatchee River population include reaching an average abundance of 2,000 naturally produced spawners and having a risk of quasi-extinction below 5% over a 100-year period. The criteria also emphasize the maintenance of multiple spatially distinct spawning aggregations by requiring that an average of ≥20 spawners return to four of five major spawning areas in the basin while some spawning occurs in one minor spawning area downstream of Tumwater Dam (Figure 5.1).

5.2.2 *Workshop*

We convened a group of decision makers, stakeholders, and scientific experts for a workshop to discuss information needed to make decisions about spring Chinook salmon habitat restoration and hatchery management in the Wenatchee River Basin. The meeting included co-managers and experts from the Washington Department of Fish and Wildlife, Yakama Nation Fisheries, NOAA Fisheries, the UCSRB, Grant County Public Utilities District, Chelan County Public Utilities District, and the consulting firm BioAnalysts (Table 5.1). During the workshop, we focused on three objectives: 1) identifying desired outcomes of management and associated metrics by which to measure them, 2) identifying alternative management strategies, and 3) conceptual discussions relevant to predicting how vital rates like survival would respond to management actions.

Participants identified the delisting criteria established in the Recovery Plan as the metrics of greatest importance for informing their decision. These include targets for the average abundance of natural-origin spawners, extinction risk, and diversity in spawning location and life history strategies (UCSRB and NMFS 2007). In addition, participants identified Proportionate Natural Influence (PNI) of the hatchery supplementation programs, as an additional metric of interest, because this metric would allow them to estimate the effect of the hatchery supplementation program on the natural adaptations of the wild population to its environment (Paquet et al. 2011).

Workshop participants were interested in better understanding the outcomes of a variety of habitat restoration actions in natal tributaries as well as in downstream rearing habitats. We based much of the discussion on work that had been conducted by the Upper Columbia Regional Technical Team (UCRTT 2021), of which several workshop participants were members. The UCRTT identified habitat restoration actions needed in each reach, habitat attributes that would be altered by these actions, and life stages of Chinook salmon that would benefit (Figure J1). Participants noted the difficulty of predicting the expected demographic response to individual habitat restoration actions but collectively hypothesized a moderate improvement in life stage-specific survival that might result from habitat restoration within a given habitat. Participants identified the demographic rates that would be affected by habitat restoration, including egg survival through emergence from nests, survival from emergence through a fish's first summer, and overwinter survival prior to seaward migration the following spring, for fish using the restored area.

Empirically derived effects of habitat restoration on vital rates were not available, so workshop participants collectively agreed upon a set of hypothesized effects of restoration in either natal stream or downstream habitat on survival of fish within that habitat during a particular life stage

(Table 5.2). These hypotheses were informed both by discussions with workshop participants and information developed by the Upper Columbia Regional Technical Team (UCRTT 2021). Because most habitat restoration actions have the potential to increase survival during multiple life stages (Figure J1), we assumed that actions would benefit all juvenile life stages occurring within a habitat (natal stream or downstream areas). We hypothesized that natal-stream restoration would result in 10% increases in survival during egg incubation, summer rearing, and overwintering for fish residing in the natal stream during those life stages. Restoration of downstream rearing habitat had no effect on egg survival because fish in our model did not spawn in those habitats, but it increased summer rearing and overwintering survival by 10% for fish residing in downstream habitat during those life stages. We assumed that the downstream-rearing LHP that emigrates in summer would experience a 5% increase in summer survival from habitat restoration in either habitat because they spend part of the summer in each habitat. We further assumed that benefits would be cumulative across life stages, so that the total proportional benefit was calculated as the product of the individual proportional benefits across life stages (Table 5.2). While quantitative benefits of restoration are not known (UCSRB & NMFS 2007), we were able to simulate effects of management strategies at the population level by hypothesizing specific quantitative benefits in collaboration with experts. Benefits estimated from post-restoration monitoring could readily be used to update our simulations in the future.

Participants also expressed interest in identifying what degree of hatchery supplementation, in terms of numbers of smolts produced and numbers of hatchery-origin adults allowed to spawn in the wild, would most benefit the wild population. In particular, the group expressed interest in comparing the outcome of maintaining hatchery programs at their current sizes (baseline) to reducing the size of the hatchery programs by 50%. In the baseline strategy, the target

broodstock size for the Chiwawa River program was 74 spawners and for the Nason Creek program it was 64. We modeled the second strategy by reducing hatchery broodstock size targets by 50% from the baseline, which in turn reduced the number of smolts produced and the number of hatchery-origin adults that returned to the basin and could be allowed to spawn in natal streams.

5.2.3 *Population Model*

To simulate spring Chinook salmon population trajectories under alternative habitat and hatchery management strategies, we built upon the IPM framework developed by Sorel et al. (*in prep*; Ch. 4). While this IPM framework accounted for the natural production resulting from hatchery-origin fish spawning in the wild, it did not explicitly model how hatchery-origin fish were produced. Here, we added the production of hatchery-origin fish to the IPM framework of Sorel et al. (*in prep*; Ch. 4) for the purposes of this analysis (Figure 5.2). The IPM used here included separate functions to produce natural-origin (born in the wild) and hatchery-origin (born in a hatchery) juveniles, and unique survival and return rates for fish of each origin back to the Wenatchee River Basin to spawn.

The IPM used here modeled the production of natural-origin juveniles (born in the wild to natural- and hatchery-origin spawners) expressing each of four juvenile LHPs in each natal stream in the same way as the IPM of Sorel et al. (*in prep*; Ch. 4). Of the four LHPs, three are downstream-rearing and emigrate at age 0 in spring, summer, or fall, and one is natal-reach rearing and emigrates at age 1 in spring. Production of each LHP in each stream was modeled as a modified Beverton-Holt function of the effective number of female spawners allowing both positive and negative density dependence (Myers et al. 1995; Sorel et al. *in review*; Ch. 2). The

IPM included process error in juvenile production, which is a function of streamflow covariates and random effects of year. Juvenile abundance estimates from downstream-migrant screw traps informed the juvenile production function.

The number of hatchery-origin smolts (born in a hatchery to natural- and hatchery-origin broodstock) produced per spawner in the hatchery broodstock, $\mathrm{HSS}_{t,p}$, in year *t* and hatchery program *p*, was informed by the observed number of smolts produced per spawner in the Chiwawa River and Nason Creek programs in 2001–2020 (Hillman et al. 2020). Based on these data, we assumed that the number of smolts produced per spawner in the hatchery broodstock in each year and program was lognormally distributed, $log(\mathrm{HSS}_{t,p}) \sim \mathrm{N}(\mu = 7.59, \mathrm{sd} = 0.12)$.

The IPM tracked the survival of juveniles, their probability of returning from the ocean at different ages, and their survival and return to the Wenatchee River Basin similar to that described in Sorel et al. (*in prep*; Ch. 4). However, in addition to the four naturally produced LHPs, here we accounted for an additional group, hatchery-origin juveniles, which we allowed to have separate stage-specific survival rates from the naturally produced LHPs. To estimate the survival and return rates for hatchery-origin fish, we included capture histories for PIT-tagged hatchery-origin juveniles in the model likelihood in addition to the capture histories of PIT-tagged natural-origin juveniles.

As in Sorel et al. (*in prep*; Ch. 4), the IPM used in this analysis accounted for the removal of natural- and hatchery-origin fish for use in hatchery broodstock and the release of hatchery-origin fish above Tumwater Dam to spawn naturally. It also accounted for survival between Tumwater Dam and the spawning ground and the proportion of spawners that are female. The model weighted the contribution of female spawners based on their age and origin (natural vs.

hatchery), where older fish and natural-origin females contribute more to juvenile production than younger and hatchery-origin fish.

The IPM was developed in the program TMB (Kristensen et al. 2016) in the R statistical environment (R Core Team 2021), and posterior samples were drawn using the tmbstan package (Monnahan & Kristensen 2018), which uses the no-u-turn algorithm from the Stan package (Carpenter et al. 2017). We ran three Markov chains of 2,000 posterior samples each, using 500 of those for warmup. We confirmed convergence based on potential scale reduction factors (i.e., $\hat{R}$) being less than 1.02 and Monte Carlo standard errors being < 5% of posterior standard errors.

5.2.4 *Population Projections*

We simulated future population trajectories under eight alternative strategies, which were combinations of four habitat restoration strategies and two hatchery management strategies (Table 5.3). The four habitat strategies were baseline, natal-stream restoration, downstream restoration, and restoration of both habitat types. The two hatchery strategies were baseline and 50% reduced broodstock size.

For each strategy, we simulated the population forward for 50 years, running 100 population projections with each of 500 parameter sets (50,000 total projections) from the posterior of the fitted IPM. During projections, we simulated environmental and demographic stochasticity by sampling random effects of year from their hyperdistributions and simulating future environmental conditions from a dynamic factor analysis model (Sorel et al. *in prep*; Ch. 4). To simulate habitat restoration strategies, we multiplied the abundance of juveniles expressing each LHP by the proportional change in Table 5.3, which represents the product of proportional survival increases across all juvenile life stages.

Simulating future hatchery management required coding rules for determining the number of natural and hatchery-origin adults collected for hatchery broodstock, as well as the number of hatchery-origin adult returns released to spawn naturally. We used the same rules as Sorel et al. (*in prep*; Ch. 4), which satisfy constraints on PNI and the maximum proportion of natural-origin returns that can be collected for broodstock, which are outlined in Hatchery Genetic Management Plans (Chelan PUD and WDFW 2009, Grant PUD et al. 2009) and Biological Opinions for the programs (NMFS 2015). The rules were used to calculate the number of individuals to collect and release as a function of the forecasted return of natural-origin spawners, which we simulated with a 10% coefficient of variation around the latent true return in the model to account for forecasting error.

We took the geometric mean of natural-origin female spawners across each 50-year simulated trajectory to quantify mean projected abundance. To assess the probability of the population dropping below a quasi-extinction threshold where demographic risks increase (pQET), we classified each trajectory based on whether the four-year running mean abundance of natural-origin females dropped below 15 at any point. We then calculated the proportion of the 100 trajectories simulated with each parameter set in which the population fell below this threshold. We calculated the average proportion of spawners that were of hatchery origin (pHOS), the average proportion of hatchery broodstock that were of natural origin (pNOB), and Proportion Natural Influence (PNI) = $pNOB / (pNOB + pHOS)$, across projection years for each simulated trajectory.

5.3 RESULTS

Compared to strategy 1 (baseline habitat restoration, baseline hatchery; see Table 5.3), strategy 3 (natal-stream habitat restoration, baseline hatchery) led to a 46% greater mean projected natural-

origin female spawner abundance (Figure 5.3, Figure J2), while strategy 5 (downstream habitat restoration, baseline hatchery) led to a 8% greater abundance, and strategy 7 (restoration of both habitat types, baseline hatchery) led a 60% greater abundance. The largest benefit of strategy 3 was in the White River (51% greater abundance) the largest benefit of strategy 5 was in Nason Creek (10% greater abundance), and the largest benefit of strategy 7 was in the Chiwawa River (60% greater abundance). Compared to strategy 1, strategy 2 (no habitat restoration, reduced hatchery) led to an 2% greater abundance in the Chiwawa River and a 6% lower abundance in Nason Creek; overall this translated to a 1% lower abundance under strategy 2 compared to strategy 1.

The pQET was nearly 0% under all strategies in the Chiwawa River and for the entire population (Figure 5.3, Figure J2). The pQET under strategy 3 (natal-stream habitat restoration, baseline hatchery) was lower than under strategy 1 (baseline habitat restoration, baseline hatchery) by 3% in the Chiwawa River, 22% in Nason Creek and 1% in the White River. These and all following values in the Results section represent differences in probabilities or percentages (e.g., pQET[strategy 1] – pQET[strategy 3]) rather than percent changes as used above for abundance. The pQET under strategy 5 (downstream habitat restoration, baseline hatchery) was lower than under strategy 1 by 1% in the Chiwawa River, 7% in Nason Creek and 0% in the White River. The pQET was lower under strategy 7 (restoration of both habitat types, baseline hatchery) by 3% in the Chiwawa River, 33% in Nason Creek and 1% in the White River. Compared to strategy 1, the pQET under strategy 2 (no habitat restoration, reduced hatchery) was higher by 4% in the Chiwawa River, 3% in Nason Creek and there was no difference in the White River.

Compared to strategy 1 (baseline habitat restoration, baseline hatchery), pHOS under strategy 3 (natal-stream habitat restoration, baseline hatchery) was lower by 10% for the population, under

strategy 5 (downstream habitat restoration, baseline hatchery) it was lower by 2%, and under strategy 7 (restoration in both habitat types, baseline hatchery) it was lower by 13% (Figure 5.3, Figure J2). The pHOS under strategy 2 (no habitat restoration, reduced hatchery) was lower than under strategy 1 by 6% in the Chiwawa River, 0% in Nason Creek, 3% in the White River, and 4% for the total population.

The pNOB under strategy 3 (natal-stream habitat restoration, baseline hatchery) was higher than under strategy 1 (baseline habitat restoration, baseline hatchery) by 11% in the Chiwawa River program and 17% in the Nason Creek program (Figure 5.3, Figure J2). Under strategy 5 (downstream habitat restoration, baseline hatchery), pNOB was higher than under strategy 1 by 2% in the Chiwawa River program and 3% in the Nason Creek program, and under strategy 7 (restoration of both habitat types, baseline hatchery), pNOB was higher by 13% in the Chiwawa River program and 21% in the Nason Creek program. Compared to strategy 1, pNOB under strategy 2 (no habitat restoration, reduced hatchery) was higher by 17% in the Chiwawa River program and 31% in the Nason Creek program.

Like pNOB, the PNI was greater under strategy 3 (natal-stream habitat restoration, baseline hatchery) than under strategy 1 (baseline habitat restoration, baseline hatchery) for the Chiwawa River program (10%) and the Nason Creek program (16%; Figure 5.3, Figure J2). Under strategy 5 (downstream habitat restoration, baseline hatchery), PNI was higher than under strategy 1 by 2% in the Chiwawa River program and 3% in the Nason Creek program, and under strategy 7 (restoration of both habitat types, baseline hatchery), PNI was higher by 12% in the Chiwawa River program and 20% in the Nason Creek program. PNI was higher under strategy 2 (no habitat restoration, reduced hatchery) than strategy one in the Chiwawa River program (9%) and in the Nason Creek program (21%).

5.4 DISCUSSION

In our simulated future population trajectories under alternative habitat management strategies natal-stream habitat restoration led to greater improvements in population viability metrics than downstream habitat restoration. In our simulations with different hatchery management strategies, smaller hatchery broodstock size targets than are currently used reduced risks of introgression with hatchery-origin spawners while having relatively small effects on natural productivity.

The larger positive effect of restoring natal-stream habitat than downstream habitat on viability can be partially explained by our hypothesized cumulative increases in survival under the natal-stream restoration strategy for numerically dominant fall subyearling and spring yearling emigrant LHPs of 21% and 33.1% respectively (Table 5.2), because these LHPs rely on natal streams for most or all of their freshwater rearing. In contrast, we hypothesized that the downstream-restoration strategy provided no survival benefit to the spring yearling emigrant LHP that uses downstream habitats mostly as a migration corridor (Buchanan et al. 2015), and only a 10% benefit to the fall subyearling LHP that uses downstream habitat mostly for overwintering. Downstream restoration provided greater survival benefits to spring and summer subyearling emigrant LHPs that rear in downstream habitat extensively, but they comprise a smaller proportion of all juveniles (Sorel et al. *in review*; Ch. 2). The relative frequencies of the spring and summer subyearling emigrant LHPs increased with increasing population size (Sorel et al. *in review*; Ch. 2), but the population size did not increase to the point where the spring and summer subyearling emigrant LHPs were as abundant as the fall subyearling and spring yearling LHPs.

Our projected population-level results of habitat restoration are conditional on our hypothesized changes to stage-specific survival rates in different areas for different LHPs. However, alternative hypotheses about the effects of management actions on survival rates, based on further elicitation of expert judgment (e.g., Martin et al. 2012) or empirical results, could be evaluated using our framework and may lead to different conclusions. Empirical data, collected in a robust manner, on the relationship between management actions and stage-specific survival rates would provide the most defensible predictions of population response to management, highlighting the value of monitoring the effect of management on survival rates.

Despite the smaller population response to downstream habitat restoration, restoring downstream habitats has the advantage of benefiting fish born in multiple natal streams, contributing to the recovery criteria of maintaining multiple spawning aggregations at average spawner abundances >20. All the strategies that included natal-stream restoration assumed that all three natal streams would be restored, but this may be more costly than restoring downstream habitat used by fish from multiple natal streams. Our results could be evaluated within a return-on-investment framework to consider cost in decision making (Fonner et al. 2021). Furthermore, there is a spawning aggregation that uses downstream areas for all life stages, which currently makes up <10% of the population (Hillman et al. 2020), and that we consequently did not model. Therefore, there may be advantages to downstream restoration that were not accounted for in our analysis.

Our hypothesized effects of habitat restoration on survival rates relied on several simplifying assumptions; for example, we hypothesized that habitat restoration conducted in each habitat type would benefit survival during all life stages occurring in that habitat. However, if distinct habitat restoration actions were required to improve survival during distinct life stages, then

different restoration strategies would need to be examined to assess tradeoffs among them (e.g., Honea et al. 2009). For example, outcomes could be compared between actions improving egg-incubation survival within a natal stream and improving overwinter survival within downstream habitat. Empirical data on the effect of management on survival rates could be used to parameterize simulations to make such comparisons.

This study is an example of how ecological models that account for the distribution of organisms in space and time can inform population responses to different spatial allocations of habitat restoration effort. For migratory animals, including those exhibiting individual heterogeneity in seasonal habitat use, these models must account for the proportions of a population residing in different habitats at different times (Martin et al. 2007; Runge et al. 2014). For spring Chinook salmon, the entire population relies on natal habitat for egg incubation, but some LHPs move to downstream areas to rear. Additionally, the expression of LHPs can be affected by population density and environmental factors (Sorel et al. *in review*; Ch. 2). Given this complexity, management modeling was useful for predicting population responses to alternative spatial allocations of habitat restoration effort identified by decision makers, while accounting for seasonal habitat use dynamics identified as potentially relevant to decisions by scientific experts.

Reducing hatchery broodstock sizes resulted in fewer hatchery-origin adults being produced and available to spawn in the wild and contribute to natural production; however, it also resulted in fewer natural-origin adults being removed from the population for use in hatchery broodstock. In the Chiwawa River, the loss in natural production from reducing hatchery spawners was more than compensated for by removing fewer natural-origin fish for broodstock, resulting in a small increase in average abundance of natural-origin fish. This was not the case in Nason Creek, where the loss in production from reducing hatchery-origin spawners resulted in a small net

reduction in abundance. This was largely because more natural-origin fish were removed from the Chiwawa River to be used in both the Chiwawa River and Nason Creek programs' broodstocks than were removed from Nason Creek for the Nason Creek broodstock only (NMFS 2015). The effect of reducing hatchery production on the risk of the spawning aggregations falling below the quasi-extinction threshold were relatively small.

Reducing hatchery broodstock targets led to considerable increases in PNI, indicating a reduction in the effect of introgression with hatchery-origin fish on the natural adaptations of the wild population. Because reducing target broodstock sizes did not appreciably decrease natural productivity, a higher proportion of the reduced broodstock size targets could be filled with natural-origin returns without exceeding 30% of the natural-origin returns to the Chiwawa River. These increases in pNOB, combined with small changes in pHOS, resulted in increases in PNI in both programs resulting from reducing hatchery broodstock size targets.

In their review of the effects of hatcheries on wild salmon populations, Naish et al. (2007) called for more explicit definition of the objectives of hatchery supplementation programs and formal evaluation of their efficacy in meeting those objectives. In our workshop, participants defined two potentially competing objectives of the hatchery program: 1) increasing natural production and 2) minimizing effects of supplementation on the natural adaptations of the population as measured through the PNI metric. Naish et al. (2007) also emphasize that hatchery management often involves tradeoffs between risks such as genetic effects of supplementation and those of small population sizes. However, in our case study example, it appears that reducing target broodstock sizes may increase PNI while having relatively small effects on natural production as measured through abundance and pQET. This may be an example of a win-win strategy identified through management modeling.

Principals of SDM are valuable in systems with multiple decision makers, stakeholders, and uncertainty about ecological responses to actions (Runge et al. 2020). In our case study, the decision makers and scientific experts had previously developed a Recovery Plan (UCSRB and NMFS 2007), which helped them define desired outcomes and associated metrics (objective 1 of our workshop). Furthermore, the workshop participants had previously participated in a formal prioritization exercise for habitat restoration effort (Upper Columbia Regional Technical Team 2021), and strategic planning for hatchery programs (NMFS 2015), which helped then identify management alternatives (workshop objective 2). Scientific experts in our workshop worked with us to hypothesize potential changes in survival due to habitat restoration and key aspects of the population dynamics to consider (workshop objective 3). However, considerable uncertainty remained around the expected population response to different spatial allocations of habitat restoration and hatchery program sizes, which hampered decision making. Our IPM-based management model enabled us to predict population-level metrics under the management strategies identified by the decision makers while accounting for critical aspects of population dynamics that were identified by scientific experts and informed by data.

The management modeling framework developed for this system could be used to evaluate more management strategies and hypotheses about vital rate responses to inform decisions in an ongoing collaboration between decision makers, scientific experts, and decision analysts. As is the case with many conservation decisions, management of endangered Chinook salmon in the Wenatchee River basin is incredibly complex both socially and ecologically. Despite this overwhelming complexity, combining SDM and management modeling increases the odds that management actions will achieve stakeholder's desired outcomes for critically important populations.

5.5 ACKNOWLEDGEMENTS

I thank the workshop participants for sharing their expertise and time with us. Funding for this research was provided by the National Oceanographic and Atmospheric Administration Northwest Fisheries Science Center, the Washington Cooperative Fish and Wildlife Research Unit, and the Northwest Climate Adaptation Science Center. This work would not be possible if not for the tremendous efforts of those who monitor Chinook salmon in the Wenatchee River Basin and the Columbia River and maintain databases for storing and accessing data. I thank Stacy Amburgey for feedback on a previous version of this chapter. Any use of trade, firm, or product names is for descriptive purposes only and does not imply endorsement by the U.S. Government.

5.6 TABLES & FIGURES

Table 5.1: Table of workshop participants and their roles in a workshop designed to guide management modeling for spring-run Chinook salmon in the Wenatchee River Basin. BioAnalysts is a private environmental consulting firm. Chelan and Grant PUDs are county public utility districts that operate hydroelectric dams. NOAA stands for the U.S. National Oceanographic and Atmospheric Administration, the NWFSC is their Northwest Fisheries Science Center, and the WCR is their West Coast Region unit that establishes and administers policies. Th UCSRB is the Upper Columbia Salmon Recovery Board, a non-profit organization intimately involved in the direction and implementation of salmon recovery efforts. The WDFW is the Washington State Department of Fish and Wildlife, and Yakama Nation Fisheries is the fisheries department of the Confederated Tribes and Bands of the Yakama Nation. Participation in the workshop does not imply endorsement of any management strategy or modeling approach.

Participant	Entity	Role in Wenatchee spring Chinook management
Tracy Hillman	BioAnalysts	Has conducted monitoring and research for >35 years and chairs committees that make decisions about habitat restoration and hatchery management
Catherine Willard	Chelan PUD	Oversees research and monitoring and sits on committees that make decisions about habitat restoration and hatchery management
Todd Pearsons	Grant PUD	Oversees research and monitoring and sits on committees that make decisions about hatchery management
Jeff Jorgensen	NOAA NWFSC	Develops population models
Rich Zabel	NOAA NWFSC	Develops population models

Brett Farman	NOAA WCR	Conducts hatchery permitting and sits on committees where hatchery management decisions are made
Tracy Bowerman	UCSRB	Coordinates research and the use of science to inform decision making
Andrew Murdoch	WDFW	Has overseen research and monitoring for >20 years
Michael Tonseth	WDFW	Oversees hatchery management implementation and sits on committees where hatchery management decisions are made
Keely Murdoch	Yakama Nation Fisheries	Oversees research and monitoring and sits on multiple committees that make decisions about habitat restoration and hatchery management

Table 5.2: Table of predicted proportional changes in life-stage survival for habitat restoration strategies by juvenile life history pathway (LHP) based on expert opinion. Habitat restoration could be in the *NS* = Natal-stream or *DS* = downstream habitat. Emigrants could be *Spr.0* = spring subyearling, *Sum.0* = summer subyearling, *Fal.0* = fall subyearling, and *Spr.1* = spring yearling. Survival was *Egg* = egg incubation, *Summer* = summer rearing, and *Winter* = overwintering, with *Total* = product of scalars across life stages. *Total* is the product of the hypothesized stage-specific changes.

Habitat	LHP	Egg	Summer	Winter	Total
NS	Spr.0	1.10	1.00	1.00	1.10
NS	Sum.0	1.10	1.05	1.00	1.16
NS	Fal.0	1.10	1.10	1.00	1.21
NS	Spr.1	1.10	1.10	1.10	1.33
DS	Spr.0	1.00	1.10	1.10	1.21
DS	Sum.0	1.00	1.05	1.10	1.16
DS	Fal.0	1.00	1.00	1.10	1.10
DS	Spr.1	1.00	1.00	1.00	1.00

Table 5.3: Table of eight management strategies, consisting of combinations of four alternative habitat restoration strategies (Habitat) and two hatchery management strategies (Hatchery). The columns Spr.0 through Spr.1 represent proportional changes (i.e., 1.000 = no change) in the survival of juveniles expressing the life history pathway indicated by the column title (Spr.0 = age-0 emigrants in spring, Sum.0 = age-0 emigrants in summer, Fal.0 = age-0 emigrants in fall, and Spr.1 = age-1 emigrants in spring) resulting from the habitat restoration strategy defined in the first column. The benefit for the *Baseline*, *Natal*, and *Downstream* habitat restoration strategies are from Table 2. For the *Both* habitat restoration strategy, the benefit was calculated as the product of the benefit of natal stream and downstream habitat restoration, assuming cumulative effects. The last two columns show the target broodstock sizes for the Chiwawa River and Nason Creek hatchery programs under the management strategy defined in the second column.

Strategy	Habitat	Hatchery	Spr.0	Sum.0	Fal.0	Spr.1	Chiwawa	Nason
1	Baseline	Baseline	1.00	1.00	1.00	1.00	74	64
2	Baseline	Reduced	1.00	1.00	1.00	1.00	37	32
3	Natal	Baseline	1.10	1.16	1.21	1.33	74	64
4	Natal	Reduced	1.10	1.16	1.21	1.33	37	32
5	Downstream	Baseline	1.21	1.16	1.10	1.00	74	64
6	Downstream	Reduced	1.21	1.16	1.10	1.00	37	32
7	Both	Baseline	1.33	1.33	1.33	1.33	74	64
8	Both	Reduced	1.33	1.33	1.33	1.33	37	32

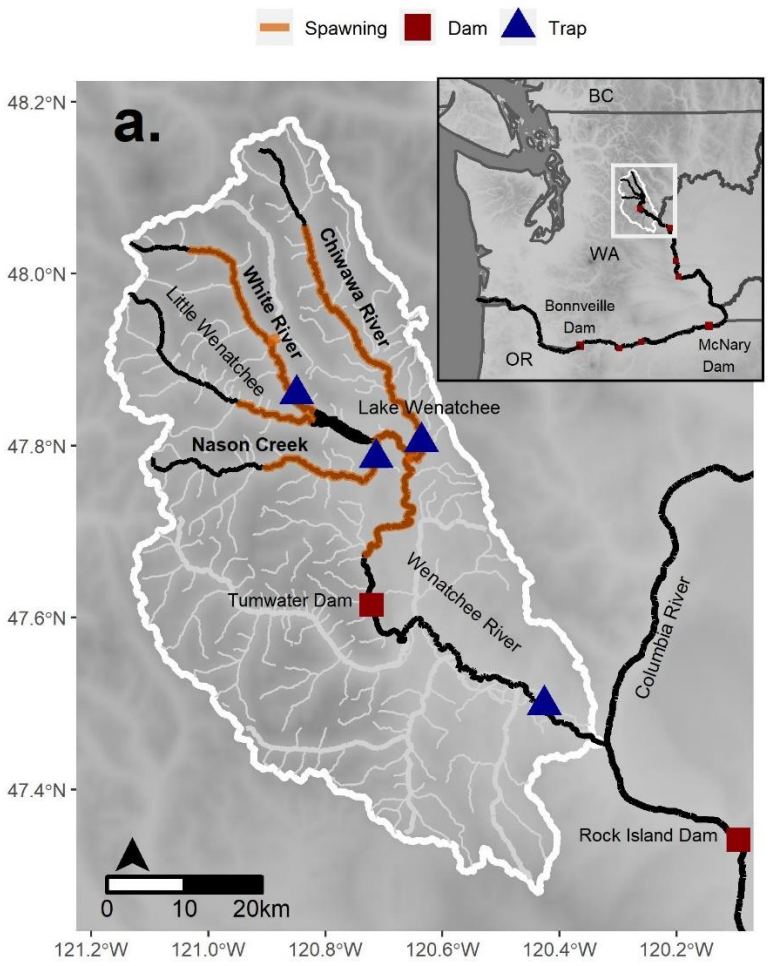

Figure 5.1: Map of the Wenatchee River Basin showing spawning habitat within the five major spawning areas for spring Chinook salmon – the Chiwawa River, White River, Little Wenatchee River, Nason Creek, and upper mainstem Wenatchee River – and the locations of downstream-migrant screw traps and dams. The spawning areas modeled in this analysis are bolded.

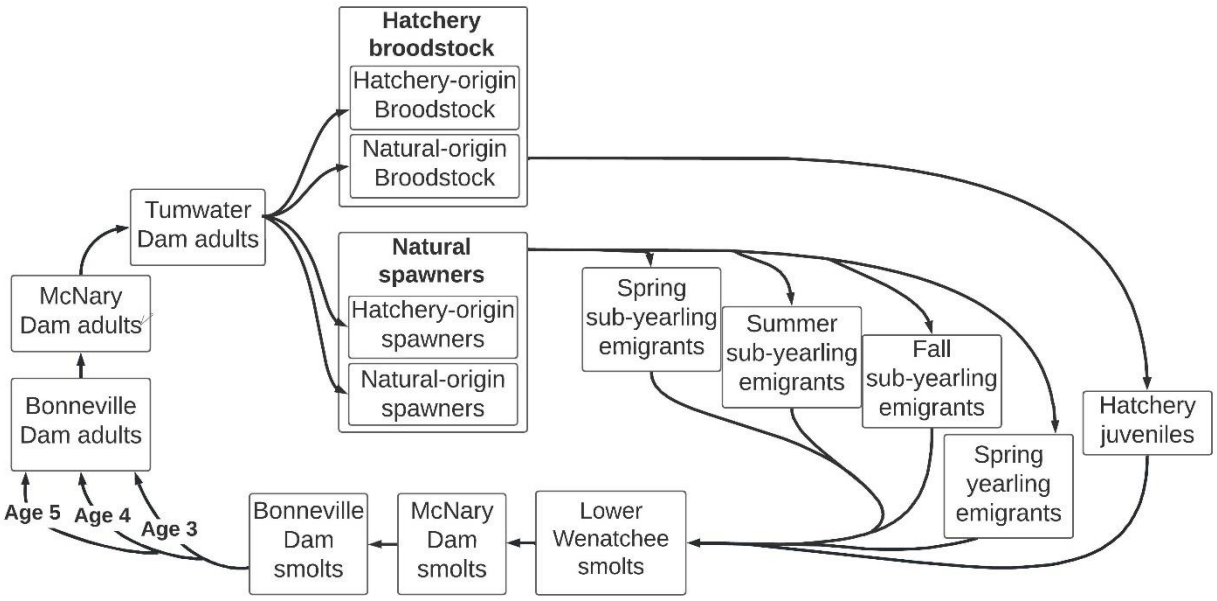

Figure 5.2: Conceptual diagram of the integrated population model for Wenatchee River Chinook salmon. Square boxes represent population states (i.e., life stage abundances), and arrows connecting boxes represent demographic rates (i.e., juvenile production, survival, and maturation) and broodstock collection. The transition between *Bonneville Dam smolts* and *Bonneville Dam adults* covers the period when fish enter the ocean and remain there between one and three years before returning to Bonneville Dam as adults.

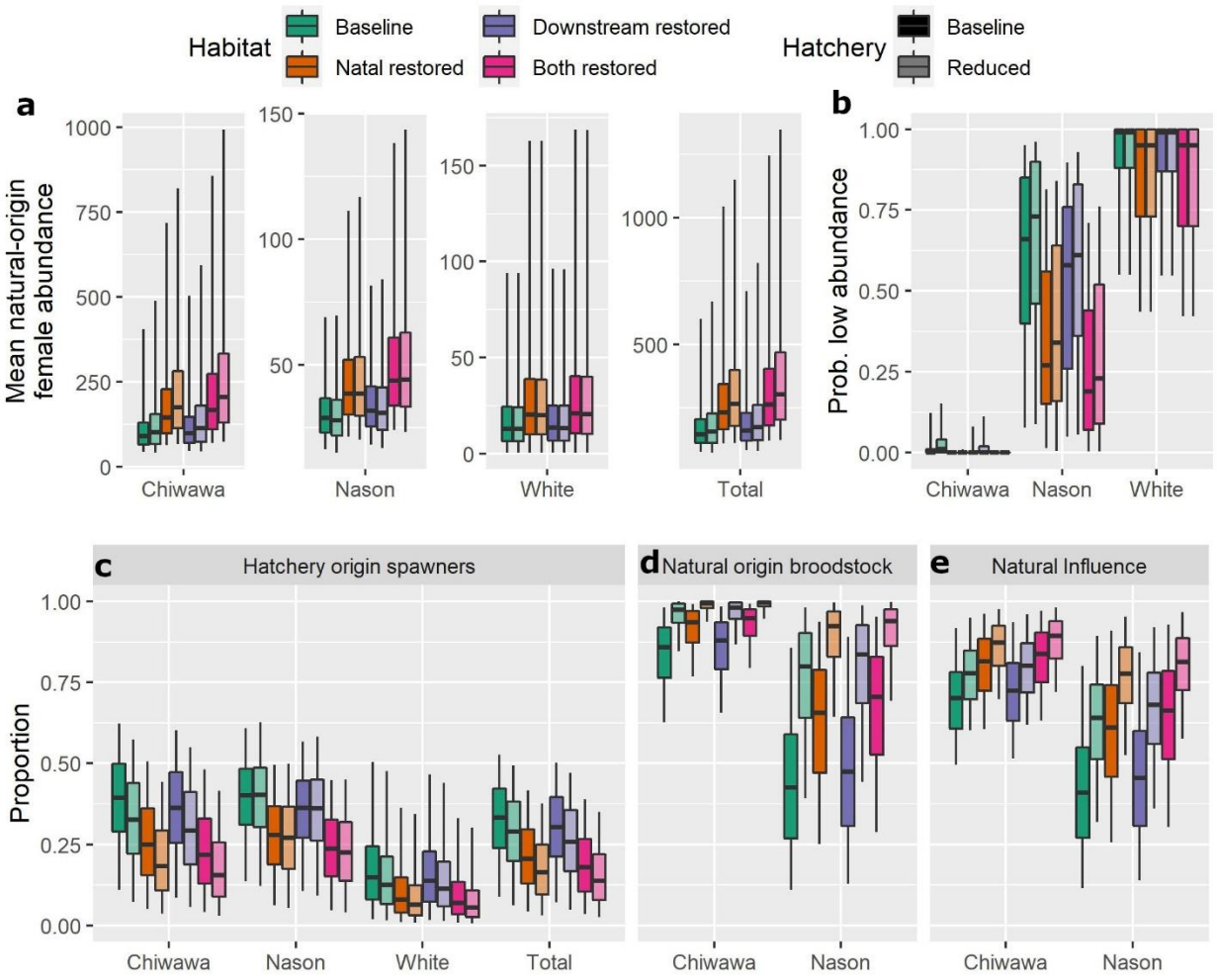

Figure 5.3: Boxplots of (a) the simulated geometric mean natural-origin female spawner abundance over 50 years (b) the probability of the four-year running mean natural-origin female spawner abundance falling below a quasi-extinction threshold of 15 (pQET), (c) the average proportion of spawners that are of hatchery origin (pHOS), (d) the average proportion of hatchery broodstock that are of natural origin (pNOB), and (e) the average Proportionate Natural Influence (PNI = pNOB / (pNOB + pHOS); a measure of the effect of introgression with hatchery-origin spawners on the natural adaptations of the wild population) by natal stream and management strategy. Box color represents habitat strategy, and box shading represents hatchery broodstock size strategy (see Table 3). Within each boxplot, the center line represents the median across simulations, the box spans the interquartile range, and the whiskers span the 90% quantile.

5.7 REFERENCES

Barnas KA, Katz SL, Hamm DE, Diaz MC, Jordan CE. 2015. Is habitat restoration targeting relevant ecological needs for endangered species? Using Pacific Salmon as a case study. Ecosphere **6**:art110.

Besbeas P, Freeman SN, Morgan BJT, Catchpole EA. 2002. Integrating mark–recapture–recovery and census data to estimate animal abundance and demographic parameters. Biometrics **58**:540–547.

Buchanan RA, Skalski JR, Mackey G, Snow C, Murdoch AR. 2015. Estimating cohort survival through tributaries for salmonid populations with variable ages at migration. North American Journal of Fisheries Management **35**:958–973.

Carpenter B, Gelman A, Hoffman MD, Lee D, Goodrich B, Betancourt M, Brubaker M, Guo J, Li P, Riddell A. 2017. Stan: a probabilistic programming language. Journal of Statistical Software **76**:1–32.

Chelan County Public Utility District No. 1 (Chelan PUD), Washington Department of Fish and Wildlife (WDFW). 2009. Hatchery and genetic management plan: Wenatchee Upper Columbia River spring Chinook: Chiwawa spring Chinook.

Fonner R, Honea J, Jorgensen JC, Plummer M, McClure M. 2021. Considering intervention intensity in habitat restoration planning: An application to Pacific salmon. Journal of Environmental Management **299**:113536.

Forsythe AB, Day T, Nelson WA. 2021. Demystifying individual heterogeneity. Ecology Letters **24**:2282–2297.

Gibson RJ. 2017. Salient needs for conservation of Atlantic Salmon. Fisheries **42**:163–174. Taylor & Francis.

Gregory R, Failing L, Harstone M, Long G, McDaniels T, Ohlson D. 2012. Structured decision making: a practical guide to environmental management choices. John Wiley & Sons, Incorporated, Hoboken, UNITED KINGDOM. Available from http://ebookcentral.proquest.com/lib/washington/detail.action?docID=862851 (accessed June 12, 2020).

Hemming V et al. 2022. An introduction to decision science for conservation. Conservation Biology **36**:e13868.

Hillman TW et al. 2020. Monitoring and evaluation of the Chelan and Grant County PUD s hatchery programs: 201 9 annual report. Report to the HCP and PRCC Hatchery Committees. Report to the HCP and PRCC Hatchery Committees. Wenatchee and Ephrata, WA. Available from https://www.grantpud.org/templates/galaxy/images/images/Downloads/ResourceCommittees/OtherDocuments/2017_Final_Annual_Report_with_Appendices.pdf (accessed November 16, 2018).

Honea JM, Jorgensen JC, McClure MM, Cooney TD, Engie K, Holzer DM, Hilborn R. 2009. Evaluating habitat effects on population status: influence of habitat restoration on spring-run Chinook salmon. Freshwater Biology **54**:1576–1592.

Jorgensen JC, Honea JM, McClure MM, Cooney TD, Engie K, Holzer DM. 2009. Linking landscape-level change to habitat quality: an evaluation of restoration actions on the freshwater habitat of spring-run Chinook salmon. Freshwater Biology **54**:1560–1575.

Kareiva P, Marvier M, McClure M. 2000. Recovery and management options for spring/summer Chinook salmon in the Columbia River Basin. Science **290**:977–979.

Keeney RL. 2004. Making Better Decision Makers. Decision Analysis **1**:193–204. INFORMS.

Kristensen K, Nielsen A, Berg C, Skaug H, Bell B. 2016. TMB: automatic differentiation and Laplace approximation. Journal of Statistical Software, 70(5), 1-21.

Martin TG, Burgman MA, Fidler F, Kuhnert PM, Low-Choy S, Mcbride M, Mengersen K. 2012. Eliciting Expert Knowledge in Conservation Science. Conservation Biology **26**:29–38.

Martin TG, Chades I, Arcese P, Marra PP, Possingham HP, Norris DR. 2007. Optimal conservation of migratory species. PloS one **2**:e751. Public Library of Science San Francisco, USA.

McClure MM, Holmes EE, Sanderson BL, Jordan CE. 2003. A Large-Scale, Multispecies Status Assessment: Anadromous Salmonids in the Columbia River Basin. Ecological Applications **13**:964–989.

Monnahan CC, Kristensen K. 2018. No-U-turn sampling for fast Bayesian inference in ADMB and TMB: Introducing the adnuts and tmbstan R packages. PloS one **13**:e0197954. Public Library of Science San Francisco, CA USA.

Myers RA, Barrowman NJ, Hutchings JA, Rosenberg AA. 1995. Population dynamics of exploited fish stocks at low population levels. Science **269**:1106–1108. American Association for the Advancement of Science.

Naish KA, Taylor JE, Levin PS, Quinn TP, Winton JR, Huppert D, Hilborn R. 2007. An evaluation of the effects of conservation and fishery enhancement hatcheries on wild populations of salmon1. Pages 61–194 Advances in Marine Biology. Academic Press. Available from http://www.sciencedirect.com/science/article/pii/S0065288107530026 (accessed December 5, 2018).

National Marine Fisheries Service (NMFS). 2015. Reinitiation of the Issuance of Three Section 10(a)(1)(A) Permits for the Upper Columbia River: Chiwawa River, Nason Creek, and White River Spring Chinook Salmon Hatchery Programs.

Nehlsen W, Williams JE, Lichatowich JA. 1991. Pacific salmon at the crossroads: stocks at risk from California, Oregon, Idaho, and Washington. Fisheries **16**:18.

Paquet P et al. 2011. Hatcheries, conservation, and sustainable fisheries—achieving multiple goals: results of the Hatchery Scientific Review Group's Columbia River basin review. Fisheries **36**:547–561. Wiley Online Library.

Peters CN, Marmorek DR. 2001. Application of decision analysis to evaluate recovery actions for threatened Snake River spring and summer chinook salmon (Oncorhynchus tshawytscha). Canadian Journal of Fisheries and Aquatic Sciences **58**:2431–2446.

Public Utility District No 2 of Grant County(Grant PUD), Washington Department of Fish and Wildlife, Yakama Nation. 2009. Hatchery and genetic management plan: Upper Columbia River spring-run Chinook salmon – Nason Creek supplementation program.

R Core Team. 2021. R: A Language and Environment for Statistical Computing. R Foundation for Statistical Computing, Vienna, Austria. Available from https://www.R-project.org/.

Ruckelshaus MH, Levin P, Johnson JB, Kareiva PM. 2002. The Pacific Salmon Wars: What Science Brings to the Challenge of Recovering Species. Annual Review of Ecology and Systematics **33**:665–706.

Runge CA, Martin TG, Possingham HP, Willis SG, Fuller RA. 2014. Conserving mobile species. Frontiers in Ecology and the Environment **12**:395–402. Wiley Online Library.

Runge MC, Converse SJ, Lyons JE, Smith DR. 2020. Structured Decision Making: Case Studies in Natural Resource Management. Johns Hopkins University Press, Baltimore. Available from http://muse.jhu.edu/book/74951 (accessed May 2, 2022).

Scheuerell MD, Hilborn R, Ruckelshaus MH, Bartz KK, Lagueux KM, Haas AD, Rawson K. 2006. The Shiraz model: a tool for incorporating anthropogenic effects and fish–habitat relationships in conservation planning. Canadian Journal of Fisheries and Aquatic Sciences **63**:1596–1607.

Schmolke A, Thorbek P, DeAngelis DL, Grimm V. 2010. Ecological models supporting environmental decision making: a strategy for the future. Trends in Ecology & Evolution **25**:479–486.

Schroeder RK, Whitman LD, Cannon B, Olmsted P. 2015. Juvenile life-history diversity and population stability of spring Chinook salmon in the Willamette River basin, Oregon. Canadian Journal of Fisheries and Aquatic Sciences **73**:921–934.

Servanty S, Converse SJ, Bailey LL. 2014. Demography of a reintroduced population: moving toward management models for an endangered species, the Whooping Crane. Ecological Applications **24**:927–937.

Slaney TL, Hyatt KD, Northcote TG, Fielden RJ. 1996. Status of Anadromous Salmon and Trout in British Columbia and Yukon. Fisheries **21**:20–35.

Sorel MH, Jorgensen JC, Zabel RW, Murdoch AR, Kamphaus CM, Converse SJ. *in prep*. Integrating individual heterogeneity into an integrated population model to inform viability analysis.

Sorel MH, Murdoch AR, Zabel RW, Kamphaus CM, Buhle ER, Scheuerell MD, Converse SJ. *in review*. Effects of population density and environmental conditions on life-history expression in a migratory fish.

Upper Columbia Regional Technical Team. 2021. Habitat action prioritization within the Upper Columbia River Basin. Available from https://www.ucsrb.org/mdocs-posts/habitat-action-prioritization-strategy-v-3/.

Upper Columbia Salmon Recovery Board (UCSRB), United States National Marine Fisheries Service (NMFS), editors. 2007. Upper Columbia Spring Chinook Salmon and Steelhead Recovery Plan. Available from https://repository.library.noaa.gov/view/noaa/15990.

Volkman JM, McConnaha WE. 1993. Through a glass, darkly: Columbia River salmon, the endangered species act, and adaptive management. Environmental Law **23**:1249–1272. Temporary Publisher.

Williams RN et al. 1999. Return to the river: scientific issues in the restoration of salmonid fishes in the Columbia River. Fisheries **24**:10–19. Taylor & Francis.

APPENDIX A

Supplementary tables and figures (Chapter 2)

Table A1: Parameter estimates for modified Beverton-Holt models of the abundances of juvenile emigrants expressing four alternative life-history strategies as a function of female spawner abundance. α, γ, and J^{max} are the parameters of the modified Beverton-Holt model, *lcl* represents the lower 95% confidence limit and *ucl* is the upper 95% confidence limit. *Spr-0* = spring subyearling, *Sum-0* = summer subyearling, *Fall-0* = fall subyearling, and *Spr-1* = spring yearling emigrants.

stream	LH	α	α lcl	α ucl	Γ	γ lcl	γ ucl	J^{max}	J^{max} lcl	J^{max} ucl
Chiwawa	Spr-0	4.5	1.7	11.6	1.84	1.45	2.34	14884	1184	186493
Nason	Spr-0	5.5	2.3	12.9	1.25	0.89	1.76	14769	1147	189665
White	Spr-0	5.6	3.0	10.7	1.59	1.07	2.36	14808	1153	187409
Chiwawa	Sum-0	45.7	30.3	69.0	1.39	1.19	1.62	19743	2589	150045
Nason	Sum-0	51.6	23.2	114.9	1.04	0.75	1.46	19153	2294	161315
White	Sum-0	28.2	18.2	43.7	0.91	0.59	1.41	19183	2286	159249
Chiwawa	Fall-0	104.3	63.7	171.3	1.16	0.71	1.88	1325	640	2766
Nason	Fall-0	101.7	47.3	218.1	1.2	0.69	2.08	1515	590	3910
White	Fall-0	75.4	42.7	132.1	0.71	0.34	1.53	1365	479	3916
Chiwawa	Spr-1	474.7	333.8	677.5	0.35	0.22	0.56	14901	1148	203007
Nason	Spr-1	112.9	57.2	224.1	0.31	0.13	0.73	14771	1094	207672
White	Spr-1	134.2	68.0	265.2	0.35	0.14	0.85	14798	1111	203561

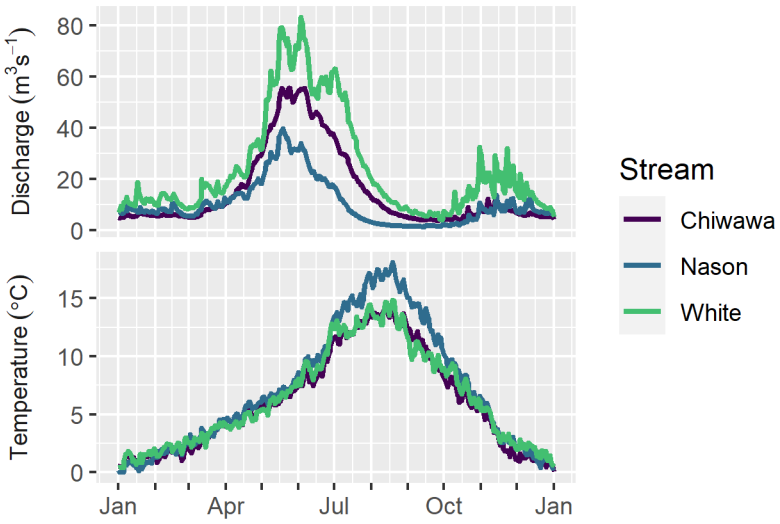

Figure A1: Average daily stream discharge (m^3s^{-1}) and temperature (°C) in the Chiwawa River, Nason Creek, and the White River in the Wenatchee River Basin. Discharge averages were taken over the years 1997–2018 in the Chiwawa, 2004–2018 in Nason Creek, and 2006–2018 in the White River. Temperature averages were taken over the years 2013–2017 in the Chiwawa River, 2012–2017 in Nason Creek, and 2014–2017 in the White River (Siegel and Volk 2019).

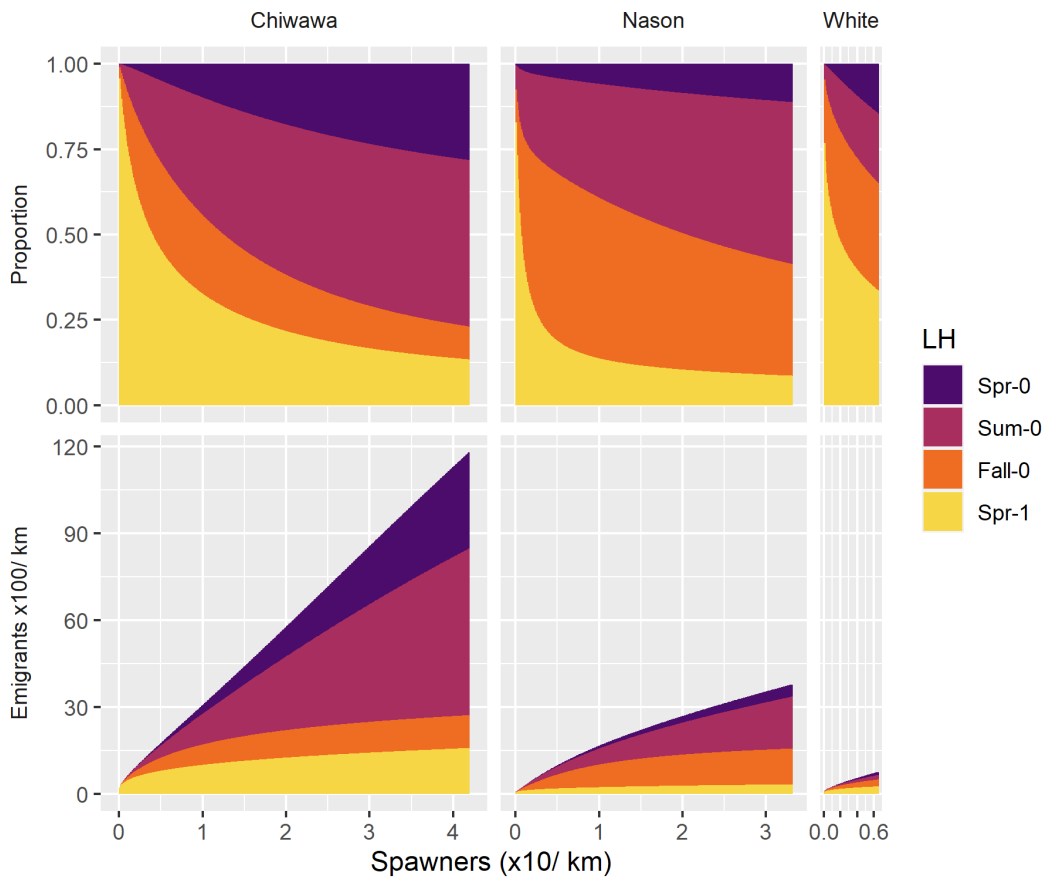

Figure A2: Proportion (top row) and expected abundance (bottom row) of juvenile emigrants expressing each of four juvenile life-history pathways (LHPs) as a function of spawner abundance, based on models that account for density dependence in the production of each LHP. Predictions span the range of spawner abundance for which estimates of juvenile abundance were available to parameterize models. Estimates represent the expectations for an average year.

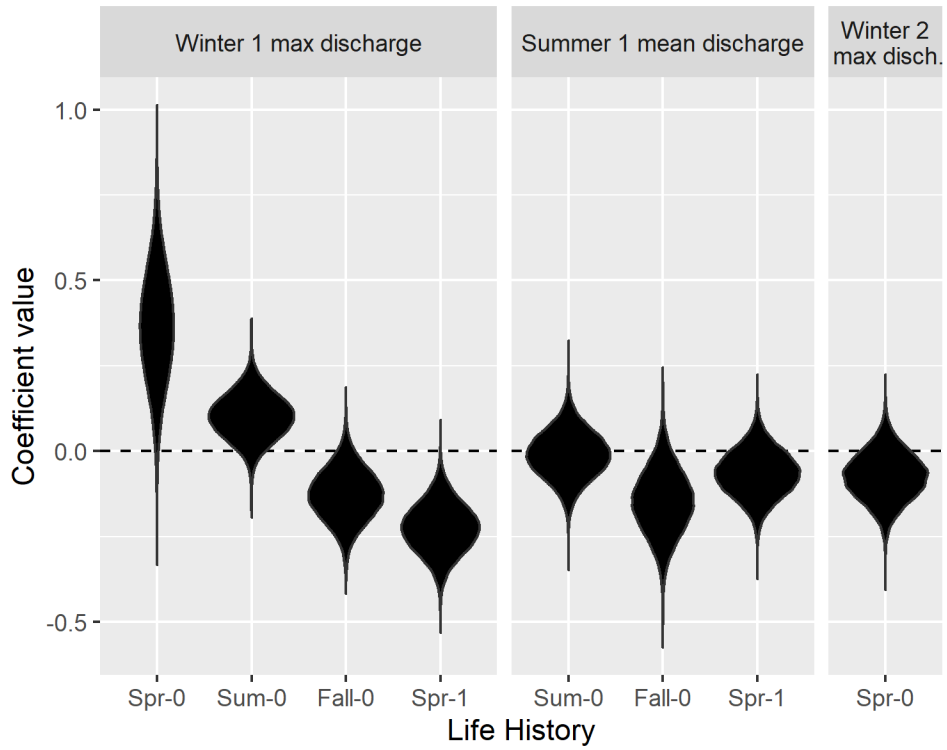

Figure A3: Coefficient values for the effects of log maximum daily stream discharge during a brood year's first winter (Winter 1), average discharge during its first summer (Summer 1), and log maximum discharge during its second winter (Winter 2) on process error in the annual abundance of each juvenile life history

References

Siegel, J. E., and C. J. Volk. 2019. Accurate spatiotemporal predictions of daily stream temperature from statistical models accounting for interactions between climate and landscape. PeerJ 7:e7892.

APPENDIX B

Age delineation based on length and capture date (Chapter 2)

This appendix documents how we assigned ages to juvenile Chinook captured in screw traps in the Wenatchee River Basin based on their length and day of year of capture. Emigration from natal streams occurred in three pulses each year (Figure S1), and the spring pulse included both age-0 and age-1 fish, which had different lengths (Figure S2 and S3).

A subset of emigrants >60 mm was implanted with passive integrated transponder tags, and a subset of those fish were detected when passing dams in the seaward-migration corridor. Based on the date of emigration and subsequent detection, we can infer the age that a fish was when it emigrated (Figure S3), because fish that emigrate at age 1 continue to the ocean in the same year and fish that emigrate at age 0 remain in the Wenatchee River Basin until the following year (Buchanan et al. 2015).

As a first step in developing a rule for classifying fish ages based on length and day of year at emigration, we determine the day of year before which 99.9% of fish that were known to have been age 1 at emigration were captured (Figure S4). The 99.9th quantile of capture days for 12,897 fish that were known to have been age 1 at emigration because they were subsequently detected in the migration corridor in the same year as emigration, was day 179. We therefore classified fish captured after day 179 as age 0.

The next step was to delineate age 0 and age 1 fish that emigration prior to day 179 based on their capture length and day of year. We used a three-step process to accomplish this task. First, we fit a mixture distribution of two normal distributions to the log-transformed lengths of all fish that had been captured within 10-day intervals (combining multiple years) starting on day 50 and ending on day 179 using the package *mixtools* in the R statistical environment (Benaglia et al.

2009; R Core Team 2021). Next, we found the length corresponding to the minimum densities between the two modes of the mixture distribution (Figure S5). Finally, we linearly interpolated between points represented by the midpoint of each 10-day interval and the length corresponding with the minimum density of the mixture distribution for that interval (Figure S6). Using the resulting line to delineate ages, this method correctly classified 99.91% of the 19,517 fish whose ages could be determined based on their date of capture and subsequent detection at dams in the migration corridor (Figure S7).

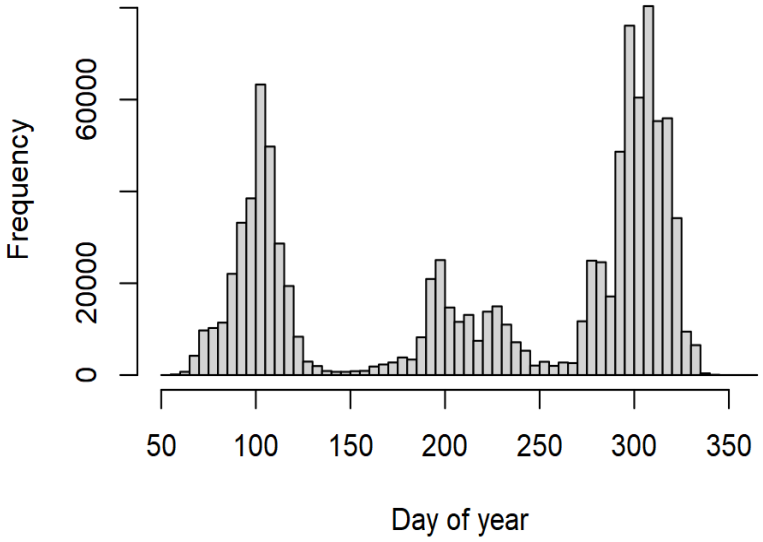

Figure B1: Histogram of the number of fish caught by day of year in three natal streams over multiple years.

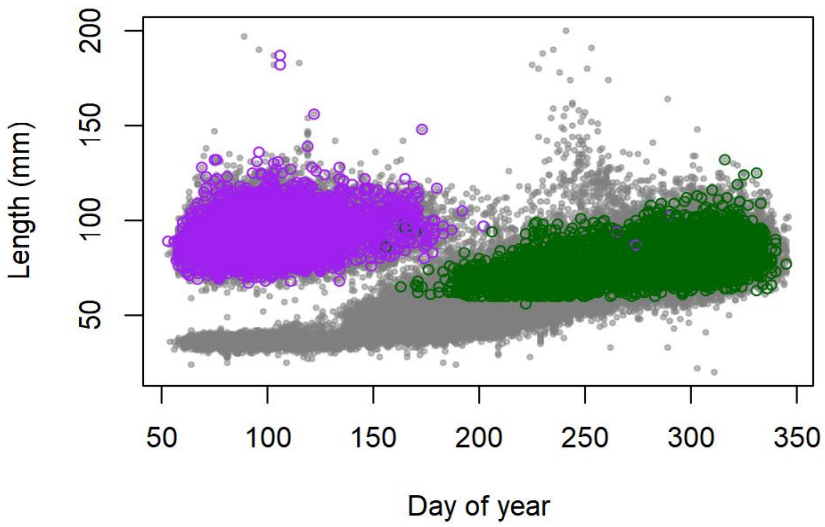

Figure B2: Length at emigration versus emigration day of year for fish that were known to have emigrated at age 1 (Purple) and age 0 (green) based on the timing of their initial capture and subsequent detections, overlain over all fish for which length and day of year at capture were available (gray).

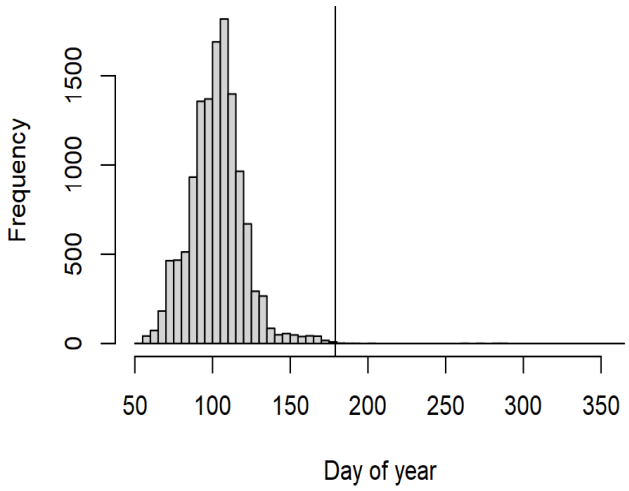

Figure B3: Histogram of capture day of year of fish that were tagged at screw traps and subsequently detected at mainstem dams when migrating downstream in the same year they were tagged. The vertical line represents the 99.9th quantile of capture day of year for these fish.

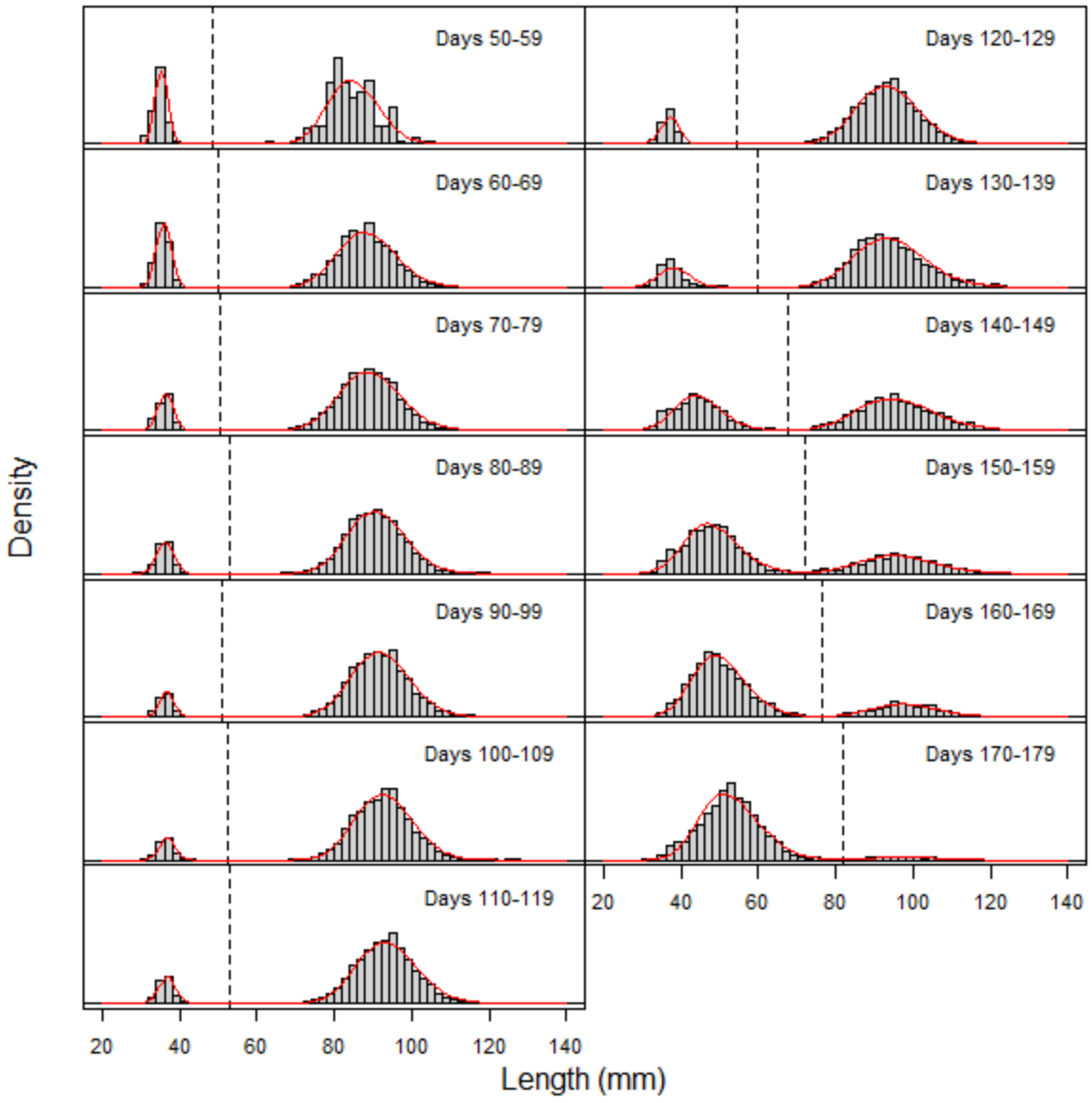

Figure B4: Histograms of the lengths of fish captured within 10-day intervals overlain with two-lognormal mixture distributions fit to these data (red line). The dashed vertical lines represent the minimum density of the mixture distribution between the two modes.

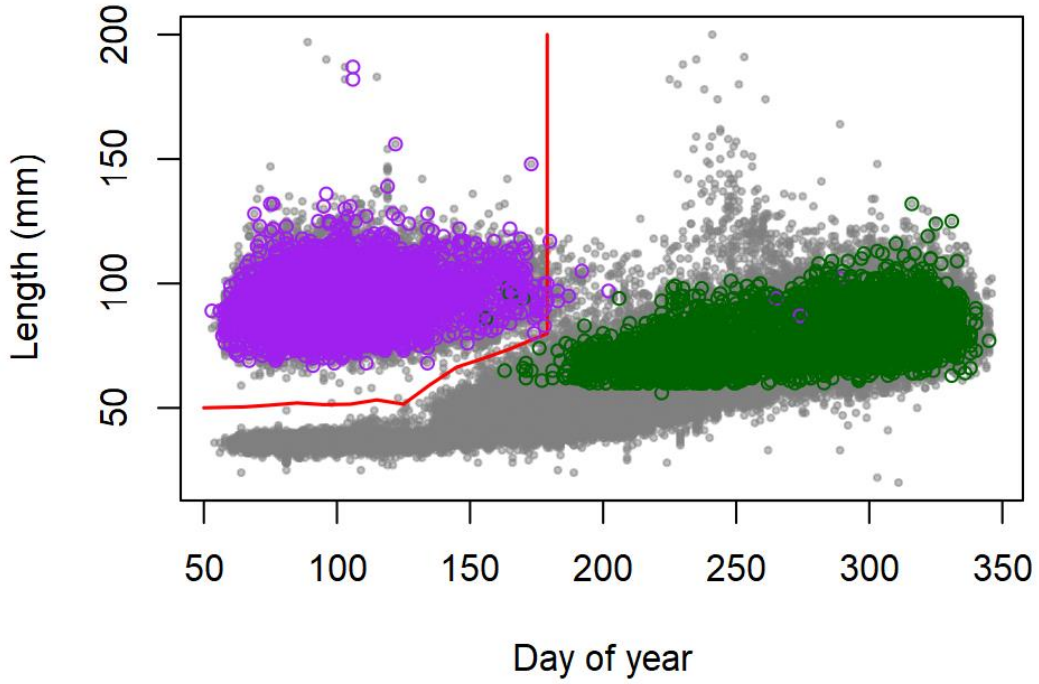

Figure B5: Cutoff line (red) for delineating age 1 (above line) from age 0 (below line) fish a based on their length and day of year of capture during emigration from natal streams. Grey points represent observed lengths and days of year of captured fish, purple points represent fish that were presumed to be age 1 at emigration based on the timing of their initial capture and subsequent detection in the migration corridor, and green points represent fish presumed to have been age 0 at emigration based on this information.

References

Benaglia T, Chauveau D, Hunter DR, Young D. 2009. mixtools: An R package for analyzing finite mixture models. Journal of Statistical Software **32**:1–29.

Buchanan RA, Skalski JR, Mackey G, Snow C, Murdoch AR. 2015. Estimating cohort survival through tributaries for salmonid populations with variable ages at migration. North American Journal of Fisheries Management **35**:958–973.

R Core Team. 2021. R: a language and environment for statistical computing. R Foundation for Statistical Computing, Vienna, Austria. Available from https://www.R-project.org/.

APPENDIX C

Supplementary tables and figures (Chapter 3)

Table C1: random effects of year included in models of: ϕ - survival probabilities following each detection occasion, ψ - probabilities of fish returning from the ocean at different ages, and p - detection probabilities on each occasion. *LHP* = juvenile life history strategy, and *NR.DS* = juvenile life history pathways where summer and fall subyearlings are grouped (i.e., natal-reach vs. downstream rearing). Detection probability at Tumwater Dam for adults was assumed to be 1.0.

Occasion	random effects of year
ϕ	
Natal emigration	Year + LHP*Year
Lower Wenatchee	Year + NR.DS*Year
McNary	Year + NR.DS*Year
Bonneville	Year + NR.DS*Year
Bonneville.ad	Year
McNary.ad	Year
ψ	
Bonneville	Year
p	
Lower Wenatchee	Year + LHP*Year
McNary	Year + NR.DS*Year
Bonneville	Year + NR.DS*Year
Bonneville.ad	Year
McNary.ad	Year
Tumwater.ad	-

Table C2: Estimates of survival across years by occasion, juvenile life history, natal stream, and fish age. The three juvenile life history pathways are fish that emigrated from their natal stream as subyearlings in summer (*Sum.0*) or fall (*Fal.0*), or as yearlings in spring (*Spr.1*). *DSR* represents both downstream-rearing life histories (summer and fall subyearlings) on occasions when they were assumed to be the same. *LHP* = life history pathway, *Lcl* = lower 95% confidence limit and *ucl* = upper 95% confidence limit.

Interval	LHP	Stream	Age	Median	lcl	ucl
1	Sum.0	Chiwawa	2	0.241	0.163	0.344
1	Sum.0	Nason	2	0.166	0.121	0.222
1	Sum.0	White	2	0.118	0.052	0.245
1	Fal.0	Chiwawa	2	0.401	0.268	0.552
1	Fal.0	Nason	2	0.336	0.254	0.430
1	Fal.0	White	2	0.152	0.096	0.232
1	Spr.1	Chiwawa	2	0.889	0.728	0.959
1	Spr.1	Nason	2	0.853	0.642	0.951
1	Spr.1	White	2	0.547	0.301	0.778
2	DSR	Chiwawa	2	0.347	0.230	0.481
2	DSR	Nason	2	0.388	0.295	0.487
2	DSR	White	2	0.419	0.316	0.531
2	Spr.1	Chiwawa	2	0.434	0.365	0.503
2	Spr.1	Nason	2	0.396	0.316	0.479
2	Spr.1	White	2	0.351	0.222	0.506
3	DSR	Chiwawa	2	0.709	0.538	0.832
3	DSR	Nason	2	0.708	0.536	0.833
3	DSR	White	2	0.708	0.536	0.833
3	Spr.1	Chiwawa	2	0.708	0.536	0.834
3	Spr.1	Nason	2	0.708	0.536	0.834
3	Spr.1	White	2	0.708	0.537	0.833
4	DSR	Chiwawa	-	0.027	0.021	0.037
4	DSR	Nason	-	0.028	0.019	0.042
4	DSR	White	-	0.027	0.012	0.060
4	Spr.1	Chiwawa	-	0.013	0.010	0.018
4	Spr.1	Nason	-	0.015	0.010	0.023
4	Spr.1	White	-	0.018	0.008	0.038
5	All	All	3	0.849	0.816	0.876
5	All	All	4	0.849	0.816	0.876

Interval	LHP	Stream	Age	Median	lcl	ucl
5	All	All	5	0.849	0.816	0.876
6	All	All	3	0.877	0.846	0.904
6	All	All	4	0.878	0.847	0.904
6	All	All	5	0.877	0.845	0.904

Table C3: Estimates of proportions of fish returning at ages three through five across years by occasion, juvenile life history, natal stream, and fish age. *DSR* = downstream-rearing life histories (summer and fall subyearling emigrants) and *Spr.1* = natal-reach-rearing life history. *LHP* = life history pathway, *Lcl* = lower 95% confidence limit and *ucl* = upper 95% confidence limit.

LHP	Age	Median	lcl	ucl
DSR	3	0.123	0.075	0.192
DSR	4	0.750	0.680	0.803
DSR	5	0.126	0.078	0.193
Spr.1	3	0.065	0.035	0.117
Spr.1	4	0.739	0.660	0.801
Spr.1	5	0.195	0.131	0.277

Table C4: Estimates of detection probabilities across years by occasion, juvenile life history, natal stream, and life history pathway. The three juvenile life history pathways are fish that emigrated from their natal stream as subyearlings in summer (*Sum.0*) or fall (*Fal.0*), or as yearlings in spring (*Spr.1*). *DSR* represents both downstream-rearing life histories (summer and fall). *LHP* = life history pathway, *Lcl* = lower 95% confidence limit and *ucl* = upper 95% confidence limit.

Occasion	LHP	Stream	Age	Median	lcl	ucl
2	Sum.0	Chiwawa	2	0.005	0.003	0.011
2	Sum.0	Nason	2	0.006	0.002	0.015
2	Sum.0	White	2	0.011	0.004	0.032
2	Fal.0	Chiwawa	2	0.008	0.005	0.013
2	Fal.0	Nason	2	0.008	0.005	0.013
2	Fal.0	White	2	0.007	0.003	0.014
2	Spr.1	Chiwawa	2	0.012	0.008	0.016
2	Spr.1	Nason	2	0.010	0.006	0.016
2	Spr.1	White	2	0.005	0.001	0.016
3	DSR	Chiwawa	2	0.257	0.222	0.294
3	DSR	Nason	2	0.256	0.221	0.294
3	DSR	White	2	0.254	0.217	0.294
3	Spr.1	Chiwawa	2	0.252	0.220	0.287
3	Spr.1	Nason	2	0.252	0.219	0.288
3	Spr.1	White	2	0.253	0.217	0.293
4	DSR	Chiwawa	2	0.126	0.094	0.166
4	DSR	Nason	2	0.126	0.092	0.169
4	DSR	White	2	0.112	0.069	0.176
4	Spr.1	Chiwawa	2	0.108	0.082	0.141
4	Spr.1	Nason	2	0.129	0.093	0.173
4	Spr.1	White	2	0.119	0.076	0.180
5	All	All	3	0.931	0.790	0.980
5	All	All	4	0.995	0.976	0.999
5	All	All	5	0.954	0.895	0.981
6	All	All	3	0.984	0.967	0.992
6	All	All	4	0.984	0.967	0.992
6	All	All	5	0.984	0.967	0.992

Table C5: Standard deviations of Gaussian hyper-distributions of random effects of year on survival by occasion and juvenile life history pathway (LHP). The three juvenile life history pathways are fish that emigrated from their natal stream as subyearlings in summer (*Sum.0*) or fall (*Fal.0*), or as yearlings in spring (*Spr.1*). *DSR* represents both downstream-rearing life histories (summer and fall). *LHP* = life history pathway, *Lcl* = lower 95% confidence limit and *ucl* = upper 95% confidence limit.

Interval	LH	Median	lcl	ucl
1	All	0.074	0.010	0.521
1	Fal.0	0.138	0.049	0.398
1	Spr.1	0.079	0.009	0.691
1	Sum.0	0.136	0.037	0.485
2	All	0.234	0.125	0.436
2	Spr.1	0.079	0.013	0.479
2	DSR	0.072	0.011	0.458
3	All	0.022	0.002	0.238
3	Spr.1	0.021	0.002	0.230
3	DSR	0.022	0.002	0.230
4	All	0.203	0.073	0.558
4	Spr.1	0.153	0.024	1.065
4	DSR	0.099	0.013	0.702
5	All	0.024	0.002	0.260
6	All	0.024	0.002	0.274

Table C6: Standard deviations of Gaussian hyper-distributions of random effects of year on detection probabilities by occasion and juvenile life history strategy (LH). The three juvenile life history pathways are fish that emigrated from their natal stream as subyearlings in summer (*Sum.0*) or fall (*Fal.0*), or as yearlings in spring (*Spr.1*). *DSR* represents both downstream-rearing life histories (summer and fall). *LHP* = life history pathway, *Lcl* = lower 95% confidence limit and *ucl* = upper 95% confidence limit.

Occasion	LH	Median	lcl	ucl
2	All	0.392	0.217	0.717
2	Fal.0	0.240	0.083	0.693
2	Spr.1	0.190	0.043	0.875
2	Sum.0	0.640	0.290	1.478
3	All	0.259	0.159	0.420
3	Spr.1	0.080	0.016	0.398
3	DSR	0.145	0.058	0.361
4	All	0.298	0.157	0.558
4	Spr.1	0.116	0.024	0.526
4	DSR	0.202	0.086	0.469
5	All	0.024	0.002	0.267
6	All	0.023	0.002	0.274

Table C7: Marginal standard deviations and correlation of random effects of year on age proportions of returning adults. The proportions were modeled with a multinomial logit link, where age 4 was the reference age. *Lcl* = lower 95% confidence limit and *ucl* = upper 95% confidence limit.

Age	Median	lcl	ucl
3	0.5	0.218	1.174
5	0.542	0.299	0.98
Corr	-0.624	-0.931	0.705

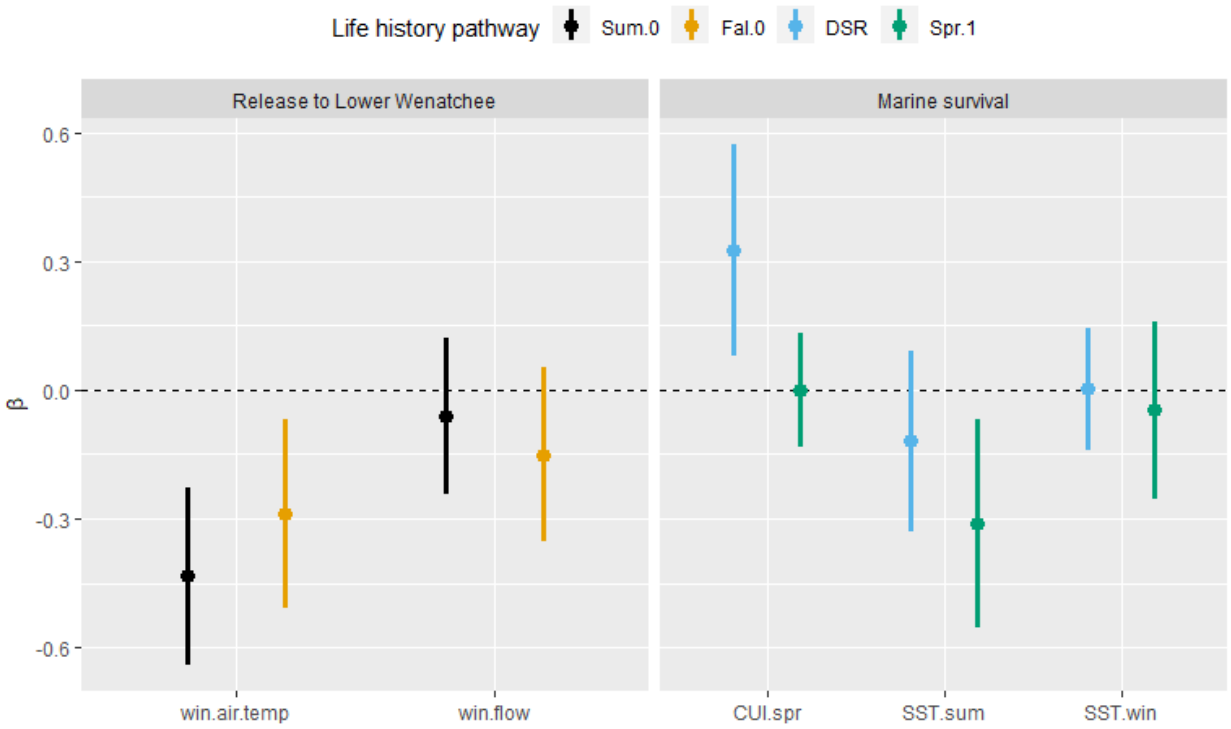

Figure C1: Effects of environmental covariates on survival by occasion (column) and juvenile life history pathway (color). The three juvenile life history pathways are fish that emigrated from their natal stream as subyearlings in summer (*Sum.0*) or fall (*Fal.0*), or as yearlings in spring (*Spr.1*). *DSR* represents both downstream-rearing life histories (summer and fall subyearlings). *CUI.spr* = coastal upwelling index during spring, *SST.sum* = sea surface temperature off the Washington coast during summer, and *SST.win* = sea surface temperature in an arc of the northeast Pacific Ocean defined by Johnstone and Mantua (2014) during the winter prior to when juveniles enter the marine environment. Points represent mean estimates and lines span 95% confidence intervals.

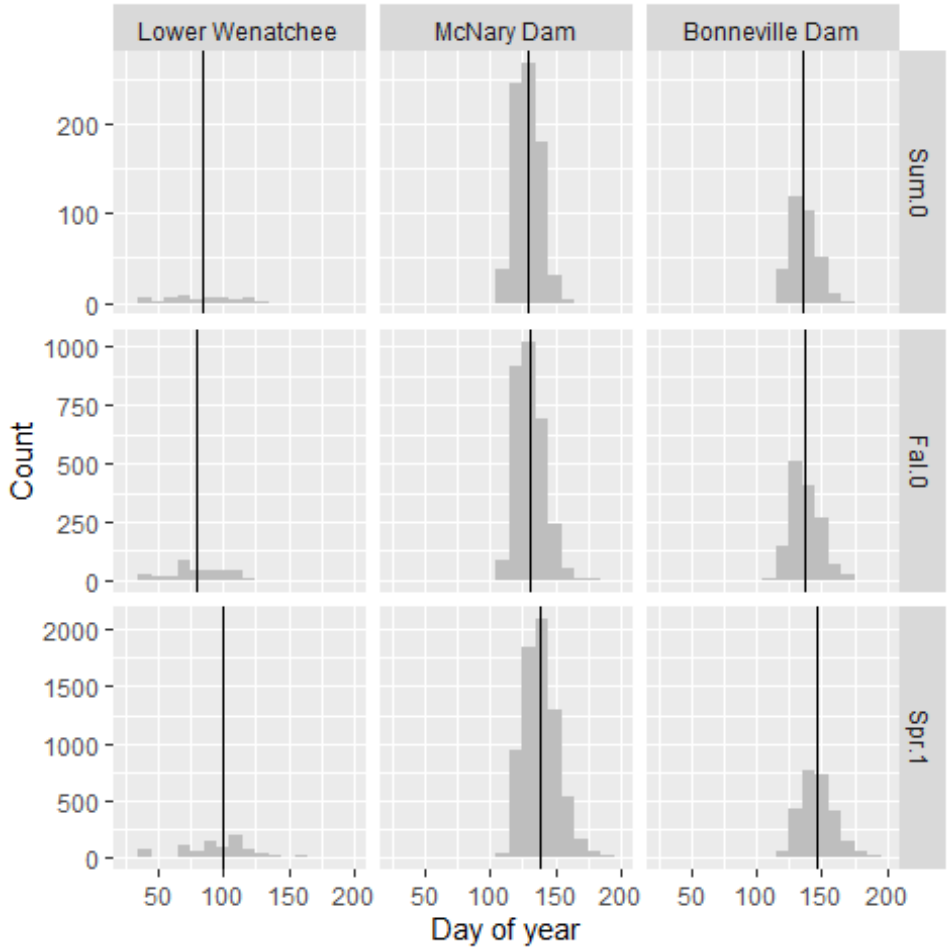

Figure C2: Day of year of detections at three sites (columns) by juvenile life history pathways (rows). Fish from all study years and natal streams are represented. Vertical lines indicate median detection days. Summer (*Sum.0*) and fall (*Fal.0*) subyearling emigrants (downstream-rearing fish) had very similar detection timing to each other. downstream-rearing fish were detected 19 days earlier than yearling (*Spr.1*) emigrants (natal-reach-rearing fish) in the Lower Wenatchee River trap,9 days earlier at McNary Dam, and 10 days earlier at Bonneville Dam on average.

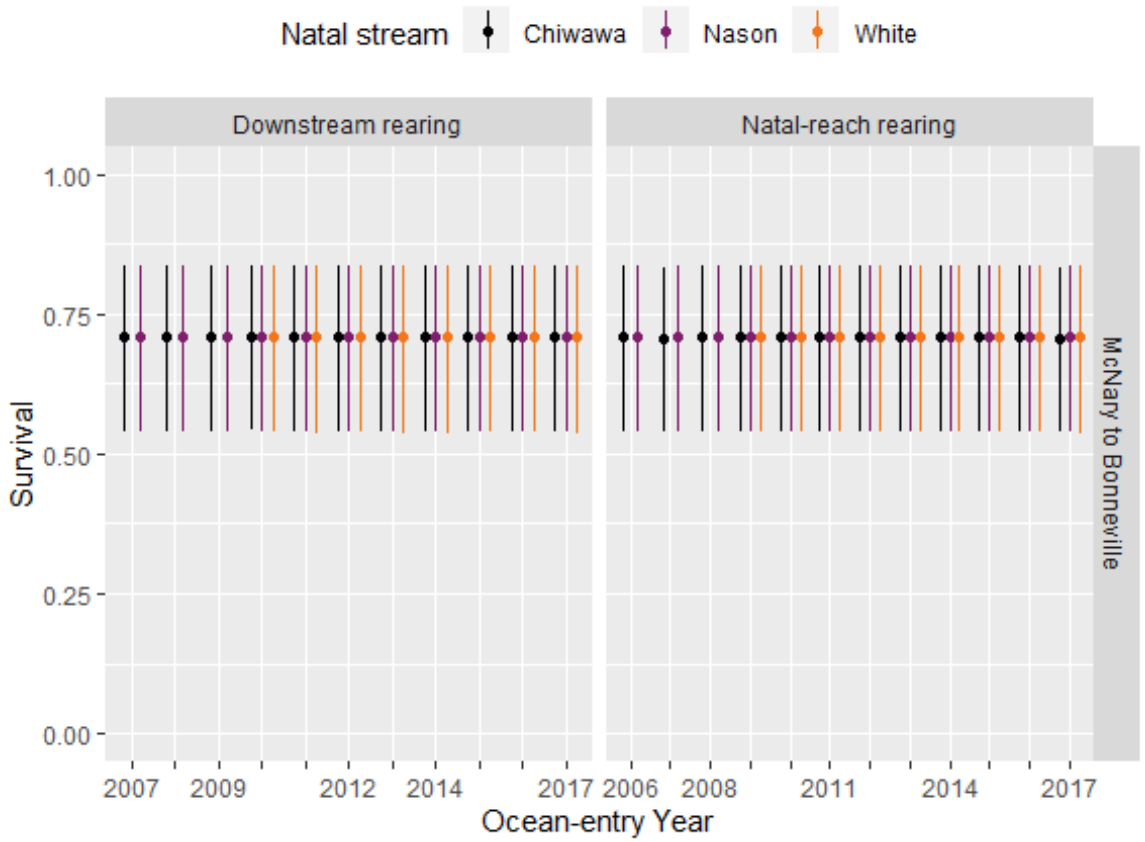

Figure C3: Annual survival estimates between McNary Dam and Bonneville Dam by natal stream (color) and juvenile life history pathway (column): Points represent mean estimates and lines span 95% confidence intervals. As with all effects, the lack of year-to-year variability does not imply that survival is constant, but rather that this model and data did not provide evidence of year-varying survival rates.

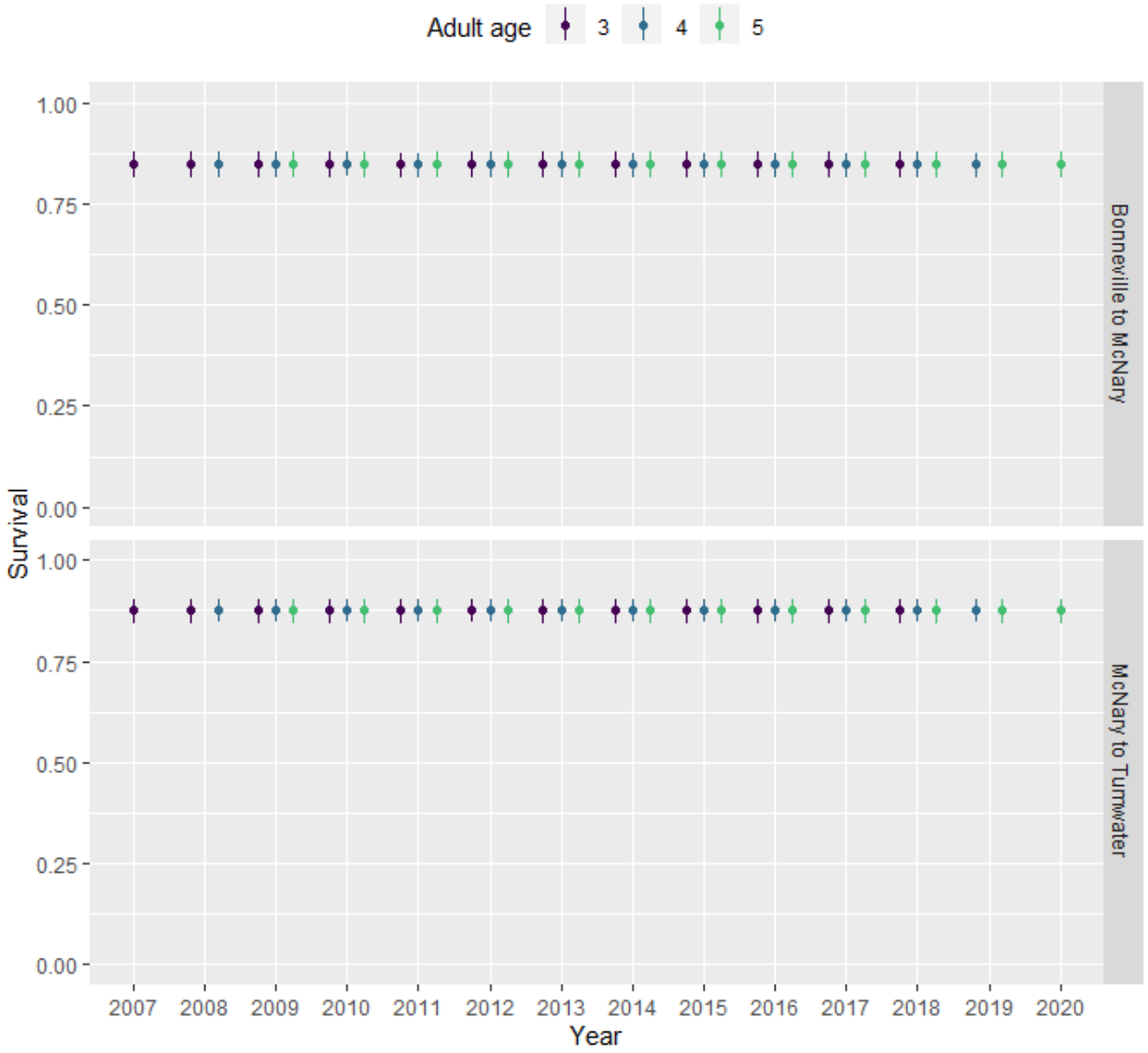

Figure C4: Annual survival estimates for upstream migrating adult Chinook salmon between Bonneville Dam and McNary Dam (top row) and McNary Dam and Tumwater Dam (bottom row), where color represents adult age. Points represent mean estimates and lines span 95% confidence intervals.

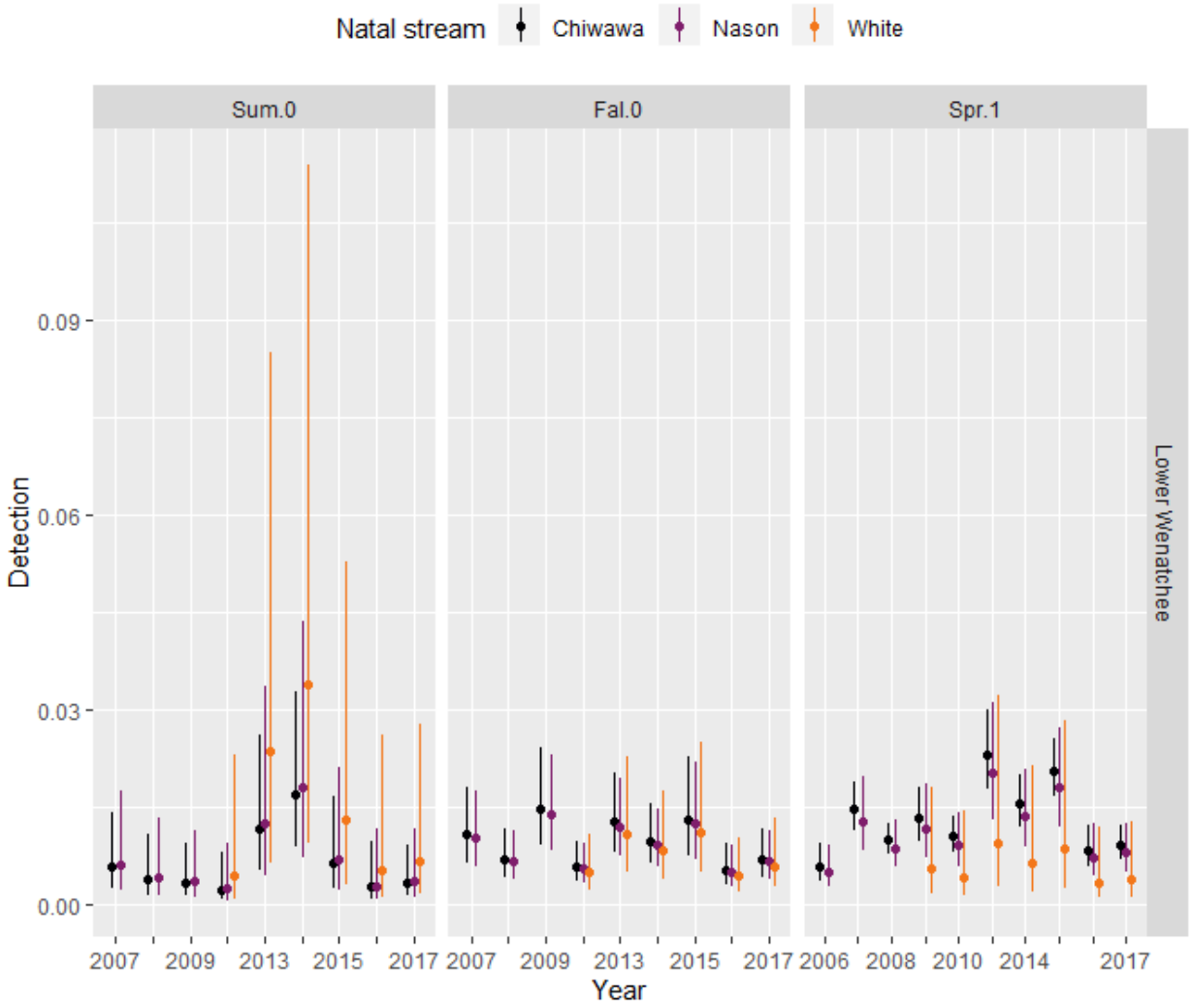

Figure C5: Annual detection probability estimates for downstream-migrating juvenile Chinook salmon at the lower Wenatchee River screw trap by natal stream (colors) and juvenile life history strategy (columns). The three juvenile life history pathways are fish that emigrated from their natal stream as subyearlings in summer (*Sum.0*) or fall (*Fal.0*), or as yearlings in spring (*Spr.1*). Points represent mean estimates and lines span 95% confidence intervals.

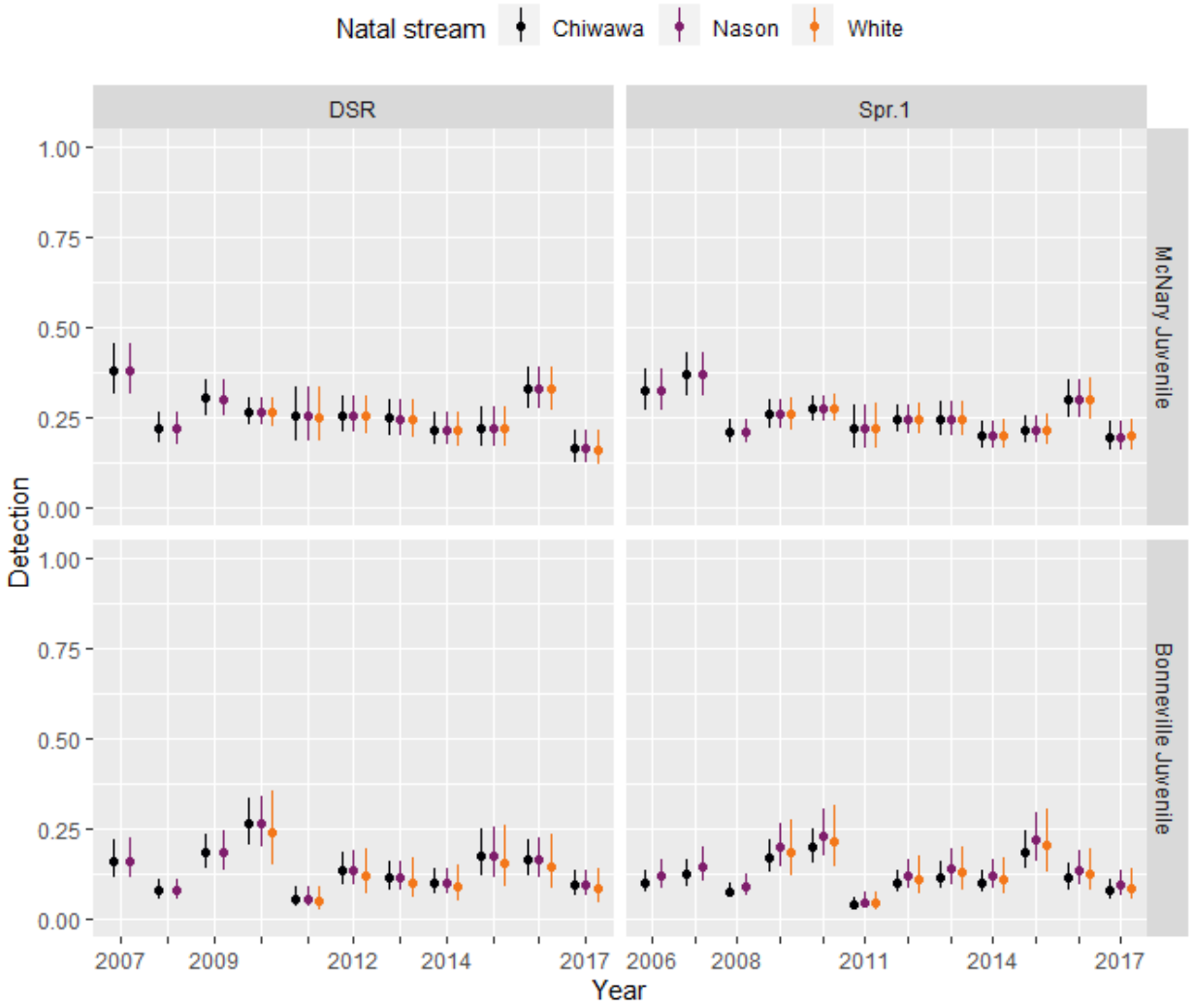

Figure C6: Annual detection probability estimates for downstream-migrating juvenile Chinook salmon at McNary Dam (top row) and Bonneville Dam (bottom row) by natal stream (colors) and juvenile life history pathway: *DSR* = downstream-rearing life histories (summer and fall subyearling emigrants) and *Spr.1* = natal-reach-rearing life history (spring yearling emigrants). Points represent mean estimates and lines span 95% confidence intervals.

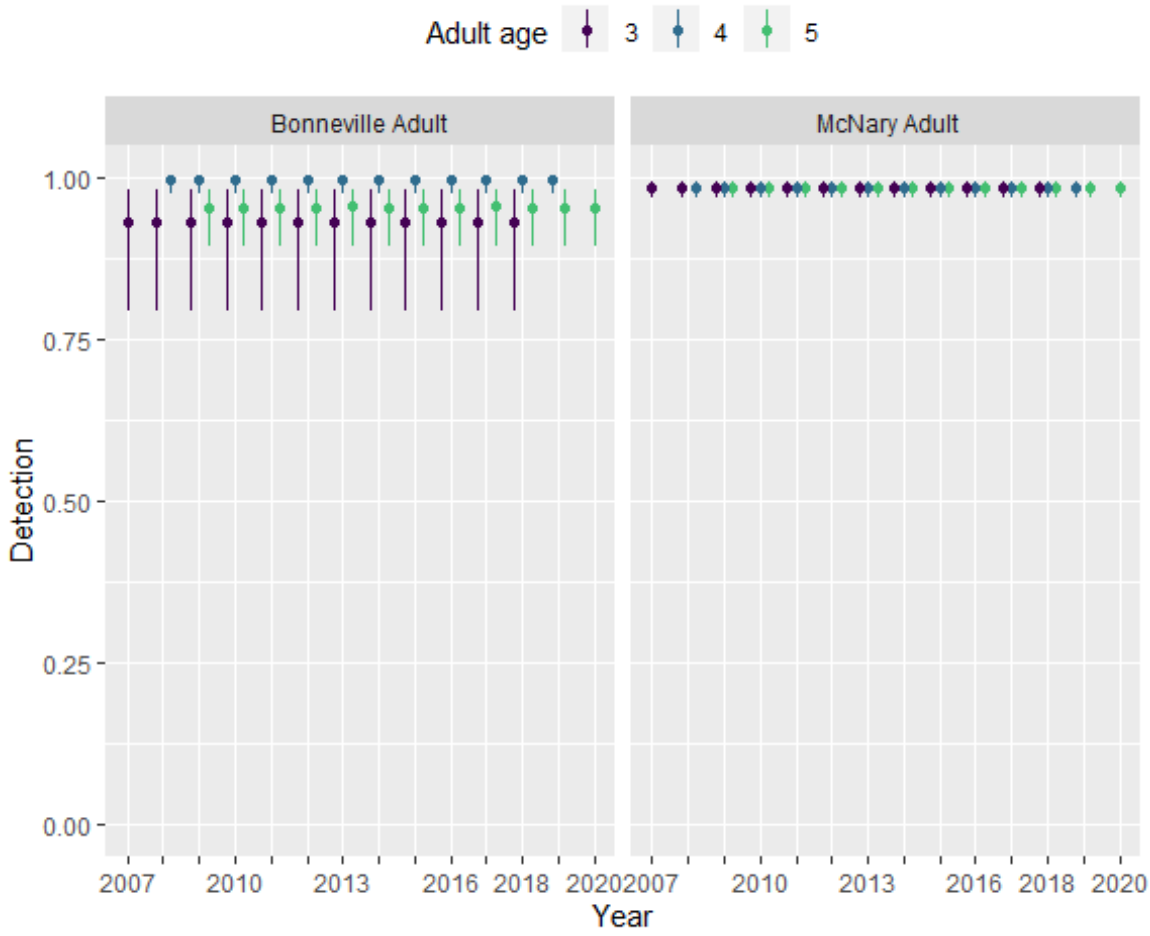

Figure C7: Annual detection probability estimates for upstream-migrating adult Chinook Salmon at Bonneville Dam (top row) and McNary Dam (bottom row), where color represents adult age. Points represent mean estimates and lines span 95% confidence intervals.

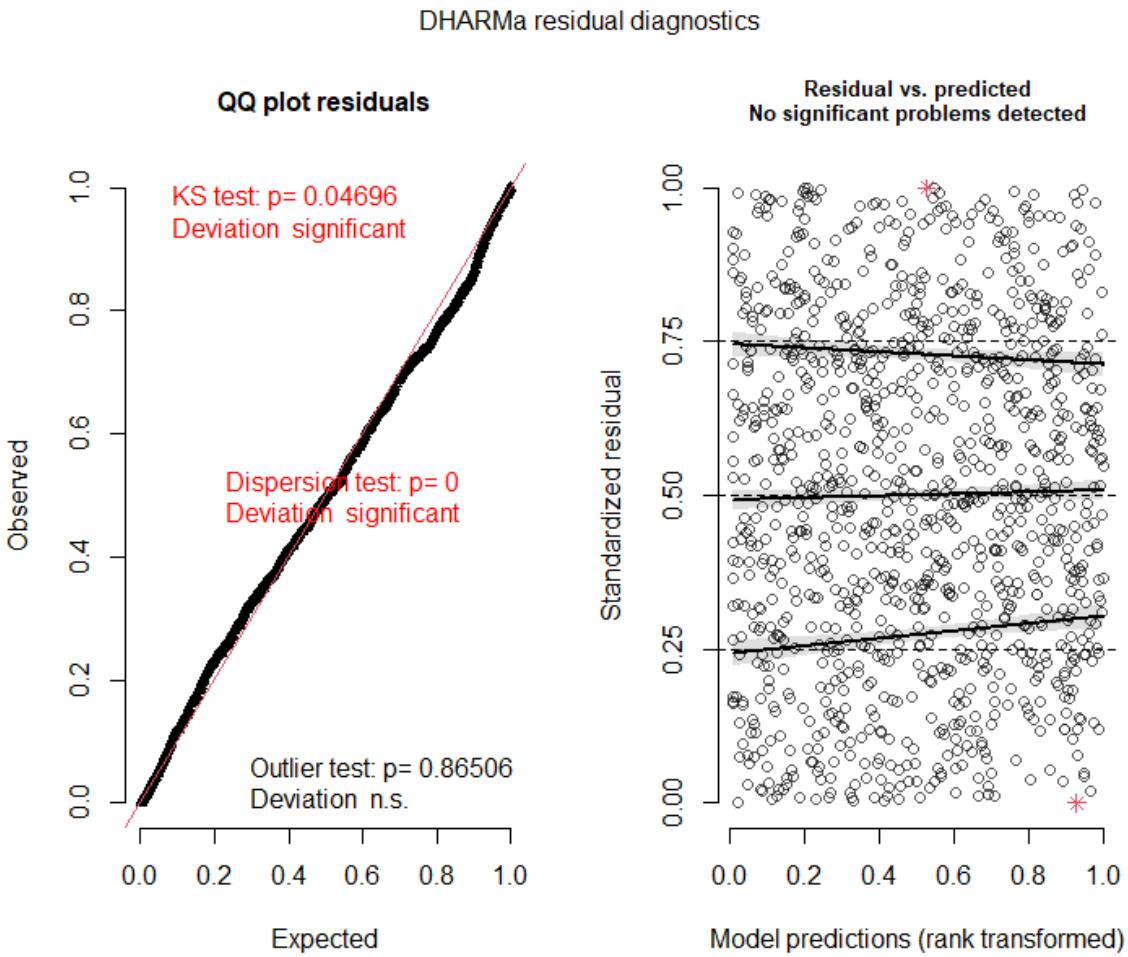

Figure C8: DHARMa residual diagnostics for simulated quantile residuals conditional on fitted random effects. The left panel shows a Q-Q plot and the right show a plot of residuals versus rank-transformed model predictions. Red asterisks indicate outliers, and the thick lines show a quantile regression fit to the residuals, which should follow the dashed horizontal lines if the residuals are uniformly distributed along the y-axis as expected.

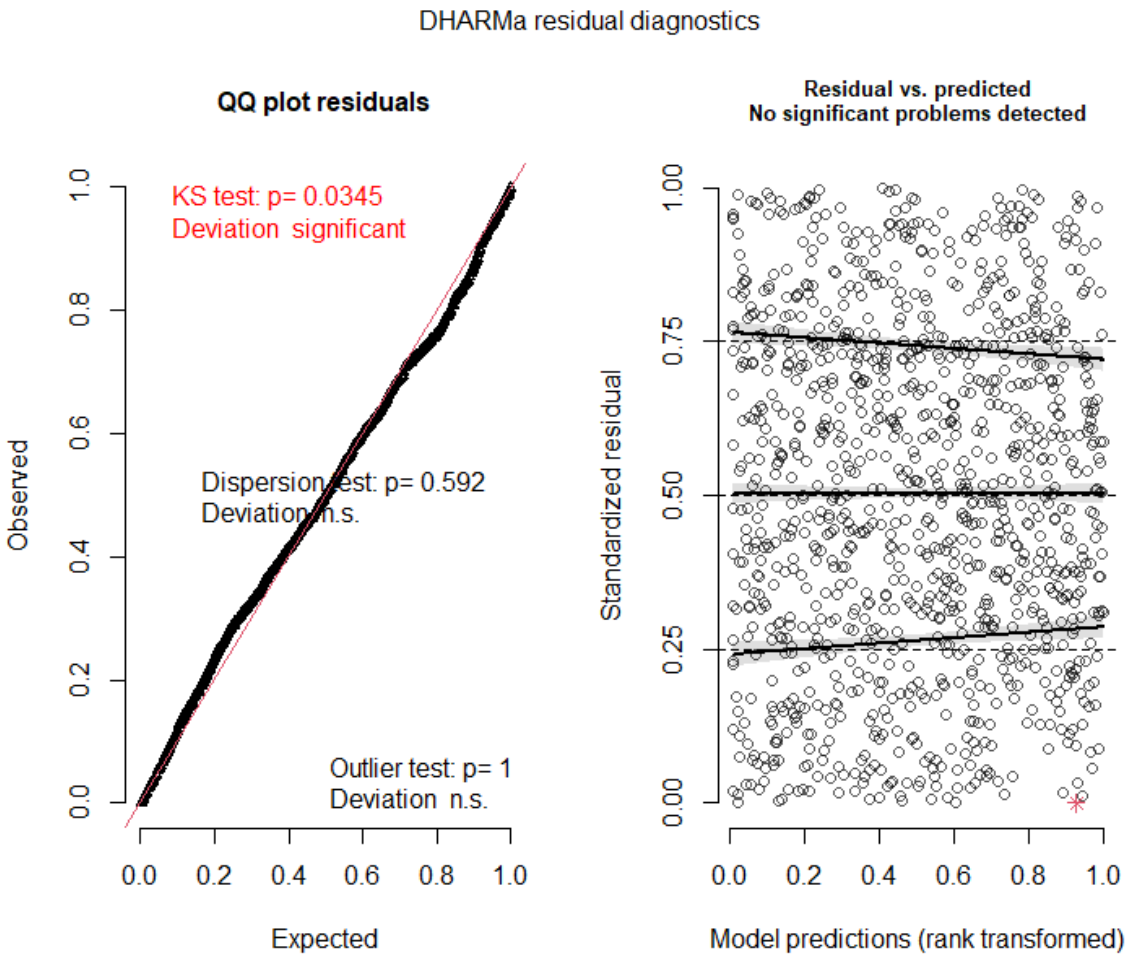

Figure C9: DHARMa residual diagnostics for standardized quantile residuals marginalized over random effects of year. The left panel shows a Q-Q plot and the right show a plot of residuals versus rank-transformed model predictions. Red asterisks indicate outliers, and the thick lines show a quantile regression fit to the residuals, which should follow the dashed horizontal lines if the residuals are uniformly distributed along the y-axis as expected.

APPENDIX D

Description of juvenile production model within integrated population model (Chapter 4)

The model of the production of juvenile emigrants in the integrated population model (IPM) follows the model of juvenile production described in Sorel et al (*in review*). In the description below, we highlight differences between the model in that paper and the model in the IPM.

As described in the main manuscript text, juvenile emigrant abundance, $Juv_{h,y,s,}$, expressing LHP *h* and emigrating in year *y* from stream *s* was calculated as a function of the effective number of female spawners, $S_{y_h,s}$, in year y_h, which is one year before the emigration year for subyearling emigrants and two years previous for yearling emigrants. To allow for both positive and negative density-dependence in the production of juvenile emigrants from natal streams, we modeled juvenile production using the modified Beverton-Holt function of Myers et al. (1995),

$$Juv_{h,y,s} = \frac{\alpha_{h,s} S_{y_h,s}^{\gamma_{h,s}}}{1 + \frac{\alpha_{h,s} S_{y_h,s}^{\gamma_{h,s}}}{J_{h,s}^{\max}}} \exp\left(\epsilon_{h,y,s}^{J}\right) \quad (1)$$

with shape parameters $\alpha_{h,s}$, $\gamma_{h,s}$, and $J_{h,s}^{\max}$ (Sorel et al. *in review*; Ch. 2).

The shape parameters of the modified Beverton-Holt function, $\alpha_{h,s}$, $\gamma_{h,s}$, and $J_{h,s}^{\max}$, were modeled hierarchically across streams, *s*, and within life history pathways, *h*, such that $\alpha_{h,s} \sim \text{logNormal}(\mu_h^{\alpha}, \sigma_h^{\alpha})$, with corresponding hyperdistributions for $\gamma_{h,s}$ and $J_{h,s}^{\max}$. Exponential priors were applied to the hyperdistribution standard deviations, [e.g., $\sigma_h^{\alpha} \sim exp(\lambda)$], to help with fitting in light of there being only three streams (Gelman 2006,

Simpson et al. 2017). The same rate parameter, λ, which controls the strength of penalization was applied for all three Beverton-Holt rate parameters and four LHPs.

We penalized deviations of the hyperdistribution log-means, μ_h^γ, for shape parameter, $\gamma_{h,s}$, for each life history pathway, *h*, from zero to put prior weight on a model with less density dependence,

$$\mu_h^\gamma \sim N\left(0, \tau_h^\gamma\right), \quad \tau_h^\gamma \sim \text{Exp}(\lambda^\gamma), \tag{2}$$

where the parameter λ^γ controls the strength of penalization and was applied for all four life history pathways. We penalized deviations of the hyperdistribution log-mean, $\mu_h^{J^{\max}}$, for the shape parameter $J_{h,s}^{\max}$ from the natural log of 1.5e4, which was greater than the upper limit of the 95% confidence interval of the largest observed abundance of emigrants in the dataset (1.26e4) to put prior weight on a model with less density dependence,

$$\mu_h^{J^{\max}} \sim N\left(\log(1.5e4), \tau_h^{J^{\max}}\right), \quad \tau_h^{J^{\max}} \sim \exp\left(\lambda^{J^{\max}}\right) \tag{3}$$

where the parameter $\lambda^{J^{\max}}$ controls the strength of penalization and was applied for all four life history pathways. Unlike in Sorel et al. (*in review*; Ch. 2), we applied a weakly informative prior on the hyperdistribution log-means, μ_h^α, for the shape parameters, $\alpha_{h,s}$, for spawner to juvenile productivity, $\mu_h^\alpha \sim N(4, 3)$, to regulate productivity away from unrealistically high values.

Process errors around the Beverton-Holt function, $\epsilon_{h,y,s}^{J}$, for life history pathway *h*, year *y*, and stream *s* were modeled as,

$$\epsilon_{h,y,s}^{J} = \boldsymbol{x}'_{h,y,s}\boldsymbol{\beta}_h^\epsilon + \omega_y l_{h,s} + \eta_{h,y,s}, \tag{4}$$

with effects, $\boldsymbol{\beta}_h^{\epsilon}$, of environmental covariates $\boldsymbol{x}_{h,y,s}$, effect $l_{h,s}$ of latent covariate ω_y, and idiosyncratic random term $\eta_{h,y,s}$. The latent covariate, $\omega_y \sim N(0,1)$, reflected environmental drivers that were not otherwise accounted for and could lead to correlated process error among life history pathways and natal streams. The error, $\eta_{h,y,s} \sim N(0, \sigma_{h,s}^{\eta})$, accounted for variability among years that was uncorrelated among LHPs and streams.

The environmental covariates included in $\boldsymbol{x}_{h,y,s}$ varied by life history pathway *h* to reflect the amount of time that each life history spent in the natal stream. For all life history pathways, we included an effect of log maximum daily winter (November–February) stream discharge during fish's first winter**.** For all but spring subyearling emigrants, we included an effect of mean daily summer (June-September) discharge. Finally, for spring yearling emigrants only, we included an effect of log maximum daily winter stream discharge during their second winter. We assumed that the effect of each environmental covariate was the same across natal streams but could differ among life history pathways. We scaled the stream discharge covariates by their stream-specific means and standard deviations to model effects of standardized annual deviations from average discharge within each stream. Records of streamflow in the Chiwawa River were obtained from the U.S. Geological Survey's gauge using the *dataRetrieval* package in R (Hirsch et al. 2015), and data on streamflow in Nason Creek and the White River was obtained from Washington Department of Ecology stream gauges (Washington Department of Ecology 2020).

Unlike in Sorel et al. (*in review*; Ch. 2), we applied penalized-complexity priors on the effects of stream-discharge covariates, $\boldsymbol{\beta}_h^{\epsilon} \sim N(0, \sigma_h^{\beta})$, $\sigma_h^{\beta} \sim \exp(\lambda^{\beta})$, to balance bias and variance in predictions (Simpson et al. 2017). Effects of the latent covariates were assumed to arise from a zero-centered normal hyperdistribution, $l_{h,s} \sim N(0, \sigma^{l})$, with penalization on the standard deviation, $\sigma^{l} \sim \exp(\lambda^{\epsilon})$, to help with model fitting. An exponential prior was applied on the

standard deviations of the idiosyncratic errors, $\sigma_{h,s}^{\eta} \sim \exp(\lambda^{\epsilon})$, where the penalization rate, λ^{ϵ}, was the same rate parameter used in the prior on the latent covariate effect hyperdistribution standard deviation. On all penalization rate parameters, $\lambda, \lambda^{\gamma}, \lambda^{J^{\max}}, \lambda^{\beta} and\ \lambda^{\epsilon}$, we applied a half-normal prior, $\lambda \sim \text{half} - \text{normal}(0, 25)$.

References

Gelman, A. 2006. Prior distributions for variance parameters in hierarchical models (comment on article by Browne and Draper). Bayesian Analysis 1:515–534.

Hirsch, R., L. DeCicco, and D. Lorenz. 2015. User guide to Exploration and Graphics for River Trends (EGRET) and dataRetrieval: R packages for hydrologic data. U.S. Geological Survey.

Myers, R. A., N. J. Barrowman, J. A. Hutchings, and A. A. Rosenberg. 1995. Population dynamics of exploited fish stocks at low population levels. Science 269:1106–1108.

Simpson, D., H. Rue, A. Riebler, T. G. Martins, and S. H. Sørbye. 2017. Penalizing model component complexity: a principled, practical approach to constructing priors. Statistical Science 32:1–28.

Sorel, M. H., A. R. Murdoch, R. W. Zabel, C. M. Kamphaus, E. R. Buhle, M. D. Scheuerell, and S. J. Converse. in review. Effects of population density and environmental conditions on life-history expression in a migratory fish.

Washington Department of Ecology. 2020. Flow Monitoring Network. https://fortress.wa.gov/ecy/eap/flows/regions/state.asp.

APPENDIX E

Description of survival and marine-return model within the integrated population model (Chapter 4)

Based on Sorel et al. (*in review*; Ch. 3), we used a multi-state mark-recapture model to estimate downstream survival and ocean return rate, $\phi_{t,l,s,y}$, by interval t, juvenile LHP l, natal stream s, and year y; upstream adult survival, $\phi_{t,y,a}$, by interval, year, and age a; and conditional return-age probabilities, $\psi_{l,y,a}$, by juvenile LHP, year, and age (Arnason 1973, Brownie et al. 1993). Because fish could not be observed after passing downstream of Bonneville Dam unless they returned to Bonneville Dam one to three years later (occasion five; Table 1), annual marine survival and maturation (i.e., return) probabilities were confounded and not separately identifiable without making assumptions such as constant annual survival. Instead, we modeled the probability of return at any age for fish entering the ocean each year (i.e., return rate), and conditional on return, the probability, $\psi_{l,y,a}$, of returning at a given age *a* (Buhle et al. 2018).

Survival and marine-return rates — We modeled survival of juveniles and return rates from the ocean, $\phi_{t,l,s,y}$, for interval t, juvenile LHP l, natal stream s, and year y; as:

$$\begin{aligned} \text{logit}\left(\phi_{t,l,s,y}\right) &= \alpha_t + \boldsymbol{x}_{t,l,s,y}\boldsymbol{\beta} + \delta_{t,y} + \epsilon_{t,l,y} \\ \delta_{t,y} &\sim \text{N}(0, \sigma_t) \\ \epsilon_{t,l,y} &\sim \text{N}\left(0, \tau_{t,l}\right) \end{aligned} \qquad (1)$$

with interval-specific intercept, α_t, covariate and categorical effect vector, $\boldsymbol{x}_{t,l,s,y}$, coefficient vector, $\boldsymbol{\beta}$, random effect of year specific to each time interval, $\delta_{t,y}$, and random effects of year specific to each time interval and LHP, $\epsilon_{t,y,l}$ [where downstream-rearing LHPs (*spr.0*, *sum.0*, and *fal.0*) were grouped after the first interval]. Synchronous random effect of year, $\delta_{t,y}$, that

affected all LHPs were included to account for correlation in survival across LHPs among-years. We assumed that both the synchronous and asynchronous random effects of year were normally distributed around zero with standard deviations σ_t and $\tau_{t,l}$, respectively.

Penalized-complexity priors (Simpson et al. 2017) were applied on coefficients and random effects of year to balance variance and bias and help with model fitting. The prior on each coefficient was a zero-centered normal distribution, $\beta_n \sim \mathrm{N}(0.0, \upsilon_{\beta_n})$, with unique standard deviation, υ_{β_n}, for each coefficient, on which we applied an exponential penalty, $\upsilon_{\beta_n} \sim \exp(\lambda_t)$. The strength of the penalty was determined by the rate parameter, λ_t, which we applied to all υ_{β_n} within a given interval. Exponential penalties were also applied to standard deviations of the hyper-distributions for the random effects of year, $\sigma_t \sim \exp(\lambda_t^{\mathrm{rand}})$, and $\tau_{t,l} \sim \exp(\lambda_t^{\mathrm{rand}})$, with a unique penalty rate parameter ($\lambda_t^{\mathrm{rand}}$) applied in each interval *t*. We fit the penalty rate parameters, λ_t and $\lambda_t^{\mathrm{rand}}$, as part of the model and applied half-normal priors, e.g., $\lambda_t \sim \mathrm{half-normal}(0,\ 25)$, to constrain those that were not well informed by the data. Table 1 details the effects included in each survival interval and Table 2 details the random effects of year. For categorical variables, sum-constraint coding was used in the design vectors ($\boldsymbol{x}_{t,l,s,y}$) such that the penalized coefficients represented deviations from across-group means.

We allowed survival during the first survival interval, from initial release to the screw trap at the Wenatchee River-Columbia River confluence, to vary by juvenile LHP, natal stream, and their interaction (Table 1). During the second through fourth survival intervals, downstream-rearing LHPs (*spr.0*, *sum.0*, and *fal.0*), were assumed to have common survival. Specifically, we fit effects of LHP type (downstream- and natal-reach reach rearing), natal stream, and their

interaction during the second through fourth survival intervals, where the fourth interval represented return from the ocean at any adult age.

We included effects of environmental covariates on survival during the first and fourth intervals (Table 1). For survival during the first interval, which represents rearing in the mainstem Wenatchee River for downstream-rearing LHPs, we modeled an effect of average annual winter (November–February) air temperature and Wenatchee River discharge for downstream-rearing LHPs only (Favrot and Jonasson 2020). These covariate effects were allowed to differ between *spr.0*/*sum.0* and *fal.0* LHPs and were assumed to be the same among natal streams. For survival during the fourth interval, representing the probability of returning from the ocean at any age, we included effects of coastal upwelling anomalies off the coast of Washington State in the spring when fish entered the ocean, and sea surface temperature off the coast of Washington State during fish's first marine summer (Crozier et al. 2021). Effects of these covariates were allowed to differ between downstream- and natal-reach-rearing LHPs and were assumed to be common among natal streams. We normalized all environmental covariates prior to inclusion.

Wenatchee River discharge data were from obtained from USGS gauge 12459000 using the dataRetrieval package in R version 4.0.4 (R Core Team 2021; De Cicco et al. 2018) and data on air temperature at Wenatchee Pangborn Airport were obtained using the National Weather Service's NOWData webtool (https://w2.weather.gov/climate/xmacis.php?wfo=otx).
Average coastal upwelling anomaly data at 45°N by 125°W from March through May (https://www.pfeg.noaa.gov/products/PFELData/upwell/monthly/upanoms.mon) and sea surface temperature within a 2° x 2° square (46°–48°N by 124°–126°W) off the Washington Coast during June–August (https://www1.ncdc.noaa.gov/pub/data/cmb/ersst/v5/netcdf/) were obtained from the GitHub repository (bchasco/SAR_paper) associated with Chasco et al. (2021).

For survival intervals representing adult upstream migration (five and six), we assumed that survival was common among LHPs and natal streams but allowed for differences by adult return age *a*, which might arise due to age-specific migration timing differences and temporally varying fisheries or physical river conditions (Tables 1 and 2). Adult survival was modeled as:

$$\begin{aligned} \text{logit}\left(\phi_{t,y,a}\right) &= \alpha_t + \boldsymbol{x}_{t,y,a}\boldsymbol{\beta} + \delta_{t,y} \\ \delta_{t,y} &\sim \text{N}(0, \sigma_t) \end{aligned} \qquad (2)$$

where α_t is an interval-specific intercept, $\boldsymbol{x}_{t,y,a}$ is a row of the design matrix coding age effects, $\boldsymbol{\beta}$ is a coefficient vector, and $\delta_{t,y}$ are random effects of year specific to each time interval. We did not fit asynchronous year effects for upstream survival due to smaller sample sizes of returning adults annually.

Return ages — Probabilities, $\boldsymbol{\psi}_{l,y}$, of returning from the ocean at ages three, four, or five conditional on a fish returning were modeled in multinomial logit space,

$$\begin{aligned} \text{mlogit}\left(\boldsymbol{\psi}_{l,y}\right) &= \boldsymbol{\alpha}^{\psi} + \boldsymbol{x}_{l,y}^{\psi}\boldsymbol{\beta}^{\psi} + \boldsymbol{\delta}_{y}^{\psi} \\ \boldsymbol{\delta}_{y}^{\psi} &\sim \text{N}\left(0, \boldsymbol{\Sigma}^{\psi}\right). \end{aligned} \qquad (3)$$

where $\boldsymbol{\alpha}^{\psi}$ is a vector of age-specific intercepts, with the intercept for age four fixed at 0. We fit effects, $\boldsymbol{\beta}^{\psi}$, of grouped LHPs, which were coded in the vector $\boldsymbol{x}_{l,y}^{\psi}$, and applied the same penalized complexity prior as on coefficients for survival, but with a unique penalty rate parameter, λ^{ψ}. We fit random effects of year, $\boldsymbol{\delta}_{y}^{\psi}$, for ages three and five, which were bivariate normally distributed with covariance matrix $\boldsymbol{\Sigma}^{\psi}$. We allowed for correlation between the random effects of year for each age because if a greater proportion of fish return at one age that affects the proportion returning at other ages (Buhle et al. 2018). We penalized the marginal standard

deviations of the random effects of year, $\boldsymbol{\sigma}^{\psi} = \text{diag}\left(\boldsymbol{\Sigma}^{\psi}\right)^{0.5}$, $\boldsymbol{\sigma}^{\psi} \sim \exp\left(\lambda^{\psi^{\text{rand}}}\right)$, in the same fashion as with other random effects of year. We applied a regularizing prior on the transformed correlation parameter, ρ, in the bivariate normal distribution to keep it away from boundaries at -1 or 1. The prior was, $\rho \sim \text{N}(0, 0.625)$, where the correlation was $\rho/(1+\rho^2)^{0.5}$, such that 95% of the prior probability mass for the correlation was between -0.77 and 0.77.

Detection

We modeled detection probabilities with the same categorical effects (Table 1) and random effects of year (Table 2) as for survival but with different effects of environmental covariates. For detection probability on the third and fourth recapture occasions (juvenile detection at McNary and Bonneville Dams), we modeled effects of average daily discharge and spill percentage in May–June at McNary and Bonneville Dams, which may affect the probability that fish pass dams via juvenile bypass systems, where they can be detected, as opposed to spillways or turbines, where they cannot. We fit unique effects of flow and spill on detection probabilities of natal-reach and downstream-rearing LHPs, because of their different migration timing, but assumed common effects across natal streams as was also the case for environmental effects on survival. We obtained discharge and spill data from the Columbia Basin Research Data Access in Real Time webtool (http://www.cbr.washington.edu/dart/query/river_graph_text). We applied the same penalized complexity priors on coefficients and random effects of year as were applied for survival, but fit unique penalty rate parameters for detection probability, λ_t^p and $\lambda_t^{p^{\text{rand}}}$, with a unique penalty rate for each occasion *t*.

Detection probability on the final occasion (Tumwater Dam) was fixed at 1.0, which ensured identifiability of the final interval-specific survival rate. This assumption was supported based on

the observation that 464 out of 465 fish (99.78%) that were known to pass Tumwater Dam as adults, because they were detected in adult fish ladders downstream of Tumwater Dam and then subsequently on in-stream arrays upstream of Tumwater Dam, were detected at Tumwater Dam.

Spr.0 emigrant survival — Downstream-rearing fish that emigrated from their natal streams in spring (*Spr.0*) were too small to be implanted with PIT tags, so their survival and return ages could not be directly informed by data. We assumed that their survival after the first interval, and their return ages, were the same as other downstream-rearing LHPs. However, to calculate *spr.0* survival during the first interval, ${\phi^1}_{\text{spr.0},y,s}$, we added an effect, β_{DOY}, of average emigration day of year (DOY) relative to the average emigration DOY for the *sum.0* LHP, Δ^{DOY}, to the linear predictor for the survival of *sum.0* LHP: $\text{logit}\left({\phi^1}_{\text{spr.0},y,s}\right) = \text{logit}\left({\phi^1}_{\text{sum.0},y,s}\right) + \beta_{\text{DOY}}\,\Delta^{\text{DOY}}$. We developed an informed prior, $\beta_{\text{DOY}} \sim N(0.36, 0.06)$, from a separate model of the same dataset of PIT-tagged fish, which included an individual-level covariate effect of release DOY on the survival of the *sum.0* LHP.

Table E1: Variables included in models of survival probabilities (ϕ) following each capture occasion, conditional probabilities of age at return from the ocean given survival (ψ), and detection probabilities (p) on each occasion. *LHP* = juvenile life history pathway, *DS* = downstream rearing (only summer and fall subyearling LHPs), *NR.DS* = juvenile life history pathways where summer and fall subyearlings are grouped (i.e., natal-reach vs. downstream rearing), *Ad.age* = adult age, *Stream* = natal stream, *Win.flow* = winter discharge in the Wenatchee River, *Win.air* = winter air temperature in the Wenatchee Basin, *CUI.Spr* = coastal upwelling off of the coast of Washington State in spring, *SST.WA.Sum* = sea surface temperature off the coast of Washington State in summer, *Flow* = discharge measured at a dam of detection, and *Spill* = percentage of water spilled at dam of detection. Detection probability at Tumwater Dam for adults was assumed to be 1.0.

Occasion/interval	Variables
$\boldsymbol{\phi}$	
1-Natal emigration	LHP + Stream + LHP*Stream + DS*Win.flow + DS*Win.air
2-Lower Wenatchee	NR.DS + Stream + NR.DS*Stream
3-McNary.juv	NR.DS + Stream + NR.DS*Stream
4-Bonneville.juv	NR.DS + Stream + NR.DS*Stream + NR.DS*CUI.Spr + NR.DS*SST.WA.Sum
5-Bonneville.ad	Ad.age
6-McNary.ad	Ad.age
$\boldsymbol{\psi}$	
4-Bonneville	NR.DS
$\boldsymbol{p}$	
2-Lower Wenatchee	LHP + Stream + LHP*Stream
3-McNary.juv	NR.DS + Stream + NR.DS*Stream + NR.DS*Flow + NR.DS*Spill
4-Bonneville.juv	NR.DS + Stream + NR.DS*Stream + NR.DS*Flow + NR.DS*Spill
5-Bonneville.ad	Ad.age
6-McNary.ad	Ad.age
7-Tumwater.ad	-

Table E 2: random effects of year included in models of: ϕ - survival probabilities following each capture occasion, ψ - probabilities of fish returning from the ocean at different ages, and p - detection probabilities on each occasion. *LHP* = juvenile life history strategy, and *NR.DS* = juvenile life history pathways where summer and fall subyearlings are grouped (i.e., natal-reach- vs. downstream-rearing). Detection probability at Tumwater Dam for adults was assumed to be 1.0.

Occasion	random effects of year
$\boldsymbol{\phi}$	
1-Natal emigration	Year + LHP*Year
2-Lower Wenatchee	Year + NR.DS*Year
3-McNary	Year + NR.DS*Year
4-Bonneville	Year + NR.DS*Year
5-Bonneville.ad	Year
6-McNary.ad	Year
$\boldsymbol{\psi}$	
4-Bonneville	Year
$\boldsymbol{p}$	
2-Lower Wenatchee	Year + LHP*Year
3-McNary	Year + NR.DS*Year
4-Bonneville	Year + NR.DS*Year
5-Bonneville.ad	Year
6-McNary.ad	Year
7-Tumwater.ad	-

References

Arnason, A. N. 1973. The estimation of population size, migration rates and survival in a stratified population. Researches on population ecology 15:1–8.

Brownie, C., J. E. Hines, J. D. Nichols, K. H. Pollock, and J. B. Hestbeck. 1993. Capture-Recapture Studies for Multiple Strata Including Non-Markovian Transitions. Biometrics 49:1173–1187.

Buhle, E. R., M. D. Scheuerell, T. D. Cooney, M. J. Ford, R. W. Zabel, and J. T. Thorson. 2018. Using integrated population models to evaluate fishery and environmental impacts on Pacific salmon viability. NOAA Technical Memorandum.

Crozier, L. G., B. J. Burke, B. E. Chasco, D. L. Widener, and R. W. Zabel. 2021. Climate change threatens Chinook salmon throughout their life cycle. Communications Biology 4:1–14.

Simpson, D., H. Rue, A. Riebler, T. G. Martins, and S. H. Sørbye. 2017. Penalizing model component complexity: a principled, practical approach to constructing priors. Statistical Science 32:1–28.

Sorel, M. H., A. R. Murdoch, R. W. Zabel, J. C. Jorgensen, C. M. Kamphaus, and S. J. Converse. in review. Juvenile life history diversity is associated with lifetime demographic heterogeneity in a migratory fish.

APPENDIX F

Description of hatchery management model used in population projections (Chapter 4)

For the Chiwawa River program, the total number of natural-origin adults collected for broodstock across ages, $B_{y,\text{Chiwawa}}$, in year y was,

$$B_{y,\text{Chiwawa}} = \begin{cases} F_{y,\text{Chiwawa}}^{\text{Tum}} * p^{\text{Collect}}, & \text{if } \left(F_{y,\text{Chiwawa}}^{\text{Tum}} * p^{\text{Collect}}\right) < B_{\text{Chiwawa}}^{\text{Target}} \\ B_{\text{Chiwawa}}^{\text{Target}}, & \text{otherwise} \end{cases} \quad (1)$$

where $F_{y,\text{Chiwawa}}^{\text{Tum}}$ is a forecasted return to Tumwater Dam, which was simulated with a CV of 10% around the latent true return, p^{Collect} is the maximum proportion of the forecasted return that can be collected (specified as part of the control rule), and $B_{\text{Chiwawa}}^{\text{Target}}$ is the target broodstock size (specified as part of the control rule). The calculation of broodstock collected for the Nason Creek program was slightly different because collections include returns from both the Chiwawa River and Nason Creek. To ensure that the total proportion of forecasted Chiwawa River returns collected was $\leq p^{\text{Collect}}$, the maximum proportion of combined Nason Creek and Chiwawa River returns collected for the Nason program was $p_{\text{Nason}}^{\text{Collect}} = \left(p^{\text{Collect}} - \left(B_{y,\text{Chiwawa}} / F_{y,\text{Chiwawa}}\right)\right)$. The number of combined Chiwawa River and Nason Creek returns collected for the Nason Creek program broodstock was,

$$B_{y,Nason} = \begin{cases} F_{y,\text{ChNa}}^{\text{Tum}} * p_{Nason}^{\text{Collect}}, & \text{if } \left(F_{y,\text{ChNa}}^{\text{Tum}} * p_{\text{Nason}}^{\text{Collect}}\right) < B_{\text{Nason}}^{\text{Target}} \\ B_{\text{Nason}}^{\text{Target}}, & \text{otherwise} \end{cases} \quad (2)$$

where $F_{y,\mathrm{ChNa}}^{\mathrm{Tum}}$ is the combined forecasted returns from the Chiwawa River and Nason Creek less removals for the Chiwawa River program, $F_{y,\mathrm{ChNa}}^{\mathrm{Tum}} = \left(F_{y,\mathrm{Nason}}^{\mathrm{Tum}} + F_{y,\mathrm{Chiwawa}}^{\mathrm{Tum}} - B_{y,\mathrm{Chiwawa}}\right)$. Based on the management plans, $p^{\mathrm{Collect}} = 0.30$, $B_{\mathrm{Chiwawa}}^{\mathrm{Target}} = 74$, and $B_{\mathrm{Nason}}^{\mathrm{Target}} = 64$.

The abundance of hatchery-origin returns from each stream, *s*, (which are differentiable based on tag location) released to spawn naturally above Tumwater Dam in each year *y*, $A_{y,s}^{\mathrm{HO.Tum}}$, was based on the forecasted natural-origin return, $F_{y,s}$, and the total number of natural-origin adults from stream *s* removed for broodstock, $B_{y,s}^{\mathrm{Rem}}$, as ,

$$A_{y,s}^{\mathrm{HO.Tum}} = \begin{cases} H_{y,s}^{\mathrm{Max}} - F_{y,s} + B_{y,s}^{\mathrm{Rem}}, & \text{if } \left(F_{y,s} - B_{y,s}^{\mathrm{Rem}}\right) < H_{y,s}^{\mathrm{Max}} \\ 0, & \text{otherwise} \end{cases} \quad (3)$$

where $H_{y,s}^{\mathrm{Max}}$ is the maximum number of hatchery-origin fish that can be released above Tumwater Dam. To fit within Proportionate Natural Influence constraints in the management plans, $H_{y,\mathrm{Chiwawa}}^{\mathrm{Max}} = 400$ and $H_{y,\mathrm{Nason}}^{\mathrm{Max}} = 100$ (Chelan PUD and WDFW 2009, Grant PUD et al. 2009). We assumed that there would be sufficient returns of hatchery-origin spawners to implement this decision rule in all years. We simulated homing and straying of hatchery-origin fish from the stream where they were released at the following rates:

	Chiwawa	Nason	White
Chiwawa	0.89	0.09	0.02
Nason	0.01	0.98	0.01

where rows represent the stream of origin, columns represent the stream of return, and cell values are the proportions of hatchery fish from each stream spawning in each stream (Hillman et al. 2020).

References

Chelan County Public Utility District No. 1 (Chelan PUD), and Washington Department of Fish and Wildlife (WDFW). 2009. Hatchery and genetic management plan: Wenatchee Upper Columbia River spring Chinook: Chiwawa spring Chinook.

Hillman, T. W., M. Miller, M. Hughes, C. Moran, W. Williams, M. Tonseth, C. Willard, S. Hopkins, J. Caisman, T. N. Pearsons, and P. Graf. 2020. Monitoring and evaluation of the Chelan and Grant County PUD s hatchery programs: 201 9 annual report. Report to the HCP and PRCC Hatchery Committees. Wenatchee and Ephrata, WA.

Public Utility District No 2 of Grant County (Grant PUD), Washington Department of Fish and Wildlife, and Yakama Nation. 2009. Hatchery and genetic management plan: Upper Columbia River spring-run Chinook salmon – Nason Creek supplementation program.

APPENDIX G

Covariate simulation for population projection (Chapter 4)

Methods

There were nine environmental variables used in the integrated population model, which we needed to simulate future time series of to use as covariates in population projections. The variables were winter and summer discharge in each of three natal streams (total of six variables), winter air temperature in the Wenatchee River Basin, average coastal upwelling anomaly data for 45°N by 125°W from March through May, and average sea surface temperature within a 2° x 2° square (46°–48°N by 124°–126°W) off the Washington Coast during June–August. Details on the covariate data and their sources are provided in appendices S.1 and S.2.

To simulate time series of environmental variables, we fit time-series models using the MARSS package in R, and simulated projections using the *MARSS::MARSSsimulate* function. While the IPM was fit to 21 years of data, we fit the time-series models to data that extended further back in time to provide more statistical power (Figure 1). The longest time series was of summer sea surface temperature, which extended back to 1900, whereas upwelling extended back to 1946, air temperature to 1958, and stream discharge to 1991 in the Chiwawa River and 2008 in Nason Creek and the White River. We log transformed stream flow covariates before fitting the model to ensure that there was no support for negative flows, whereas the temperature covariates could be negative, and the upwelling covariate was an anomaly from the average and could therefore also be negative.

Streamflow was highly correlated among natal streams within seasons (summer and winter), and we therefore modeled it as three observations of a single latent trend for each season. We

evaluated models with different specifications of latent trends, where they could be biased or unbiased non-stationary random walks or lag-1 autocorrelated stationary trends [AR(1)] with common or unique autocorrelation coefficients. We allowed process error variances to be either common or unique between seasons in the random walk and AR(1) models. We also evaluated models with no latent trend, but which could have bias, equivalent to a linear regression with an effect of time. In all models, observation errors were assumed to be independent and identically distributed among years, natal-streams, and seasons. Data support for different models was based on the Akaike Information Criteria, with correction for small sample size (AICc).

Because air temperature, upwelling, and sea surface temperature were not strongly correlated, we fit unique models for each covariate. We evaluated candidate models with the same specification of trends as were evaluated for log flow – biased and unbiased non-stationary random walks, AR(1), and no latent trend. Models either assumed that observation error was negligible because air temperature and sea surface temperature are measured with high precision and the upwelling covariate is a derived product or included process error. Support for different model specifications was evaluated based on AICc.

Results

The most supported model of streamflow based on AICc had AR(1) latent states with a shared autocorrelation coefficient and process variance (Table 1). The autocorrelation coefficient for the log streamflow covariates was 0.15 (95% CI = -0.15, 0.45). The most supported model for air temperature was AR(1) with autocorrelation coefficient 0.41 (0.2, 0.62) and no observation error (Table 2). For upwelling, the most supported model had no latent trend but bias with a slope of -0.01 (-0.02, 0) standard deviations per year, and observation error (Table 3). The best model of

sea surface temperature also had no latent trend but bias with a slope of 0.01 (0.01, 0.02) standard deviations per year and observation error (Table 4).

Table G1: Δ Akaike Information Criteria (AIC) scores for models of log stream flow. The autocorrelation form could be, *none*, a *random walk*, or a stationary autoregressive model of order 1, *AR(1)*, with *unique* or *common* autocorrelation coefficients between seasons. Process error variance could be *IID* = independent and identically distributed or *INID* = independent and not identically distributed. There could be no bias, or unique bias for the two seasons. *logLik* is the log likelihood and *K* is the number of parameters in the model.

Autocorrelation form	Process error variance	Bias	logLik	K	$\Delta AICc$
Common AR(1)	IID	Zero	-125.0	9	0.0
Unique AR(1)	IID	Zero	-124.5	10	1.4
Common AR(1)	INID	Zero	-124.9	10	2.2
Unique AR(1)	INID	Zero	-124.5	11	3.7
Common AR(1)	IID	Unique	-124.9	11	4.6
Unique AR(1)	IID	Unique	-124.5	12	6.2
Common AR(1)	INID	Unique	-124.9	12	7.0
Unique AR(1)	INID	Unique	-124.4	13	8.5
Random walk	IID	Zero	-138.2	8	24.1
Random walk	INID	Zero	-138.0	9	26.1
Random walk	IID	Unique	-138.1	10	28.6
Random walk	INID	Unique	-138.0	11	30.7

Table G2: Δ Akaike Information Criteria (AIC) scores for models of winter air temperature. The autocorrelation form could be *none*, a *random walk*, or a stationary autoregressive model of order 1, *AR(1)*. *logLik* is the log likelihood and *K* is the number of parameters in the model.

Autocorrelation form	Bias	Process error variance	Observation error	logLik
AR(1)	None	IID	No	-77.2
AR(1)	None	IID	Yes	-77.2
None	Bias	None	Yes	-85.8

Table G3: Δ Akaike Information Criteria (AIC) scores for models of spring coastal upwelling. The autocorrelation form could be *none*, a *random walk*, or a stationary autoregressive model of order 1, *AR(1)*. *logLik* is the log likelihood and *K* is the number of parameters in the model.

Autocorrelation form	Bias	Process error variance	Observation error	logLik
None	Bias	None	Yes	-100.7
AR(1)	None	IID	No	-101.6
Random walk	Bias	IID	Yes	-100.7

Table G4: Δ Akaike Information Criteria (AIC) scores for models of summer sea surface temperature. The autocorrelation form could be *none*, a *random walk*, or a stationary autoregressive model of order 1, *AR(1)*. *logLik* is the log likelihood and *K* is the number of parameters in the model.

Autocorrelation form	Bias	Process error variance	Observation error	logLik	K	$\Delta AICc$
None	Bias	None	Yes	-154.8	3	0.0
Random walk	Bias	IID	Yes	-154.8	4	2.1
AR(1)	None	IID	No	-156.7	3	3.8
AR(1)	None	IID	Yes	-156.0	4	4.7
Random walk	None	IID	Yes	-157.6	3	5.7
None	None	None	Yes	-168.4	2	25.1
Random walk	None	IID	No	-176.9	2	42.2
Random walk	Bias	IID	No	-176.9	3	44.3

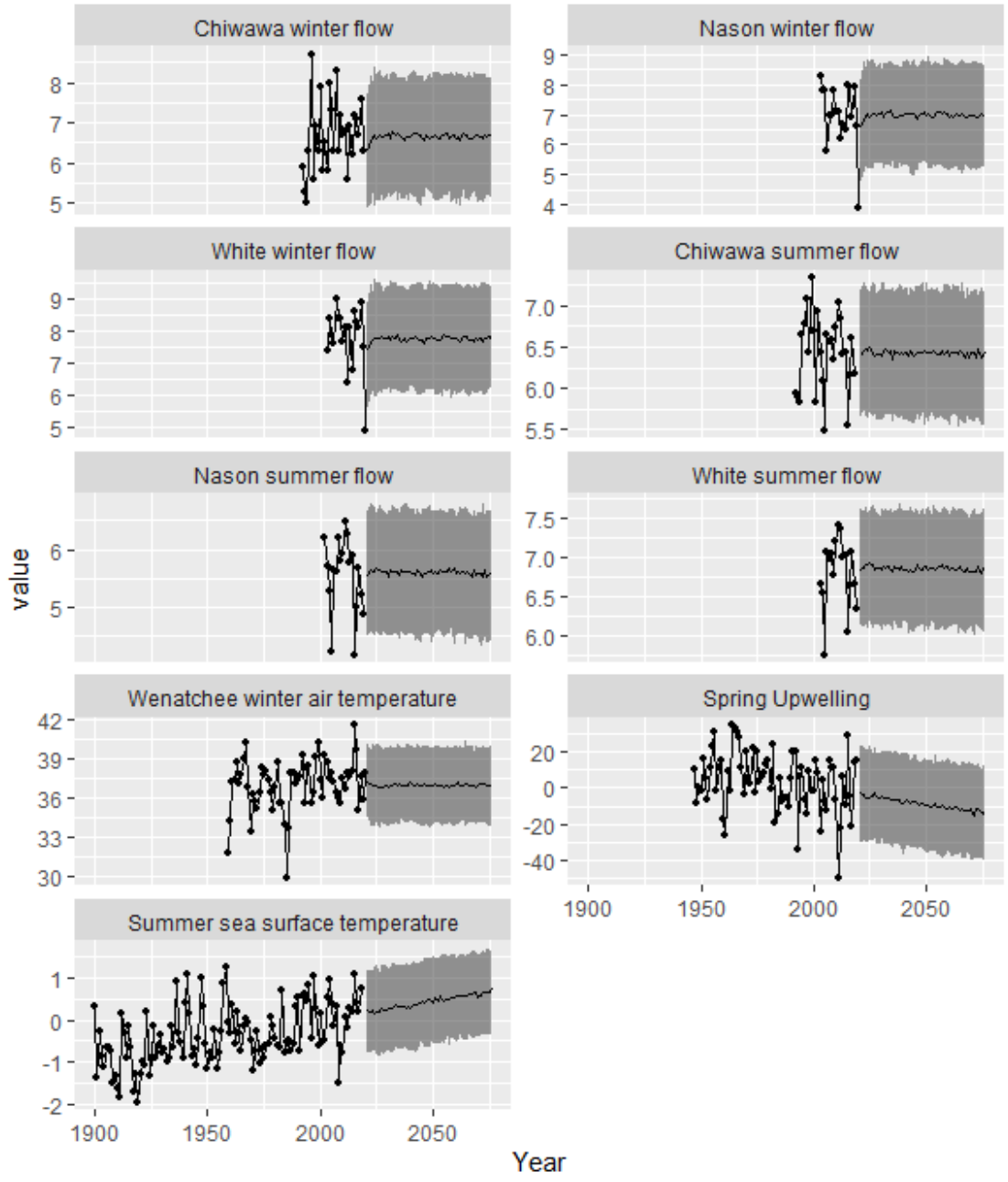

Figure G1: Time series of environmental variable data, which the model was fit to, and simulations of future data. The black line in the projections represents annual medians from 100 simulated time series and the shaded envelope spans 90% quantiles of simulated annual values.

References

Holmes, E. E., E. J. Ward, and K. Wills. 2012. MARSS: multivariate autoregressive state-space models for analyzing time-series data. R journal 4.

R Core Team. 2021. R: A Language and Environment for Statistical Computing. R Foundation for Statistical Computing, Vienna, Austria.

APPENDIX H

Sensitivity analysis for projected abundance with an integration population model (Chapter 4)

Methods

To evaluate the sensitivity of population trajectories to parameter uncertainty, we examined correlations between the geometric mean of abundance in projections and parameter values or derived quantities from posterior samples that were used to generate the projection. In the sensitivity analysis, we examined correlations between projected abundance and the log-transformed $\alpha_{h,s}$, $\gamma_{h,s}$, and $J_{h,s}^{\max}$ parameters from the juvenile production function for each stream and LHP, which controlled the rate of juvenile production and its relationship with spawner density. We also examined correlations between abundance and the logit-transformed expected median values of the following demographic rates for each LHP: survival during the first interval (from release to the Lower Wenatchee River screw trap); downstream survival between the Lower Wenatchee River screw trap and Bonneville Dam; smolt-to-adult return rates back to Bonneville Dam; proportions of adults returning at ages three and five; upstream survival back to Tumwater Dam; pre-spawn survival; the proportion of adults that were female, and the relative reproductive success of hatchery-origin spawners relative to natural-origin spawners.

Results

For the Chiwawa River, natural-origin female spawner abundance was most correlated with the expected smolt-to-adults return rate of natal-reach-rearing emigrants, followed by the return rate of downstream-rearing emigrants (Table S.1). The relative reproductive success of hatchery-origin spawners (RRS) was negatively correlated with projected abundance. However, this was likely because RRS was negatively correlated with several of the α and γ parameters in the models of natural juvenile productivity (Figure S.1). The prespawn survival rate and the average percentage of spawners that were female were positively correlated with female spawner abundance.

Projected female abundance in Nason Creek was positively correlated with smolt-to-adult return rates of downstream-rearing emigrants and to a lesser degree with return rates of natal-reach-rearing emigrants (Table S.1). Female abundance was also positively correlated α parameters in models of juvenile emigrant production, especially for the fall subyearling LHP, and with the percentage of spawners that were female.

Projected abundance in the White River was most positively correlated with the α parameter in the model of juvenile production, especially for the natal-reach-rearing emigrant (*spr.1*) LHP (Table S.1). Counterintuitively, abundance was negatively correlated with the γ parameter; however, this may have been because the α and γ parameters were negatively correlated with one another (Figure S.3). Female abundance was also positively correlated with smolt-to-adult return rates.

Table H1: Correlation between the simulated log geometric mean abundance of natural-origin female spawners in 2020-2069 and parameters or derived quantities for each natal stream (Columns). α, γ, and *Jmax* are parameters in models of the production of juveniles downstream-rearing juveniles that emigrate in spring (*Spr.0*), summer (*Sum.0*), and Fall (*Fal.0*), and natal-reach-rearing emigrants in spring (*Spr.1*). These parameters were all log transformed before correlations were assessed. *Time 1* ϕ represents survival between emigrating from the natal stream and entering the mainstem Columbia River migration corridor, which includes the overwinter period for downstream-rearing LHPs. *DSR* represents all downstream-rearing life history pathways. ϕ *DS* represents downstream survival between entering the main stem of the Columbia River and passing Bonneville Dam as juveniles. *SAR* are smolt-to-adult return rates from and to Bonneville Dam. ϕ *US* is upstream survival from Bonneville Dam to Tumwater Dam. *% age* is the percent of fish returning at a given age. ϕ *PS* is survival rate between passing Tumwater Dam as an adult and spawning. *RRS* is the reproductive success of hatchery-origin spawners relative to natural-origin spawners. All rates were logit transformed prior to calculating correlations.

	Chiwawa	Nason	White
α Spr.0	0.00	0.06	0.07
α Sum.0	0.05	0.14	0.15
α Fal.0	0.08	0.24	0.15
α Spr.1	0.07	0.14	0.42
γ Spr.0	0.06	0.01	-0.08
γ Sum.0	0.04	-0.04	-0.12
γ Fal.0	0.02	-0.04	-0.15
γ Spr.1	-0.02	-0.10	-0.32
Jmax Spr.0	-0.02	-0.09	-0.04
Jmax Sum.0	0.03	-0.04	-0.04
Jmax Fal.0	-0.01	-0.01	0.01
Jmax Spr.1	0.00	-0.10	-0.05
time 1 ϕ Spr.0	0.02	0.01	-0.01
time 1 ϕ Sum.0	-0.00	0.01	-0.01
time 1 ϕ Fal.0	-0.01	0.04	-0.01
time 1 ϕ Spr.1	-0.01	0.00	0.04
ϕ DS DSR	-0.01	-0.05	-0.07
ϕ DS Spr.1	-0.03	-0.03	-0.05
SAR DSR	0.38	0.36	0.19
SAR Spr.1	0.54	0.30	0.24
ϕ US age 3	0.03	0.04	0.04
ϕ US age 4	-0.00	0.05	0.05
ϕ US age 5	0.03	0.04	0.05
% age 3 DSR	0.03	-0.01	0.04
% age 5 DSR	-0.06	-0.03	-0.08
% age 3 Spr.1	0.02	0.02	0.00
% age 5 Spr.1	-0.06	-0.02	-0.06
ϕ PS	0.11	0.07	0.07
p female	0.11	0.11	0.08
RRS	-0.09	0.09	0.05

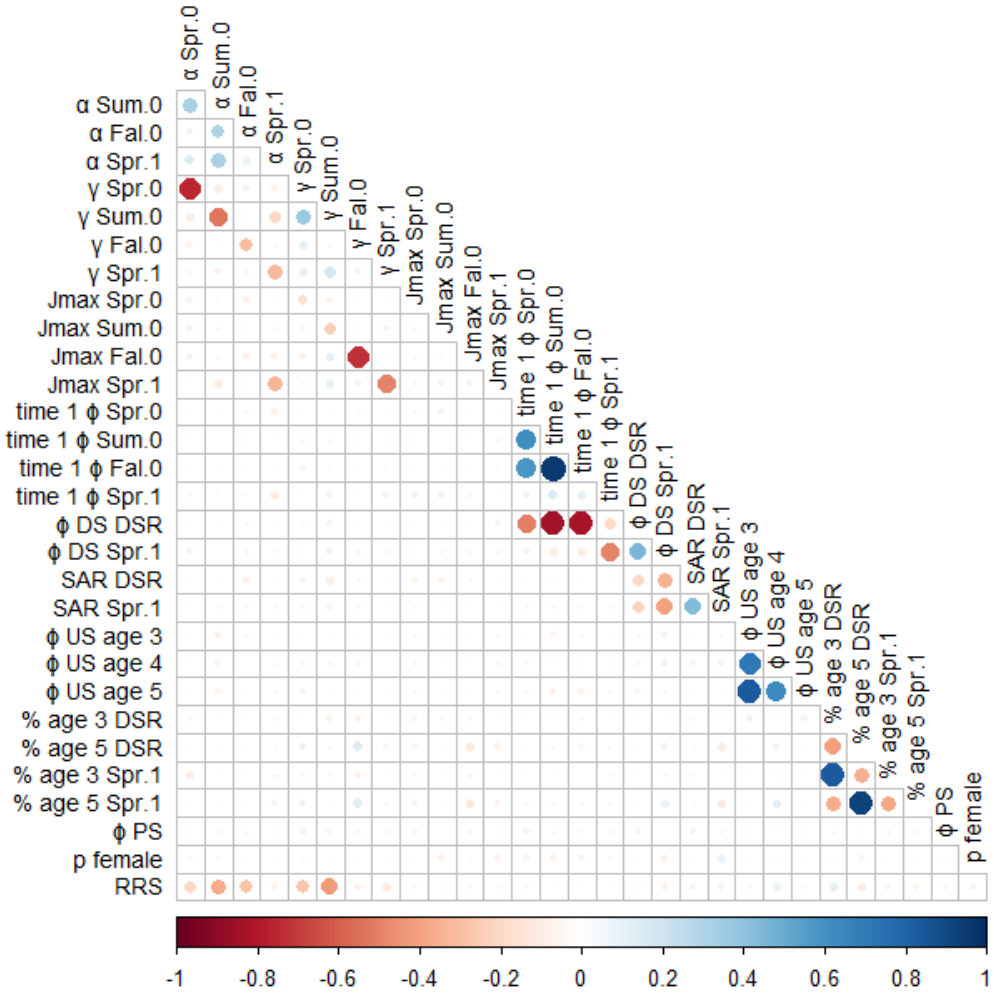

Figure H1: Correlations between parameters and derived quantities across posterior samples for the *Chiwawa River* spawning aggregation. *α*, *γ*, and *Jmax* are parameters in models of the production of juveniles emigrating at age 0 in spring (*Spr.0*), summer (*Sum.0*), and (*fal.0*), and at age 1 in spring (*Spr.1*). These parameters were all log transformed before correlation was assessed. There were some negative correlations among shape parameters within life history pathways (LHPs). *Time 1 ϕ* represents survival between emigrating from the natal stream and entering the mainstem Columbia River migration corridor, which includes the overwinter period for downstream-rearing juvenile life histories and *ϕ DS* represents downstream survival between entering the main stem of the Columbia River and passing Bonneville Dam as juveniles and *DSR* represents all downstream-rearing life history pathways. *Time 1 ϕ* and *ϕ DS* were negatively correlated within LHPs. *Time 1 ϕ* was positively correlated among downstream rearing LHPs

(which emigrate at age 0). *SAR* are smolt to adult returns from and to Bonneville Dam. ϕ *US* is upstream survival from Bonneville Dam to Tumwater Dam, which was positively correlated among ages. *% age* is the percent of fish returning at a given age, which was positively correlated between downstream- and natal-reach rearing LHPs (those emigrating from natal streams at age 0 and 1). ϕ *PS* is survival rate between passing Tumwater Dam and spawning. *RRS* is the reproductive success of hatchery-origin spawners relative to natural-origin spawners. All rates were logit transformed prior to calculating correlations.

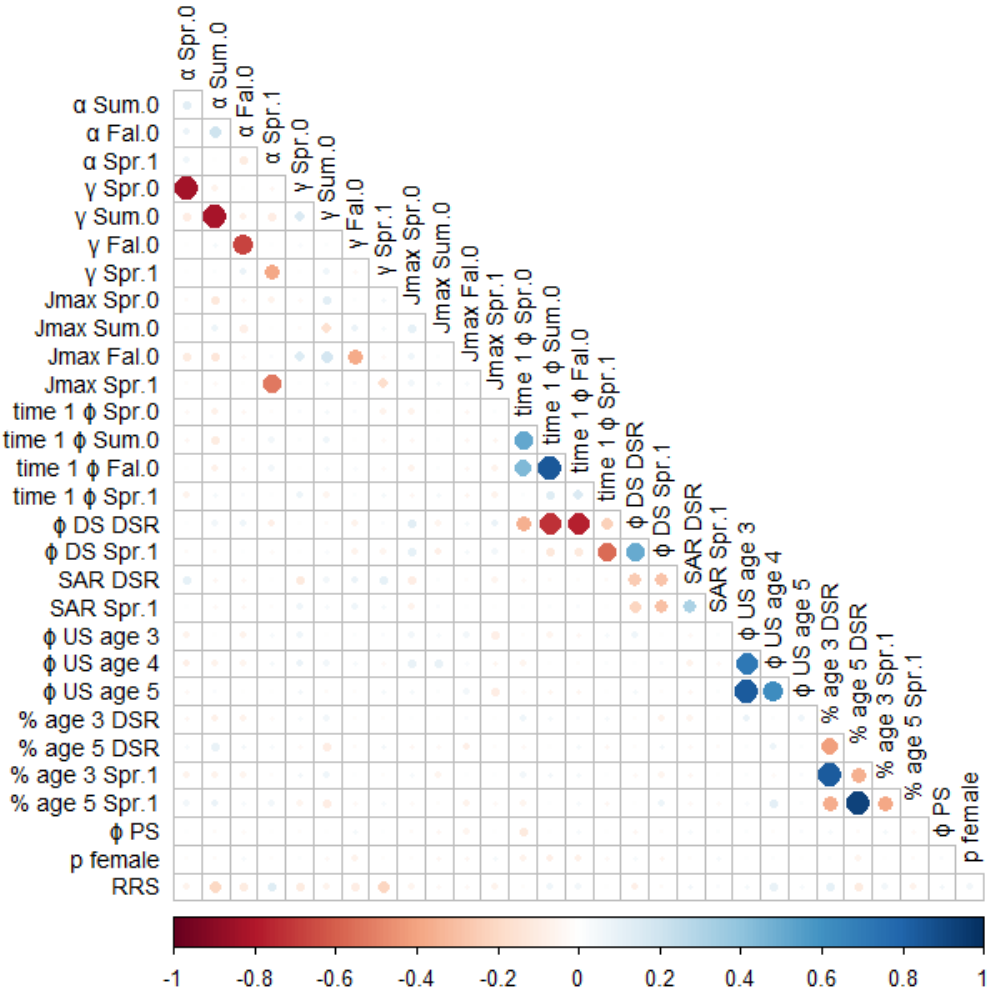

Figure H2: Correlations between parameters and derived quantity values across posterior samples for the *Nason Creek* spawning aggregation.

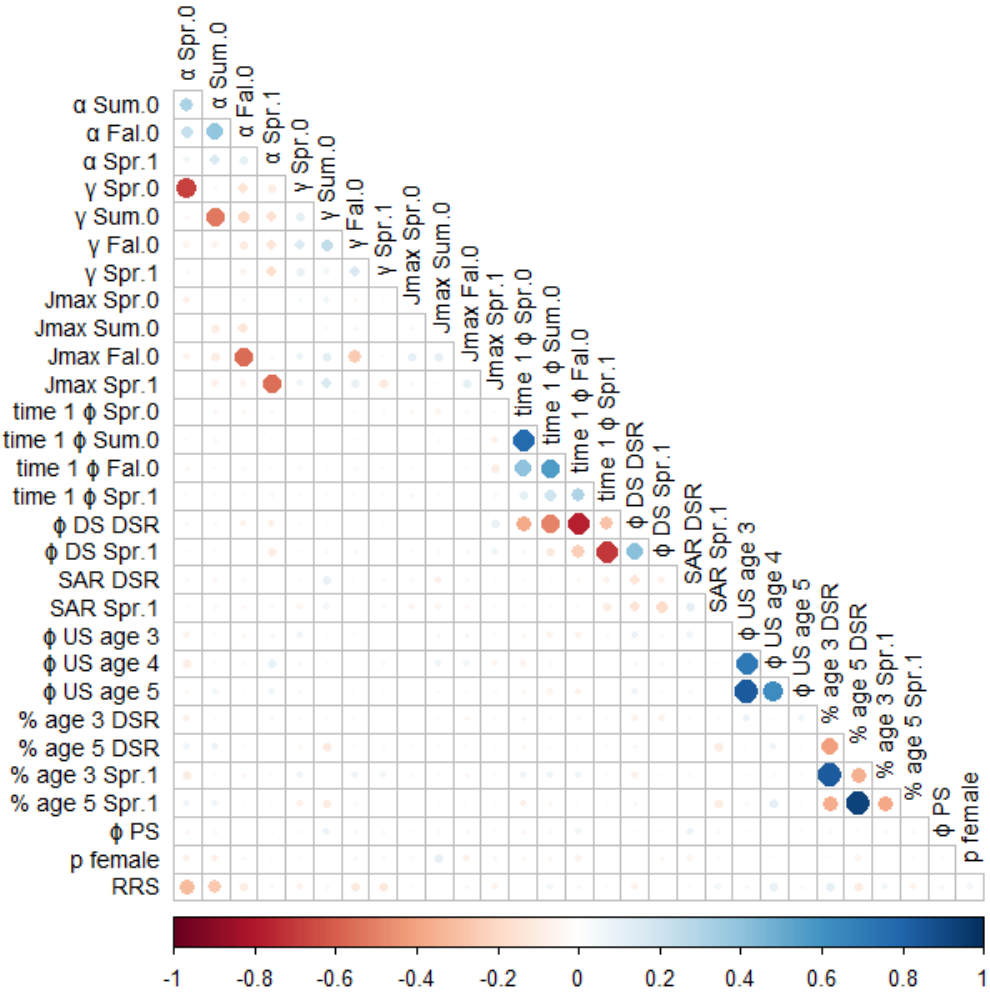

Figure H3: Correlations between parameters and derived quantity values across posterior samples for the *White River* spawning aggregation.

APPENDIX I

Supplemental figures (Chapter 4)

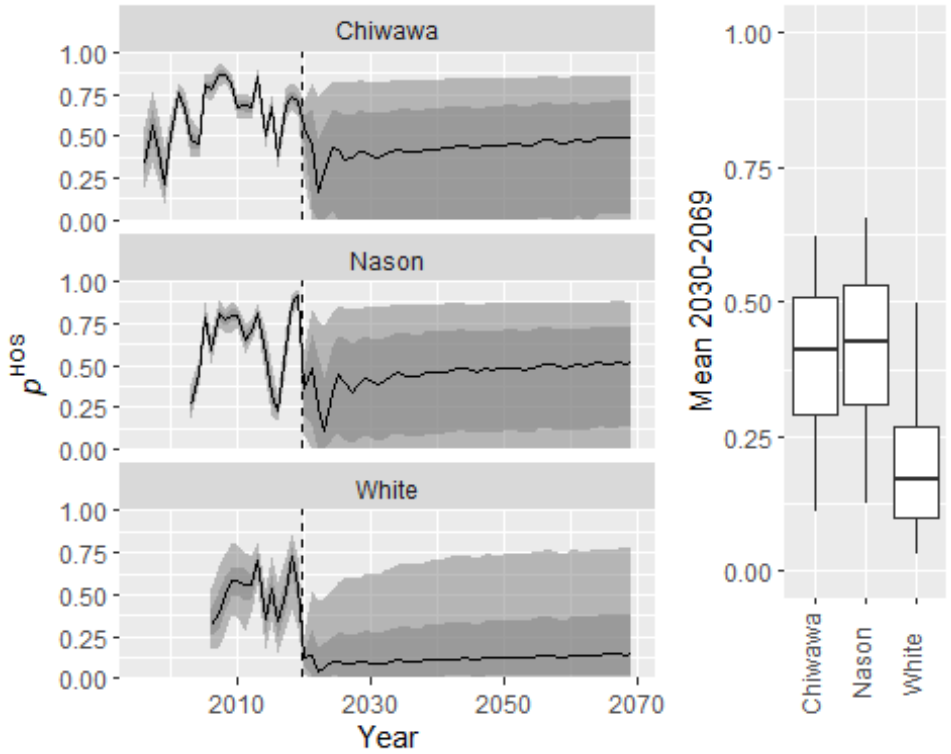

Figure I1: *Left panel*: Proportion of spawners that were of hatchery origin (p^{HOS}) by year and natal stream. Years to the left of the dotted line were fit to data and years to the right of the dotted line were projected using hatchery control rules. Lines represent medians across simulations, dark shaded envelopes represent interquartile ranges and light shaded envelopes represents 90% quantile ranges. *Right panel*: Boxplots are of the average p^{HOS} in 2020-2069. Horizontal lines represent medians, boxes span interquartile ranges and whiskers span 90% quantile ranges.

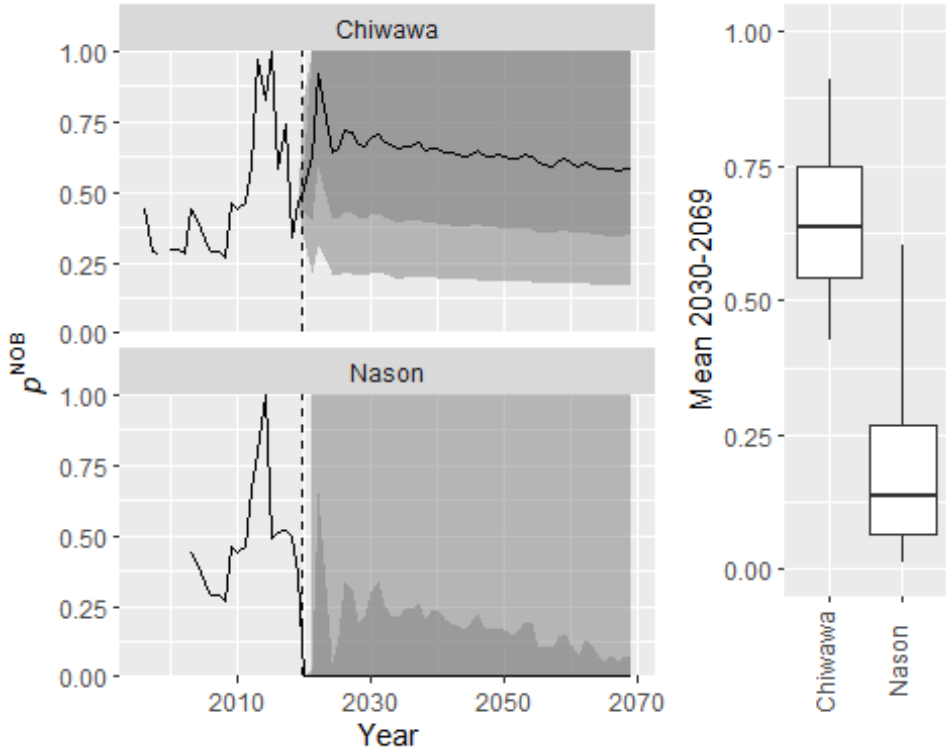

Figure I2: *Left panel*: Proportion of broodstock that are of natural origin (p^{NOB}) by hatchery program and year. Years to the left of the dotted line were fit to data and years to the right of the dotted line were projected using hatchery control rules. Lines represent medians across simulations, dark shaded envelopes represent interquartile ranges and light shaded envelopes represents 90% quantile ranges. *Right panel*: Boxplots are of the average p^{NOB} in 2020-2069 by hatchery program. Horizontal lines represent medians, boxes span interquartile ranges and whiskers span 90% quantile ranges.

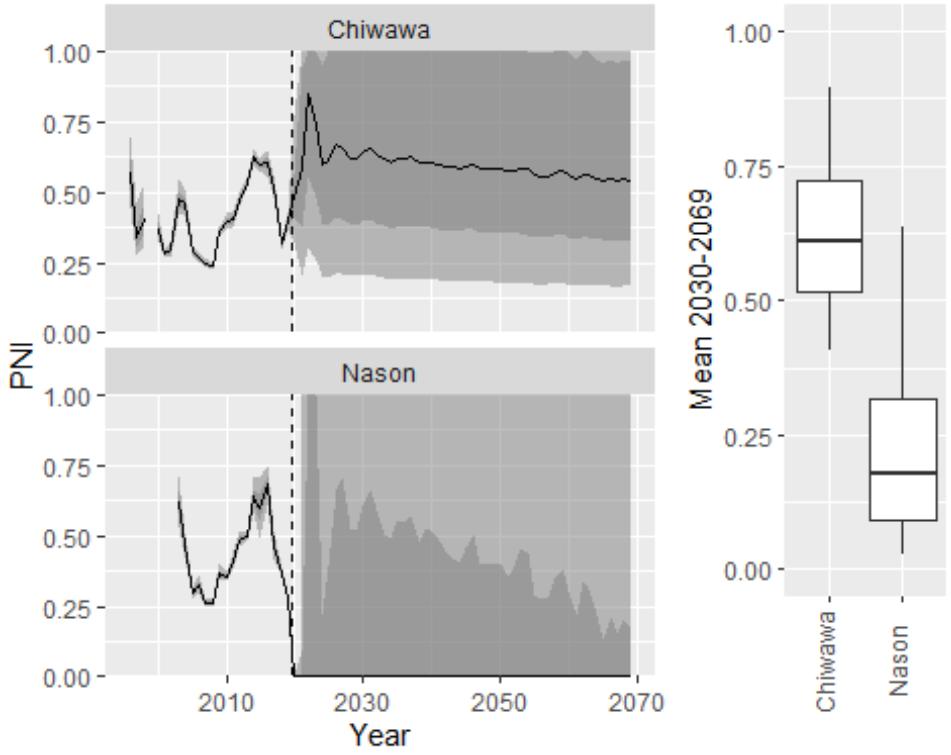

Figure I3: *Left panel*: Proportionate natural influence (PNI) by hatchery program and year. Years to the left of the dotted line were fit to data and years to the right of the dotted line were projected using hatchery control rules. Lines represent medians across simulations, dark shaded envelopes represent interquartile ranges and light shaded envelopes represents 90% quantile ranges. *Right panel*: Boxplots are of the average PNI in 2020-2069 by hatchery program. Horizontal lines represent medians, boxes span interquartile ranges and whiskers span 90% quantile ranges.

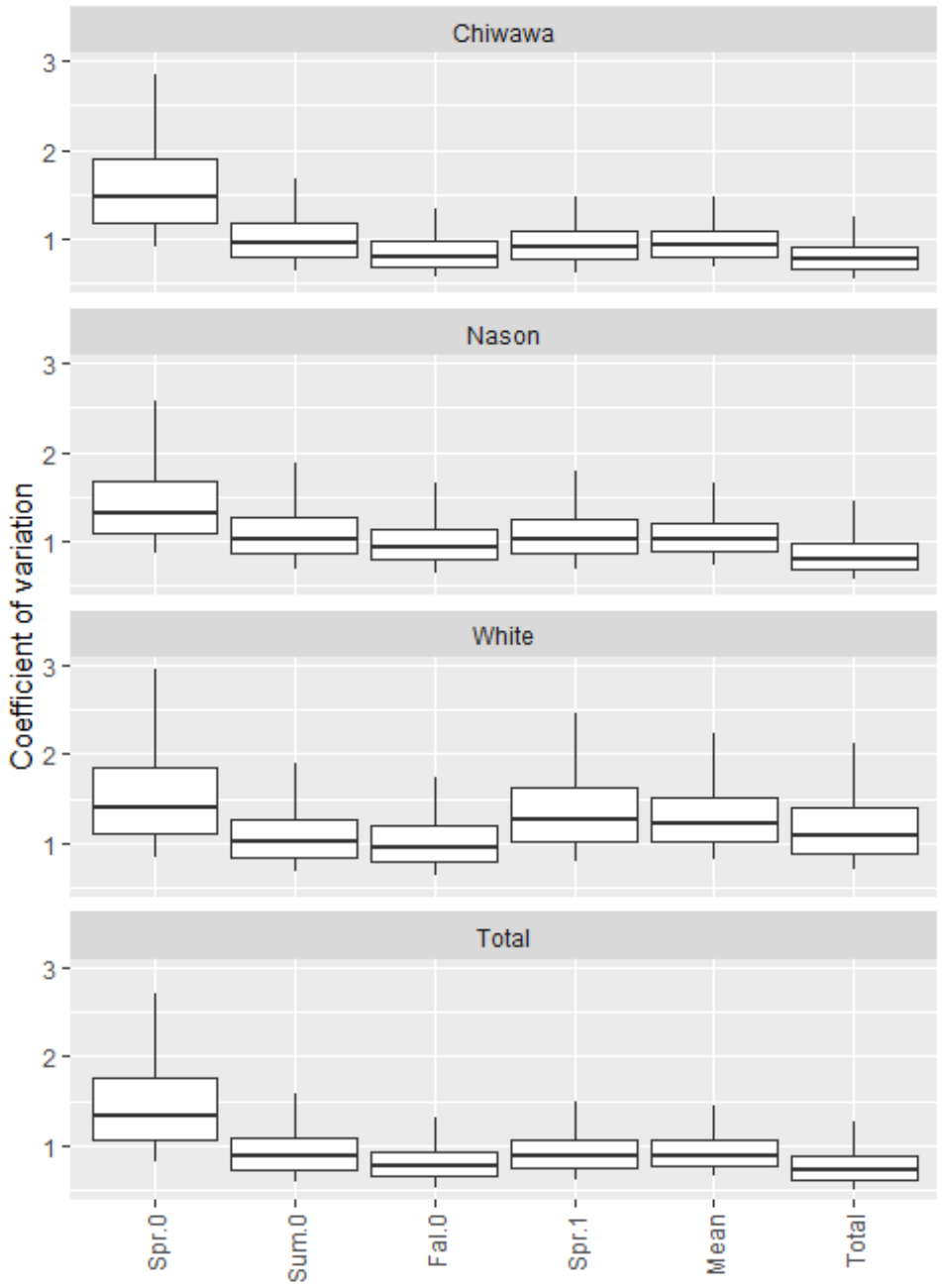

Figure I4: Boxplots of the coefficients of variation (CV) of simulated natural-origin returns to Tumwater Dam in in 2020-2069. *Mean* represents a weighted average of CVs of juvenile life history pathways within individual streams, whereas *Total* represents a CV of the sum of adults across life history pathways. The thick lines represent the median CV across 50,000 projections, the boxes span the interquartile range, and the whiskers span the 90% quantile range.

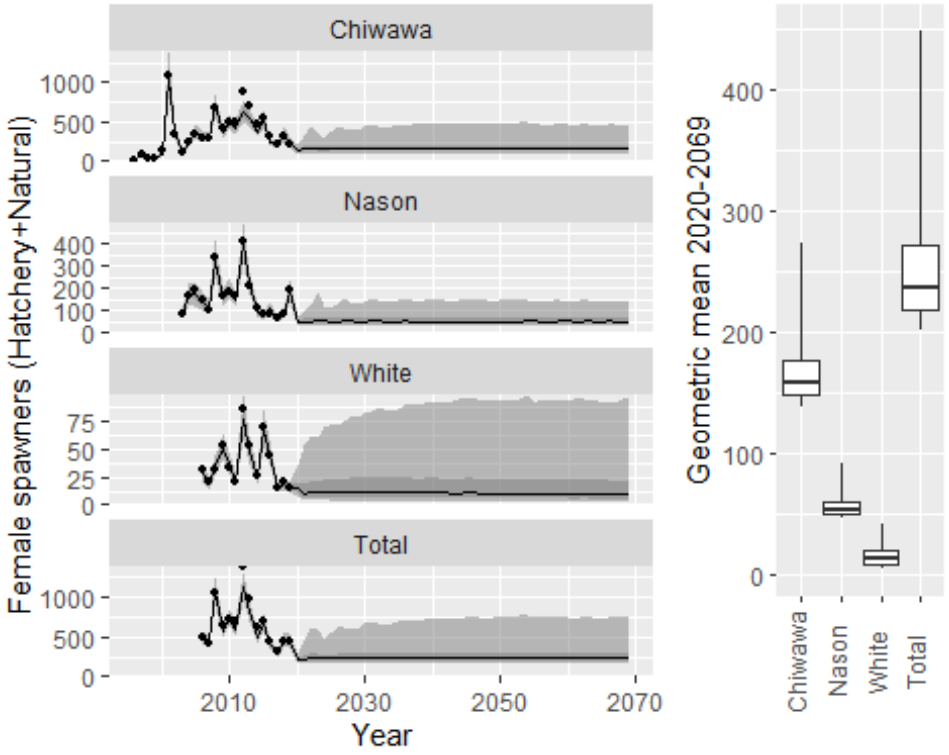

Figure I5: *Left panel*: Female spawner abundance in three natal streams by year. Points represent observations of redds, which the model was fit to. Lines represents medians across simulations, dark shaded envelopes represent interquartile ranges, and light shaded envelopes represent 90% quantile ranges. Y-axis scales differ across streams. *Right panel:* Boxplots are of the geometric mean abundance in years 2020-2069 across projections. Horizontal lines represent medians, boxes span interquartile ranges and whiskers span 90% quantile range.

APPENDIX J

Supplementary figures (Chapter 5)

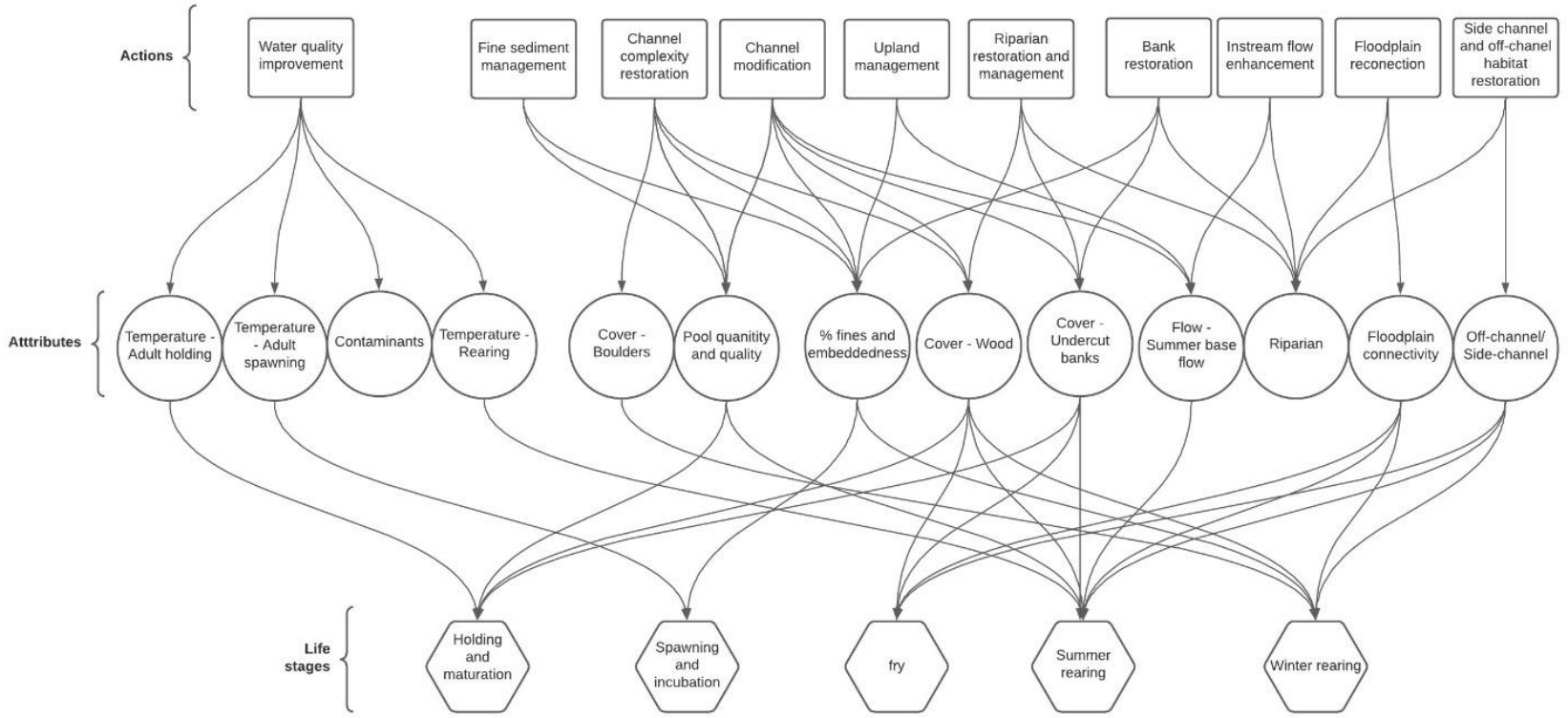

Figure J1: Conceptual diagram showing expected relationships between habitat restoration actions, habitat attributes, and life stage survival rates. This diagram is based on habitat restoration prioritization tools developed by the Upper Columbia Salmon Recovery Board and the Upper Columbia Regional Technical Team (2021). Our *egg incubation* corresponds with the *Spawning and incubation* life stage in this diagram, and our *summer rearing* life stage corresponds to the *fry* and *summer rearing* life stages in this diagram.

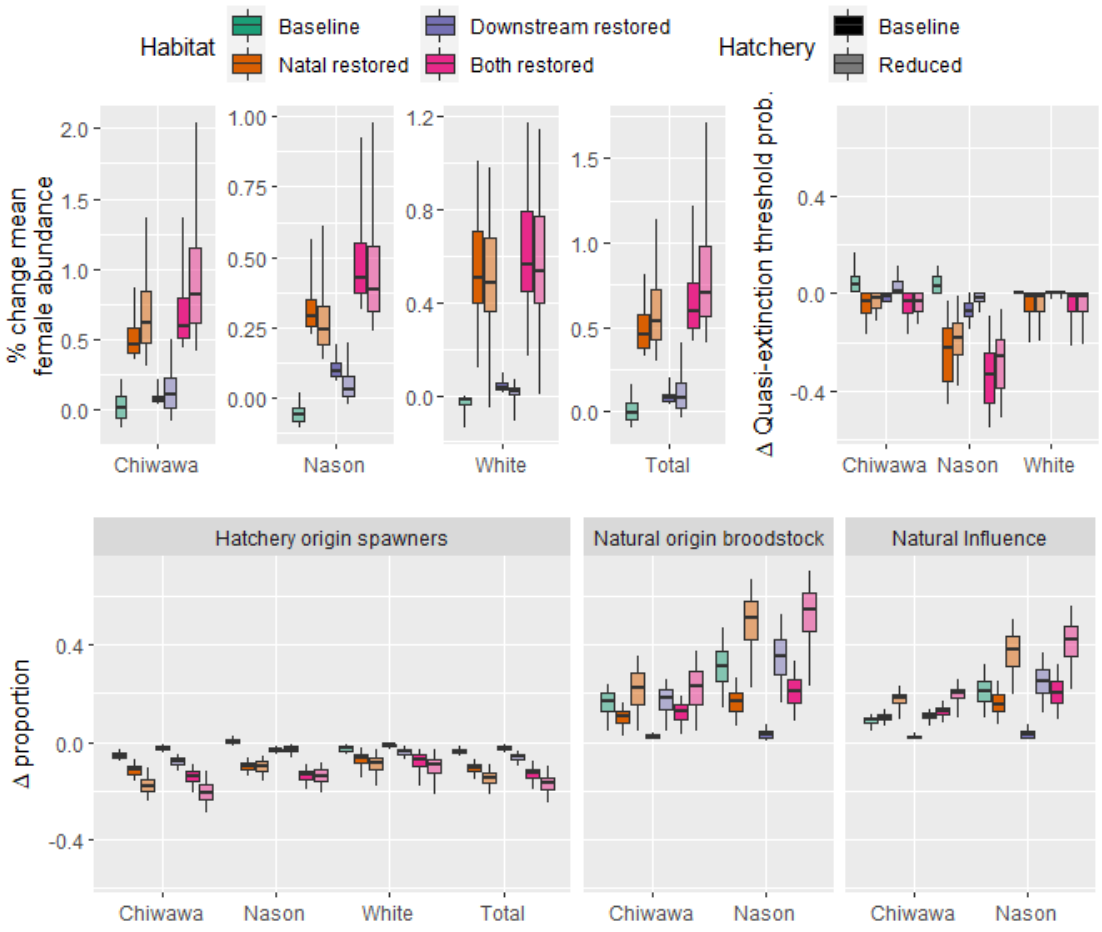

Figure J2: Boxplots of (a) the percent change in simulated geometric mean natural-origin female spawner abundance over 50 years, and the change in (b) the probability of the four-year running mean natural-origin female spawner abundance falling below a quasi-extinction threshold of 15 (pQET), (c) the average proportion of spawners that are of hatchery origin (pHOS), (d) the average proportion of hatchery broodstock that are of natural origin (pNOB), and (e) the average Proportionate Natural Influence (PNI) by natal stream relative to the baseline habitat and hatchery strategy. Box color represents habitat strategy and box shading represents hatchery broodstock size target strategies. Within each boxplot, the center line represents the median across simulations, the box spans the interquartile range, and the whiskers span the 90% quantile.